UNCLASSIFIED

AD 267 343

Reproduced
by the

ARMED SERVICES TECHNICAL INFORMATION AGENCY
ARLINGTON HALL STATION
ARLINGTON 12, VIRGINIA

UNCLASSIFIED

NOTICE: When government or other drawings, specifications or other data are used for any purpose other than in connection with a definitely related government procurement operation, the U. S. Government thereby incurs no responsibility, nor any obligation whatsoever; and the fact that the Government may have formulated, furnished, or in any way supplied the said drawings, specifications, or other data is not to be regarded by implication or otherwise as in any manner licensing the holder or any other person or corporation, or conveying any rights or permission to manufacture, use or sell any patented invention that may in any way be related thereto.

267 343

U. S. ARMY
TRANSPORTATION RESEARCH COMMAND
FORT EUSTIS, VIRGINIA

267343

TCREC TECHNICAL REPORT 61-105

WIND TUNNEL TESTS AND FURTHER ANALYSIS OF THE FLOATING WING FUEL TANKS FOR HELICOPTER RANGE EXTENSION

VOLUME 4

COUPLED WING-FUSELAGE FORCED VIBRATION ANALYSIS
45° SKEWED HINGE

Project 9X38-09-006
Contract DA 44-177-TC-550

August 1961

ASTIA

prepared by :

VERTOL DIVISION
THE BOEING COMPANY
Morton, Pennsylvania

2494—60

Project 9X38-09-006
Contract No. DA44-177-TC-550
August 1961

TCREC TECHNICAL REPORT 61-105

WIND TUNNEL TESTS AND FURTHER ANALYSIS OF THE FLOATING WING FUEL TANKS FOR HELICOPTER RANGE EXTENSION

VOLUME 4

COUPLED WING-FUSELAGE FORCED VIBRATION ANALYSIS 45° SKEWED HINGE

Report No. R-252

Prepared by:

VERTOL DIVISION
THE BOEING COMPANY
MORTON, PENNSYLVANIA

for
U. S. ARMY TRANSPORTATION RESEARCH COMMAND
FORT EUSTIS, VIRGINIA

HEADQUARTERS
U. S. ARMY TRANSPORTATION RESEARCH COMMAND
Fort Eustis, Virginia

FOREWORD

Under the terms of Contract DA 44-177-TC-550, the Vertol Division of Boeing Airplane Company has been investigating methods or means of extending the range of Army aircraft. A method presently under investigation is one in which floating-wing fuel tanks are attached to the fuselage of a helicopter through a hinge arrangement. This method holds the most promise for extending the ferry range of a helicopter of the light- or heavy-cargo type to 2,000 miles or more.

The report presented in the following pages is Volume 4 of a five-volume final report on the investigation of the floating-wing configuration. Volume 4 presents the results of the wing fuselage forced vibration study. The conclusions contained herein are concurred in by the U. S. Army Transportation Research Command, Fort Eustis, Virginia, the cognizant agency for Contract DA 44-177-TC-550.

FOR THE COMMANDER:

APPROVED BY:

Robert D. Powell Jr
ROBERT D. POWELL, JR.
USATRECOM Project Engineer

Raphael F. Garofalo
RAPHAEL F. GAROFALO
CWO-4 USA
Assistant Adjutant

TABLE OF CONTENTS

SECTION	DESCRIPTION	PAGE
	FOREWORD	ii
	LIST OF ILLUSTRATIONS	iv
	LIST OF SYMBOLS	v
	SUMMARY	1
I	INTRODUCTION	2
II	METHOD OF ANALYSIS	4
	A. General	4
	B. Matrix Fuselage-Wing Representation	10
III	WING - FUSELAGE FORCED RESPONSE	21
	A. General	21
	B. Analytical Model	21
	C. Forced Response	26
IV	CONCLUSIONS	46
V	REFERENCES	47
	APPENDICES	
	A. Coupled Mode Associated Matrix Deviation	48
	B. Method of Solution for Coupled Matrix Program	95
	DISTRIBUTION LIST	106

LIST OF ILLUSTRATIONS

Figure	Description	Page
1	Coupled Vertical-Lateral Matrix Flow Diagram	5
2	Computer Input Form	6
3	Input Sequence Chart for Coupled Matrix Program	8
4	Numerical Output for a Fuselage - Wing Forced Mode	9
5	Frame Racking Matrix	13
6	H-21 Vertical - Lateral Matrix Representation	22
7	H-21 Forward Fuselage Elastic Properties	23
8	H-21 Forward Fuselage Simulated Deflection	25
9	H-21 Aft Fuselage Elastic Properties	27
10	H-21 Reference Axis Location and Weight Distribution	28
11	Normalized Engine Modes, H-21 C-96 Shake Test	29
12	Wing Mass and Stiffness Distribution	30
13	Wing Flap Bending and Torsion Modes - 0% Fuel	31
14	Wing Flap Bending and Torsion Modes - 100% Fuel	32
15	Third Harmonic Fixed System Shaft Loads, 90 Knot RPM Sweep	33
16	Third Harmonic Forced Response 0% Wing Fuel, 90 Knots, 250 RPM	35
17	Third Harmonic Forced Response 0% Wing Fuel, 90 Knots, 258 RPM	36
18	Third Harmonic Forced Response 0% Wing Fuel, 90 Knots, 268 RPM	37
19	Matrix Residual Plot	38
20	Third Harmonic Forced Response 100% Wing Fuel, 90 Knots, 250 RPM	40
21	Third Harmonic Forced Response 100% Wing Fuel, 90 Knots, 258 RPM	41
22	Third Harmonic Forced Response 100% Wing Fuel, 90 Knots, 268 RPM	42
23	Third Harmonic Cockpit Floor Response H-21 without Floating Fuel Wings	44
24	Third Harmonic Cockpit Floor Response H-21 with Floating Fuel Wings	45

LIST OF SYMBOLS

ω	Trial frequency for matrix solution (rad./sec.)
ω_f	Forcing frequency (rad./sec.)
ω_n	Natural frequency (rad./sec.)
Ω	Rotor forcing frequency (rad./sec.)
X, Y, Z,	Linear deflections at matrix stations (in.)
α, β, γ	Angular motions at matrix station (rad.)
F_x, F_y, F_z	Forces corresponding to the X, Y, and Z directions (lb.)
M_x, M_y, M_z	Moments corresponding to the α, β, and γ rotations (in.-lb.)
n	Generalized matrix station
L	Elastic bay length (in.)
b_n	Distance from the reference axis to the neutral axis in the Y direction (in.)
c_n	Distance from the reference axis to the neutral axis in the Z direction (in.)
b_e	Distance from the reference axis to the elastic axis in the Y direction (in.)
c_e	Distance from the reference axis to the elastic axis in the Z direction (in.)
A_x	Axial compression area (in.^{2})
A_y	Effective shear area in the Y direction (in.^{2})
A_z	Effective shear area in the Z direction (in.^{2})
I_x	Torsional stiffness about the X axis (in.^{4})
I_y	Bending stiffness about the Y axis (in.^{4})
I_z	Bending stiffness about the Z axis (in.^{4})
G	Shear modulus (lb./in.^{2})
I	Bending modulus (lb./in.^{2})
$\Phi_{a\alpha}$	Linear deflection at the right side of the frame from a unit moment (in./in.-lb.)
$\Phi_{b\alpha}$	Linear deflection at the top section of the frame from a unit moment (in./in.-lb.)
$\Phi_{c\alpha}$	Linear deflection at the left side of the frame from a unit moment (in./in.-lb.)
$\Phi_{d\alpha}$	Linear deflection at the bottom section of the frame from a unit moment (in./in.-lb.)
W	Lateral distance between longerons (in.)
W_1	Lateral distance from the reference axis to the right longeron (in.)
H	Vertical distance between longerons (in.)
H_2	Vertical distance from the reference axis to the upper longeron (in.)
a, b, c	Distances from matrix station in the X, Y, Z, directions, respectively (in.)
m	Matrix station mass

I_α, I_β, I_γ	Mass moment of inertia at a matrix station (lb sec^2-in.)
K_x, K_y, K_z	Linear springs in the X, Y, and Z directions (lb/in.)
K_α, K_β, K_γ	Angular springs about the X, Y, and Z axes $\left(\frac{\text{in.-lb}}{\text{rad}}\right)$
μ_x, μ_y, μ_z	Amplification factors of linear motions
$\mu_\alpha, \mu_\beta, \mu_\gamma$	Amplification factors for angular motions
$\omega_x, \omega_y, \omega_z, \omega_\alpha, \omega_\beta, \omega_\gamma$	Uncoupled natural frequencies (rad/sec)
ω_r	Coupled engine frequency in the "r"th mode (rad/sec)
H_r	Generalized coordinate in the "r"th coupled engine mode
m_1, m_4, m_3	Rigid engine mass (lb sec^2/in.)
m_2, m_5, m_6	Rigid engine inertias about the Y, Z, and X axes respectively (lb sec^2/in.)
$e_1^{(r)}$, $e_3^{(r)}$, $e_4^{(r)}$	Engine motions in the Z, X, and Y directions respectively for the "r"th engine mode (in.)
$e_2^{(r)}$, $e_5^{(r)}$, $e_6^{(r)}$	Engine rotations about the Y, Z, and X axes respectively for the "r"th engine mode (rad)
f_1, f_3, f_4	Fuselage motions at the engine station in the Z, X, and Y directions (in.)
f_2, f_5, f_6	Fuselage rotations at the engine station about the Y, Z, and X axes, respectively (rad)
ψ_n	Azimuth variation (deg)
F_{ux}, F_{uy}, F_{uz}	Unit forces in the X, Y, and Z directions (lb)
M_{ux}, M_{uy}, M_{uz}	Unit moments about the X, Y, and Z axes (in.-lb)
F_{cx}, F_{cy}, F_{cz}	Cosine component of forces in the X, Y, and Z directions (lb)
M_{cx}, M_{cy}, M_{cz}	Cosine component of moments about the X, Y, and Z axes (in.-lb)
F_{sx}, F_{sy}, F_{sz}	Sine component of forces in the X, Y, and Z directions (lb)
M_{sx}, M_{sy}, M_{sz}	Sine component of moments about the X, Y, and Z axes (in.-lb)
ω_s	Wing natural frequency in the "S" mode (rad/sec)
H_s	Generalized coordinate in the "S" mode
$Z_{Ri}^{(s)}$, $Z_{Li}^{(s)}$	Vertical displacements relative to the undeflected fuselage of the right and left wing respectively
$\alpha_{Ri}^{(s)}$, $\beta_{Ri}^{(s)}$, $\alpha_{Li}^{(s)}$, $\beta_{Li}^{(s)}$	Angular displacements relative to the undeflected fuselage of the right and left wing respectively
m_i	Wing mass at station i
$\bar{X}_i$, $\bar{Y}_i$, $\bar{Z}_i$	Total linear displacements of the wing at station i
$\bar{\alpha}_i$, $\bar{\beta}_i$, $\bar{\gamma}_i$	Total angular displacements of the wing at station i
a_i	Longitudinal distance of wing mass from elastic axis
b_i	Lateral distance of wing from center line of aircraft

SUMMARY

Forced response calculations are performed on the H-21 helicopter equipped with floating fuel wings for the 0% and 100% fuel configurations. Using third harmonic shaft loads measured on an H-21 helicopter, and a deflection test obtained analytical model of the H-21 fuselage, the Associated Matrix Method is employed to calculate the fuselage forced response. Solutions are obtained on the Remington Rand 1103A computer installation at Wright Field. Results of the response calculations are presented as modal time histories of the fuselage for third harmonic azimuth positions of 0, 45, 90, and 135 degrees, and the resultant vertical and lateral responses at the cockpit floor during an rpm sweep.

Results of the analysis indicate that at the 0% fuel configuration, vertical response compares closely to that of the standard helicopter. Laterally, the response increases with rotor speed, having an acceptable level at the lower rotor speed range and somewhat higher amplitude at 268 rpm. For the 100% fuel configuration, the forced response calculations indicate the presence of a lateral natural frequency close to, but below, the 3Ω excitation at 250 rpm. In both the lateral and vertical directions, the calculated undamped vibration levels are high at the lower rotor speeds, but appear satisfactory at 268 rpm. Past experience indicates that predicted vibration levels near resonance are reduced by damping. Nevertheless, as a result of the calculations, it is recommended that a simplified ground shake test be performed to substantiate the calculations and provide some reasonable prediction of the effect of damping.

SECTION I

INTRODUCTION

The present wing-fuselage forced vibration study is part of an analytical and wind tunnel study being conducted under the Reference 1 Transportation Research Command contract. The program is aimed at the development of a means for helicopter ferry range extension through application of a floating fuel wing concept. An initial feasibility study of the floating wing concept was conducted by Vertol under an earlier contract, Reference 2, and the results reported in Reference 3. The present analytical and wind tunnel investigation is under the Reference 1 contract and is based on a Vertol proposal, Reference 4. This vibration investigation is a part of Phase II of the contract. Additional dynamic studies of the contract include ground and air instability reported in Reference 5 and flutter calculations reported in Reference 6.

The range of present helicopters with normal fuel load is less than 400 nautical miles. Even with additional internal tanks, the helicopter range is less than 1100 miles. With floating wings, the range can be extended to as much as 2400 miles, corresponding to the longest over-water distance on the Pacific Ocean ferry route.

Each floating wing contains compartmented fuel tankage connected by lines to the helicopter's main tank. The wing lift supports the fuel weight that it carries, and the helicopter acts as a tow to propel the wing forward. Wing attachment to the helicopter is through a hinge so as to eliminate the bending moments applied at the fuselage by conventional wings, thus avoiding the addition of extensive wing carry through structure to the helicopter. The hinge line is not longitudinal, but is skewed aft as shown.

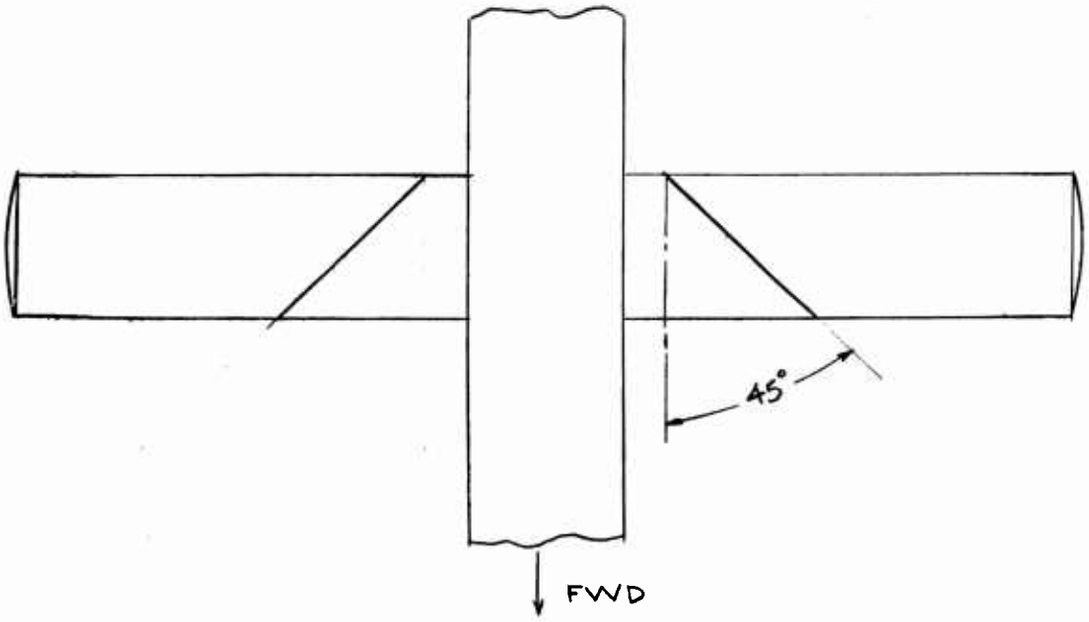

As fuel is consumed and the wing becomes lighter, it tends to flap upward about its hinge. Because of the skewed orientation, the angle of attack at any chord line is reduced as the wing flaps up, the lift is reduced, and the wing assumes a new mean position. Full span pilot controlled wing flaps are also provided, so that the trim attitude of the wing may be adjusted; these are also used as high lift devices during the running takeoff.

In-flight, the wing-helicopter combination is excited by rotor induced loads such as measured on the H-21 helicopter under Reference 7. In a previous study performed under Reference 8, the forced response of the H-21 helicopter without floating fuel wings was determined theoretically by applying measured shaft loads to an analytical representation of the fuselage which included vertical-lateral coupling. The present analyses use the coupled fuselage program of Reference 8 programmed on the Remington Rand 1103A computer. To include the floating fuel wings, the H-21 fuselage representation is expanded to include an effective wing matrix which represents the flap-torsion wing modes.

The fuselage-wing forced response is investigated here for the wing empty - 0% fuel and wing full - 100% fuel at each of the possible operating rotor speeds of 250,258 and 268 RPM for a cruise speed of 90 knots.

Section II presents the method of analysis, followed by a discussion of the results in Section III including a description of the analytical representation. Conclusions are given in Section IV, and References in Section V. The matrix derivations are presented in Appendix A, along with the method of solution in Appendix B.

SECTION II

METHOD OF ANALYSIS

A. General

The method used here for forced mode calculations is the coupled vertical-lateral analysis of Reference 8. A coupled vertical-lateral system was chosen for representing the H-21 fuselage as a result of previous investigations, both analytical and test indicating the significance of coupling. The structural deflection test of the H-21 fuselage under Reference 9, and the initially limited correlation shown between uncoupled analytical and ground shake test results in Reference 10 indicated that an analytical model of the H-21 fuselage must include vertical-lateral coupling.

The analysis includes the following basic matrix types: (1) discrete lumped masses and moments of inertia, (2) suspended lumped masses and mass moments of inertia, (3) bends permitting the selected elastic beam axis to follow the general fuselage shape, (4) sections of weightless elastic beam which permit the inclusion of bending, shear, tension and torsional stiffness properties, (5) concentrated springs which simulate the attachment of large local mass and inertia items to fuselage structure, such as the rotor transmission, and (6) ground spring matrices which permit attachment of the vibrating body to an external ground as in a bungee suspension for ground shake testing. Also, to provide the specialized representation necessary for the H-21 fuselage and to include forced response calculations, the above type of matrices were expanded to include (1) sections of weightless elastic beam, which permit frame distortion in combination with bending, shear and torsion stiffness properties, (2) stations which permit the attachment of a coupled vibration system such as the flexibly mounted engine with known modes and frequencies and (3) force matrices which permit exciting forces to be applied at any point on the vibrating body, such as the external shaker in a ground shake test or the measured flight loads at the rotor.

This existing program is adapted to the H-21 fuselage-wing combination using an effective wing matrix to transmit the dynamic wing loads to the fuselage with the uncoupled wing modes as generalized coordinates. As derived previously, with the addition of the effective wing matrix, the matrices and elements are presented in Appendix A along with the method of solution in Appendix B. Figure 1 presents the digital computer flow chart showing the basic programming procedure for the Remington Rand Univac 1103A digital computer. Application to the wing-fuselage matrix program is illustrated by Figure 2, Computer Input Forms, partially completed for the H-21 helicopter equipped with floating fuel wings, Figure 3, Input Sequence Chart for the Coupled Matrix Program and Figure 4, Numerical Output for a Fuselage-Wing Forced Mode.

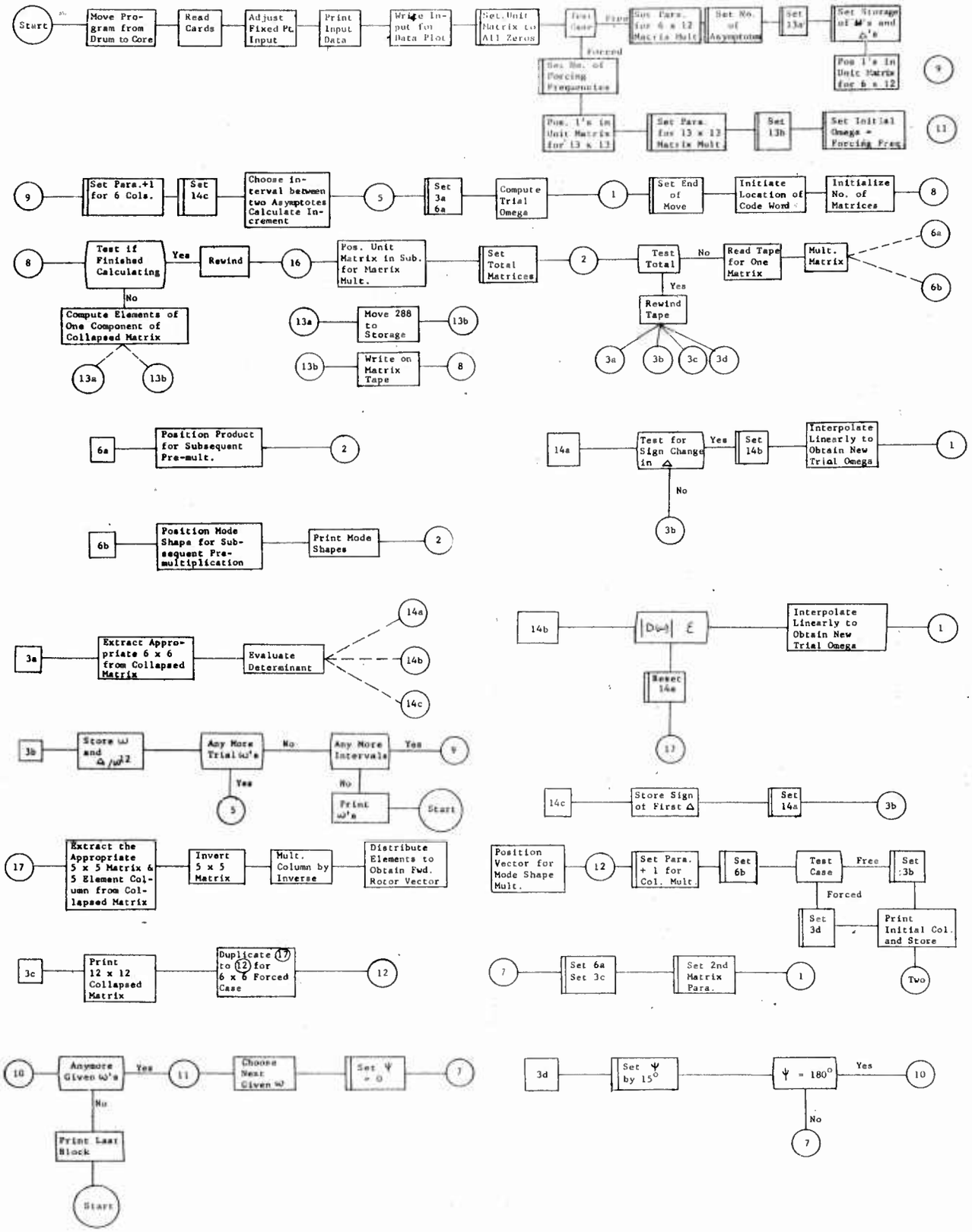

FIGURE 1. COUPLED VERTICAL-LATERAL MATRIX FLOW DIAGRAM

INPUT FOR H-21 HELICOPTER EQUIPPED WITH FLOATING FUEL WING

RO, X 051	Case
111,	Job
032861,	Date
1021	Aircraft Model No.
27100,	Gross Weight
352.00,	C. G. Station
0,	Flight No.
90,	Airspeed Knots
250,	Rotor RPM
1,	Engine (0 - Rigid, 1 - Suspended)
0,	Blades (1-On, 0-Removed)
R35SF 2.50×10^2	Rotor Speed RPM
X 1,	Collapsed Matrix (0 - No Print Out, 1 - Print Out)
50,	Total Matrices
1,	Program (0 - Free, 1 - Forced)
B 10,	Boundaries (10 - Free - Free)
X 000	Number of Forcing Frequencies
78.6,	Forcing Frequency

MATRIX INPUT
(Read Down Columns)

Rotor Shaft Loads

Loc.	Code & Elements	
1	B02026	
	F0	F_{ux}
	8.9×10^1	F_{cx}
	3.39×10^2	F_{sx}
	0	F_{uy}
	1.44×10^2	F_{cy}
	-6.40×10^1	F_{sy}
	0	F_{uz}
	-2.71×10^2	F_{cz}
	1.53×10^2	F_{sz}
	0	$M_{u\alpha}$
	3.555×10^3	$M_{c\alpha}$
	2.057×10^3	$M_{s\alpha}$
	0	$M_{u\beta}$
	5.52×10^2	$M_{c\beta}$
	-3.94×10^2	$M_{s\beta}$
	0	$M_{u\gamma}$

Rotor Shaft

Loc.	Code & Elements	
	1.013×10^3	$M_{c\gamma}$
	6.89×10^2	$M_{s\gamma}$
	0	a_f
	0	b_f
	0	c_f
	4.5×10^1	Φ
2	B01015	b_e
	0	c_e
	0	b_n
	0	c_n
	$+1.97 \times 10^1$	L
	$+1.43 \times 10^1$	A_x
	$+1.38 \times 10^1$	A_y
	$+1.38 \times 10^1$	A_z
	$+7.13 \times 10^1$	J_x
	$+3.76 \times 10^1$	I_y
	$+3.76 \times 10^1$	I_z

FIGURE 2 COMPUTER INPUT FORM

	Loc.	Code & Elements	
Rotor Shaft Spring		$+1.05 \times 10^{7}$	E
		$+4.00 \times 10^{6}$	G
	3	B07006	
		$F+1.0 \times 10^{20}$	K_x
		$+1.0 \times 10^{20}$	K_z
		$+1.0 \times 10^{20}$	K_α
		$+2.5 \times 10^{7}$	K_β
		$+2.5 \times 10^{7}$	K_γ
Transmission Elastic Bay	4	B01015	
		0	b_e
		0	C_e
		0	b_n
		0	C_n
		1.56×10^{1}	L
		1.00×10^{20}	A_x
		1.0×10^{20}	A_y
		1.0×10^{20}	A_z
		1.0×10^{20}	J_x
		1.0×10^{20}	I_y
		1.0×10^{20}	I_z
		$+1.05 \times 10^{7}$	E
		$+4.00 \times 10^{6}$	G
Transmission Mass	5	B05007	
		1.0549×10^{0}	M
		5.6×10^{1}	I_α
		6.1×10^{1}	I_β
		6.1×10^{1}	I_γ
		-3.0×10^{0}	a
		0	b
		0	c

	Loc.	Code & Elements	
Transmission Spring	6	B07006	
		$F+1.0 \times 10^{20}$	K_x
		$+3.5 \times 10^{5}$	K_y
		$+2.3 \times 10^{4}$	K_z
		$+1.0 \times 10^{20}$	K_α
		$+4.0 \times 10^{7}$	K_β
		$+7.0 \times 10^{7}$	K_γ
Pylon Elastic Bay	7	B01015	
		F 0	b_e
		0	c_e
		0	b_n
		0	c_n
		$+3.05 \times 10^{1}$	L
		1.0×10^{20}	A_x
		1.0×10^{20}	A_y
		1.0×10^{20}	A_z
		1.0×10^{20}	J_x
		1.0×10^{20}	I_y
		1.0×10^{10}	I_z
		1.05×10^{7}	E
		4.00×10^{6}	G
Pylon Bend	8	B03003	
		$F+1.6505 \times 10^{-1}$	$\cos\beta$
		-9.8629×10^{-1}	$\sin\beta$
		$+2.795 \times 10^{2}$	β

FIGURE 2 (CONTINUED) COMPUTER INPUT FORM

INPUT	TYPE CODE	INPUT SEQUENCE									
Elastic Matrix	B01017	$\cos\alpha_p$	$\sin\alpha_p$	b_e	c_e	b_n	c_n	L	A_x	A_y	A_z
		J_x	I_y	I_z	E	G					
Force Matrix	B02026	F_{ux}	F_{cx}	F_{sx}	F_{uy}	F_{cy}	F_{sy}	F_{uz}	F_{cz}	F_{sz}	$M_{u\alpha}$
		$M_{c\alpha}$	$M_{s\alpha}$	$M_{u\beta}$	$M_{c\beta}$	$M_{s\beta}$	$M_{u\gamma}$	$M_{s\gamma}$	$M_{c\gamma}$	a_f	b_f
		c_f	ψ								
Vertical Bend Matrix	B03003	$\cos\beta_p$	$\sin\beta_p$	β_p							
Shift Matrix	B04003	a	b	c							
Mass Matrix	B05007	M	I_α	I_β	I_γ	a	b	c			
Sprung Mass Matrix	B06015	M	I_α	I_β	I_γ	a	b	c	ω_x	ω_y	ω_z
Concentrated Spring Matrix	B07006	k_x	k_y	k_z	k_α	k_β	k_γ				
Ground Spring Matrix	B10011	k_x	k_y	k_z	k_α	k_β	k_γ	a	b	c	
Coupled Engine Matrix	B11056	M	I_α	I_β	I_γ	$\omega_1, \omega_2, \ldots \omega_6$		$h_1^{(1)}, h_1^{(2)} \ldots h_1^{(6)}$		$h_2^{(1)}, h_2^{(2)} \ldots h_2^{(6)}$	
		$h_3^{(1)}, h_3^{(2)} \ldots h_3^{(6)}$		$h_4^{(1)}, h_4^{(2)} \ldots h_4^{(6)}$		$h_5^{(1)}, h_5^{(2)}, \ldots h_5^{(6)}$		$h_6^{(1)}, h_6^{(2)} \ldots h_6^{(6)}$			
				$(m_1=M,\ M_2=I_\beta,\ M_3=M,\ M_4=M,\ M_5=I_\gamma,\ M_6=I_\alpha)$							
General Matrix	B12251	$a_{11}, a_{12}, a_{1n} \ldots a_{1,13}$		$a_{21}, a_{22}, a_{2n} \ldots a_{2,13}$		$a_{31}, a_{32}, a_{3n} \ldots a_{3,13}$		$a_{41}, a_{42}, a_{43} \ldots a_{4,13}$		$a_{51}, a_{52}, a_{5n} \ldots a_{5,13}$	
		$a_{61}, a_{62}, a_{6n} \ldots a_{6,13}$		$a_{71}, a_{72}, a_{7n} \ldots a_{7,13}$		$a_{81}, a_{82}, a_{8n} \ldots a_{8,13}$		$a_{91}, a_{92}, a_{9n} \ldots a_{9,13}$		$a_{10,1}, a_{10,2}, a_{10,n} \ldots a_{10,13}$	
		$a_{11,1}, a_{11,2}, a_{11,n} \ldots a_{11,13}$		$a_{12,1}, a_{12,2}, a_{12,n} \ldots a_{12,13}$		$a_{13,1}, a_{13,2}, a_{13,n} \ldots a_{13,13}$					
Frame Racking Matrix	B13022	b_n	c_n	A_x	A_y	A_z	I_y	I_z	E	G	L
		$\Phi_{a\alpha}$	$\Phi_{b\alpha}$	$\Phi_{c\alpha}$	$\Phi_{d\alpha}$	W	W_1	H	H_2		
Elastic Matrix (Collapsed)	B01015	b_e	c_e	b_n	c_n	L	A_x	A_y	A_z	J_x	I_y
		I_z	E	G							
Frame Racking Matrix (Collapsed)	B13022	b_n	c_n	A_x	A_y	A_z	I_y	I_z	E	G	L
		$\Phi_{a\alpha}$	$\Phi_{b\alpha}$	$\Phi_{c\alpha}$	$\Phi_{d\alpha}$	W	W_1	H	H_2		

FIGURE 3 INPUT SEQUENCE FOR COUPLED MATRIX PROGRAM

COUPLED VERTICAL LATERAL FUSELAGE FORCED MODES

CASE	JOB	DATE	AIRCRAFT	GROSS WT	CG STA	FLIGHT AIRSPEED KT	ROTOR RPM	ENGINE	BLADE
51	111	32861	0021	27,100		90	250	1	0

FORCING FREQUENCY RAD. PER SEC. 7.8600000 01 PER REV. 3.0 HARMONIC AZIMUTH DEG. 0.

X IN	Y IN	Z IN	ALPHA RAD	BETA RAD	GAMMA RAD	FX LB	FY LB	FZ LB	MX LB IN	Y LB IN	MZ LB IN	
1.033-02	7.414-03	-6.241-02	2.809-04	-9.215-04	-5.264-04	0.	0.	0.	0.	0.	0.	FWD Rotor Boundary
1.033-02	7.414-03	-6.241-02	2.809-04	-9.215-04	-5.264-04	8.900 01	1.440 02	-2.710 02	3.555 03	3.520 02	6.890 02	FWD Rotor Forces
1.032-02	1.058-03	-4.477-02	3.534-05	-6.159-04	-2.900-04	8.900 01	1.440 02	-2.710 02	3.555 03	-4.787 03	-2.145 03	Rotor Shaft
1.032-02	1.058-03	-4.477-02	3.534-05	-6.244-04	-2.041-04	8.900 01	1.440 02	-2.710 02	3.555 03	-4.787 03	-2.145 03	Rotor Shaft Spring
1.032-02	-2.127-03	-3.503-02	3.534-05	-6.244-04	-2.041-04	8.900 01	1.440 02	-2.710 02	3.555 03	-9.014 03	-4.394 03	Transmission Elastic Bay
1.032-02	-2.127-03	-3.503-02	3.534-05	-6.244-04	-2.041-04	1.562 02	1.341 02	-5.115 02	3.567 03	-9.971 03	-4.442 03	Transmission Mass
1.032-02	-2.510-03	-1.279-02	3.534-05	-3.751-04	-1.407-04	1.562 02	1.341 02	-5.115 02	3.567 03	-4.971 03	-4.442 03	Transmission Spring
1.032-02	-6.801-03	-1.347-03	3.534-05	-3.751-04	-1.407-04	1.562 02	1.341 02	-5.115 02	3.567 03	-9.557 04	-8.532 03	FWD Pylon Bay
3.744-04	-6.801-03	-1.040-02	-1.329-04	-3.751-04	-5.867-05	-4.767 02	1.341 02	-2.385 02	-7.827 03	-9.557 04	-4.927 03	Bend FWD Pylon
3.744-04	-6.801-03	-1.040-02	-1.329-04	-3.751-04	-5.867-05	-3.813 02	-6.822 01	-6.579 02	-1.110 04	-9.945 04	-3.301 03	Mass Station 100
5.411-04	-7.911-03	2.110-03	-1.318-04	-3.466-04	-5.745-05	-3.813 02	-6.822 01	-6.579 02	-1.110 04	-5.458 04	-3.144 03	Elastic Bay Station 100 to 119.5
5.411-04	-7.911-03	2.110-03	-1.318-04	-3.466-04	-5.745-05	-3.769 02	-1.131 02	-6.164 02	-1.115 04	-5.533 04	-3.952 03	Mass Station 119.5
8.201-04	-9.854-03	2.478-02	2.151-05	-2.622-04	-5.660-05	-3.769 02	-1.131 02	-6.164 02	-1.115 04	-7.999 04	5.715 02	Elastic Bay Station 119.5 to 159.5
8.201-04	-9.854-03	2.478-02	2.151-05	-2.622-04	-5.660-05	-3.225 02	-1.885 02	-4.129 02	-1.035 04	-8.234 04	-4.032 02	Mass 159.5
2.167-03	-1.082-02	4.169-02	1.941-05	-1.925-04	-6.264-05	-3.225 02	-1.885 02	-4.129 02	-1.035 04	-1.071 05	1.091 04	Elastic Bay Station 159.5 to 219.5
2.167-03	-1.082-02	4.169-02	1.941-05	-1.925-04	-6.264-05	-2.934 02	-2.423 02	-1.965 02	-9.751 03	-1.058 05	1.107 04	Mass 219.5
9.866-03	-1.004-02	4.169-02	1.941-05	-1.925-04	-6.264-05	-2.934 02	-2.423 02	-1.965 02	-6.063 01	-1.175 05	1.107 04	Shift from Fuselage Station to Wing
9.866-03	-1.004-02	4.169-02	1.941-05	-1.925-04	-6.264-05	6.519 01	-6.162 02	-3.319 01	1.766 04	-8.780 04	-1.309 05	Wing Elastic Axis
2.167-03	-1.082-02	4.169-02	1.941-05	-1.925-04	-6.264-05	6.519 01	-6.162 02	-3.319 01	-8.987 03	-9.041 04	-1.309 05	Shift from Wing E.A. to Fuselage Stat
3.697-03	-5.323-03	5.187-02	2.615-05	-7.442-05	4.966-05	6.519 01	-6.162 02	-3.319 01	-6.987 03	-9.306 04	-8.159 04	Elastic Bay Station 219.5 to 299.5
3.697-03	-5.323-03	5.187-02	2.615-05	-7.442-05	4.966-05	1.014 02	-7.587 02	1.170 03	1.482 03	-7.233 04	-7.929 04	Mass Station 299.5
4.454-03	4.019-03	3.645-02	4.142-04	-4.777-05	9.153-05	1.014 02	-7.587 02	1.170 03	1.482 03	-8.310 03	-3.794 04	Elastic Bay Station 299.5 to Bend
4.454-03	4.019-03	3.645-02	4.142-04	-4.777-05	9.153-05	1.940 02	-7.050 02	1.408 03	2.366 03	-8.800 03	-3.838 04	Mass at Bend
1.750-02	4.019-03	3.228-02	4.189-04	-4.777-05	-6.645-05	6.965 02	-7.050 02	1.239 03	-1.186 04	-8.800 03	-3.857 04	Fuselage Bend
1.674-02	4.803-03	3.053-02	4.306-04	-6.372-05	-4.772-05	6.965 02	-7.050 02	1.239 03	-1.186 04	4.089 04	-9.452 03	Elastic Bay Bend to Station 395
1.674-02	4.803-03	3.053-02	4.306-04	-6.372-05	-4.772-05	1.526 03	-4.409 01	2.621 03	2.128 04	3.887 04	-1.419 04	Mass Station 395
1.526-02	3.561-03	2.658-02	4.188-04	-1.066-04	-3.650-05	1.526 03	-4.409 01	2.621 03	2.126 04	1.099 05	-1.283 04	Elastic Bay Station 395 to 423
1.526-02	3.561-03	2.658-02	4.188-04	-1.066-04	-3.650-05	1.586 03	-1.791 01	2.717 03	2.149 04	1.099 05	-1.295 04	Mass Station 423
1.390-02	2.854-03	2.478-02	4.107-04	-1.575-04	-2.912-05	1.586 03	-1.791 01	2.717 03	2.149 04	1.689 05	-1.257 04	Elastic Bay Station 423 to 445
1.390-02	2.854-03	2.478-02	4.107-04	-1.575-04	-2.912-05	1.637 03	5.970	2.804 03	2.178 04	1.851 05	-1.223 04	Mass Station 445
1.014-02	1.785-04	2.403-02	2.992-04	-3.818-04	-2.368-05	1.637 03	5.970	2.804 03	2.176 04	1.025 05	-1.254 04	Elastic Bay Station 445 to 494
1.014-02	1.785-04	2.403-02	2.992-04	-3.818-04	-2.368-05	1.661 03	1.158 01	2.901 03	2.181 04	3.017 05	-1.250 04	Mass Station 494
7.586-03	-1.157-03	2.622-02	2.397-04	-5.156-04	-2.073-05	1.661 03	1.158 01	2.901 03	2.181 04	3.771 05	-1.260 04	Elastic Bay Station 494 to 521
1.455-02	2.712-03	1.249-02	2.397-04	-5.156-04	-2.073-05	1.661 03	1.158 01	2.901 03	2.165 04	3.113 05	-1.245 04	Shift to Engine C.G.
8.957-03	2.712-03	1.696-02	2.307-04	-5.156-04	6.858-05	5.007 02	1.158 01	3.318 03	2.471 04	3.113 05	-3.649 03	Rotation to Engine Axis System
8.957-03	2.712-03	1.696-02	2.307-04	-5.156-04	6.858-05	1.495 03	-3.419 02	-1.561 03	3.379 04	2.974 05	-4.099 04	Engine Mass
1.455-02	2.712-03	1.249-02	2.397-04	-5.156-04	-2.073-05	8.168 02	-3.419 02	-2.000 03	1.642 04	2.974 05	-5.052 04	Rotation to Fuselage Axis System
7.587-03	-1.157-03	2.622-02	2.397-04	-5.156-04	-2.073-05	8.168 02	-3.419 02	-2.000 03	1.180 04	2.253 05	-4.009 04	Shift from Engine Axis to Station 521
7.587-03	-1.157-03	2.622-02	2.397-04	-5.156-04	-2.073-05	8.704 02	-3.376 02	-1.855 03	1.100 04	2.219 05	-3.970 04	Mass Station 521
3.521-03	2.226-03	6.391-02	1.445-04	-6.298-04	4.972-05	8.704 02	-3.376 02	-1.855 03	1.100 04	1.468 05	-2.602 04	Elastic Bay Station 521 to 562
3.521-03	2.226-03	6.391-02	1.445-04	-6.298-04	4.972-05	8.706 02	-3.310 02	-1.652 03	1.097 04	1.419 05	-2.586 04	Mass at Station 562
1.867-03	1.386-02	1.117-01	-6.213-05	-7.687-04	1.669-04	8.706 02	-3.310 02	-1.652 03	1.097 04	5.682 04	-8.808 03	Elastic Bay Station 562 to 613.5
1.867-03	1.386-02	1.117-01	-6.213-05	-7.687-04	1.669-04	8.723 02	-2.290 02	-8.746 02	1.019 04	4.806 04	-6.168 03	Mass at Station 613.5
1.095-01	1.388-02	2.296-02	1.495-04	-7.687-04	9.678-05	-6.651 02	-2.290 02	-1.041 03	-3.816 03	4.806 04	-1.129 04	Bend, Aft Pylon
1.095-01	1.523-02	3.312-02	1.495-04	-7.687-04	9.678-05	-6.651 02	-2.290 02	-1.041 03	-3.816 03	3.348 04	-8.080 03	Aft Pylon Elastic Bay
1.095-01	1.699-02	4.061-02	1.495-04	-1.650-03	3.661-04	-6.651 02	-2.290 02	-1.041 03	-3.816 03	3.348 04	-8.080 03	Transmission Spring
1.095-01	1.699-02	4.061-02	1.495-04	-1.650-03	3.661-04	6.000	-1.020 02	-6.880 02	-3.911 03	3.036 04	-6.702 03	Transmission Mass
1.095-01	2.519-02	7.757-02	1.495-04	-1.650-03	3.661-04	6.000	-1.020 02	-6.880 02	-3.911 03	3.495 04	-4.417 03	Transmission Elastic Bay
1.095-01	2.519-02	7.757-02	1.495-04	-2.248-03	5.428-04	6.000	-1.020 02	-6.880 02	-3.911 03	3.495 04	-4.417 03	Rotor Shaft Spring
1.095-01	3.778-02	1.272-01	4.196-04	-2.656-03	7.131-04	6.000	-1.020 02	-6.880 02	-3.911 03	1.399 03	-2.408 03	Rotor Shaft
1.095-01	3.776-02	1.272-01	4.196-04	-2.656-03	7.131-04	2.880-13	-1.779-13	1.991-13	1.541-11	5.594-11	1.487-11	Aft Rotor Forces

FIGURE 4

B. MATRIX FUSELAGE - WING REPRESENTATION

Elastic Matrix - The coupled matrix provides a practical method, verified by deflection test results, for coupling the vertical-longitudinal and lateral-torsion elastic beam properties. The elastic matrix includes a reference axis, an elastic axis and a neutral axis which do not coincide, thereby coupling the two directions. Pitching, and yawing moments, and axial load are transmitted along the neutral axis, located at b_n laterally and C_n vertically from the reference axis. Vertical and lateral loads, and rolling moment (fuselage torsion) are transmitted along the elastic axis located at b_e laterally and C_e vertically from the reference axis. Loads and deflections are always referred to the arbitrary reference axis, at each end of the elastic bay. The reference axis is a convenient location chosen to meet the problem requirements for a particular aircraft; for example, waterline zero on the centerplane might be a typical reference axis location. The coupled elastic matrix is presented on page 59.

Frame Racking Matrix - In the deflection test reported in Reference 4, the deformation of the H-21 forward fuselage under torsional loading involved appreciable racking (distortion) of the fuselage frames and thus, is not definable by the simple Saint Venant torsional theory. In addition, it was determined by the test that similar frame racking resulted from symmetrical vertical loading. To include these effects in the elastic representation of the forward fuselage, the frame racking matrix was written, which in addition to normal beam bending includes frame distortion due to torque and laterally offset vertical load.

In the forward fuselage sections where frame distortion is significant, the conventional torsional representation is replaced by the following system.

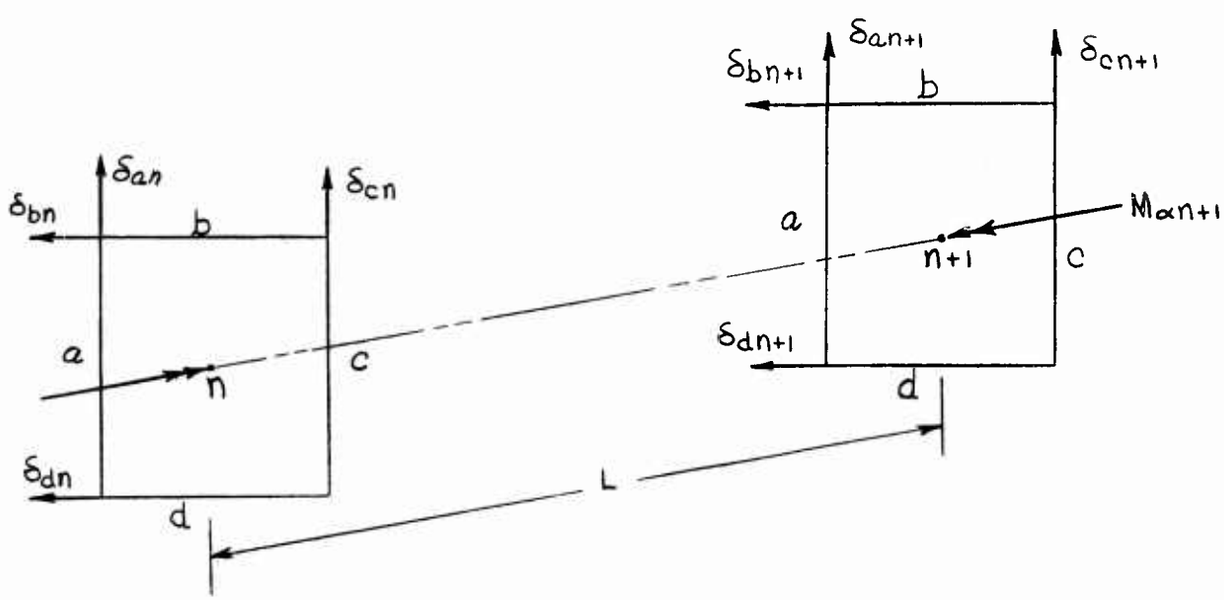

The racking coefficients are defined from the respective absolute deflections at station n and n+1.

Right Side

$$\phi_{a\alpha} = \frac{\delta_{an+1} - \delta_{an}}{M_{\alpha n}}$$

Left Side

$$\phi_{c\alpha} = \frac{\delta_{cn+1} - \delta_{cn}}{M_{\alpha n}}$$

Top

$$\phi_{b\alpha} = \frac{\delta_{bn+1} - \delta_{bn}}{M_{\alpha n}}$$

Bottom

$$\phi_{d\alpha} = \frac{\delta_{dn+1} - \delta_{dn}}{M_{\alpha n}}$$

Using the right and left side racking coefficients, the relative vertical displacement at the reference axis between station n and n+1 is obtained as shown below.

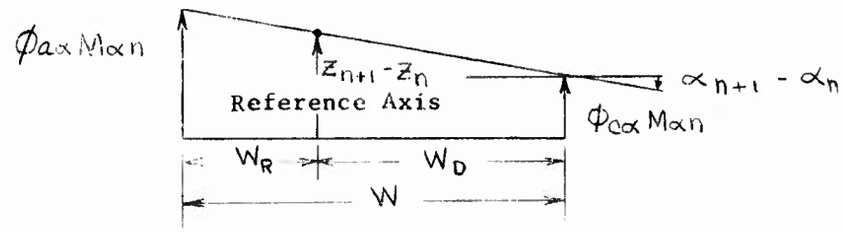

Fuselage Width

Therefore

$$\alpha_{n+1} - \alpha_n = \frac{(\phi_{\alpha a} - \phi_{c\alpha})\, M_{\alpha n}}{W}$$

And

$$z_{n+1} - z_n = \phi_{c\alpha} M_{\alpha n} + (\alpha_{n+1} - \alpha_n) W_L$$

$$= \left(1 - \frac{W_L}{W}\right) \phi_{c\alpha} M_{\alpha n} + \frac{W_L}{W} \phi_{a\alpha} M_{\alpha n}$$

Similarly, and as shown in detail in Appendix A, the lateral slope and deflection become,

$$\alpha_{n+1} - \alpha_n = \frac{(\phi_{b\alpha} - \phi_{d\alpha})}{H} M_{\alpha n}$$

$$y_{n+1} - y_n = \left(1 - \frac{H_2}{H_1}\right) \phi_{b\alpha} M_{\alpha n} - \frac{H_2}{H_1} \phi_{d\alpha} M_{\alpha n}$$

Thus, if the equations for vertical and lateral translation and rotation about the longitudinal axis are added to the existing elastic matrix, and the torsional element L/GJ is removed, the result is the frame racking matrix shown in Figure 5. It was found that an adequate representation of H-21 forward fuselage coupling required additional frame racking from vertical loads. This was accomplished by increasing the applied moment along each elastic element with an additional moment equal to the vertical shear force, F_z multiplied by a lateral arm, d. In the analytical model, this would involve a matrix prior to each frame racking matrix increasing the roll moment, M_α to $M_\alpha + F_z d$ and then, after each elastic element decreasing the roll moment to the original M_α. These matrix operations are performed in general terms and the resulting matrix illustrated in Figure 5. In the frame racking matrix as shown, the slope is defined by the vertical deflections which provide the best test correlation.

<u>Coupled Suspension Matrix</u> - The uncoupled fuselage analyses, vertical-longitudinal, and lateral-torsion reported in Phase IIa Reference 10, illustrated the importance of the engine flexibility. In the previous analyses only the uncoupled frequencies were included, but the engine shake test showed the engine modes to be highly coupled. It was therefore considered essential that the suspended engine be defined by coupled frequencies and modes. Using the notation shown on page 73 , the mass motion with respect to the fuselage can be expressed as

$$e_i = \sum_{r=1}^{6} e_i^{(r)} H_r$$

Adding the fuselage and engine motions, the kinetic energy is

$$T = \frac{1}{2} \sum_{i=1}^{6} m_i \left(\dot{\xi}_i + \dot{e}_i \right)^2$$

Or

$$T = \sum_{i=1}^{6} m_i \left(\dot{\xi}_i^2 + 2 \dot{\xi}_i \sum_{r=1}^{6} e_i^{(r)} \dot{H}_r + \sum_{r=1}^{6} e_i^{(r)2} H_r^2 \right)$$

The total potential energy of the system can be expressed in terms of the effective spring, K_r in each mode.

$$V = \frac{1}{2} \sum_{r=1}^{6} K_r H_r^2$$

Applying Lagrange's Equation and assuming the orthogonality of normal modes,

$$\xi_i \qquad m_i \ddot{\xi}_i + \sum_{r=1}^{6} m_i e_i^{(r)} \ddot{H}_r = -Q_i$$

$$H_r \qquad M_r \ddot{H}_r + K_r H_r + \sum_{j=1}^{6} m_j e_j^{(r)} \ddot{\xi}_y = 0$$

Where

$$M_r = \sum_{r=1}^{6} m_i e_i^{(r)2}$$

1												
L	1											
		1										
$\frac{C_n L^2}{2EI_y}$	$\frac{C_n L}{EI_y}$	$-\frac{C_n^2 L}{EI_y} - \frac{L}{A_x E} - \frac{b_n^2 L}{EI_z}$	1			$\frac{b_n L^2}{2EI_z}$	$-\frac{b_n L}{EI_z}$					
$-\frac{L^2}{2EI_y}$	$\frac{L}{EI_y}$	$\frac{C_n L}{EI_y}$		1								
$\frac{L^3}{6EI_y} - \frac{L}{A_z G} + d\left\{\Phi_{c\alpha}\left(1 - \frac{\omega_1}{\omega}\right) + \Phi_{a\alpha}\frac{\omega_1}{\omega}\right\}$	$\frac{L^2}{2EI_y}$	$-\frac{C_n L^2}{2EI_y}$		-L	1			$\Phi_{c\alpha}\left(1 - \frac{\omega_1}{\omega}\right) + \Phi_{a\alpha}\frac{\omega_1}{\omega}$				
						1						
						-L	1					
								1				
$d\left\{\frac{\Phi_{a\alpha} - \Phi_{c\alpha}}{\omega}\right\}$								$\frac{\Phi_{a\alpha} - \Phi_{c\alpha}}{\omega}$	1			
		$-\frac{b_n L}{EI_z}$				$\frac{L^2}{2EI_z}$	$-\frac{L}{EI_z}$			1		
$d\left\{\Phi_{b\alpha}\left(1 - \frac{H_2}{H}\right) + \Phi_{d\alpha}\frac{H_2}{H}\right\}$		$-\frac{b_n L^2}{2EI_z}$				$\frac{L^3}{6EI_z} - \frac{L}{A_y G}$		$\Phi_{b\alpha}\left(1 - \frac{H_2}{H}\right) + \Phi_{d\alpha}\frac{H_2}{H}$		L	1	
												1

FIGURE 5 FRAME RACKING MATRIX

Solving the H_r equation and substituting in the f_i equation yields,

$$M_i f_i \omega^2 + \Delta M_{ij} f_j \omega^2 = Q_i$$

where

$$\Delta M_{ij} = \sum_{r=1}^{6} \frac{\sum_{t=1}^{6} M_i M_j e_i^{(r)} e_j^{(r)}}{M_r\left(\frac{\omega_r^2}{\omega^2} - 1\right)}$$

The general force equation derived in detail in Appendix A, is expanded to the matrix representation for the coupled engine suspension shown on page 79.

<u>Uncoupled Sprung Mass Matrix</u> - To provide input generality, the analysis includes an uncoupled sprung mass matrix which is derived in Appendix A. Inasmuch as the assumed modes are uncoupled, the simplified system consists of a suspended mass mounted on six simple springs which act in the same directions as the general displacements, but are displaced from the beam station by a, b, and c, longitudinal, lateral and vertical displacements, respectively.

Using the amplification factor μ and the uncoupled frequency in each of the fuselage directions, the force expressions are:

$$F_{x\,n+1} = F_{xn} + m\mu_x \omega^2 (x + c\beta - b\gamma)$$
$$F_{y\,n+1} = F_{yn} + m\mu_y \omega^2 (y - c\alpha + a\gamma)$$
$$F_{z\,n+1} = F_{zn} + m\mu_z \omega^2 (z + b\alpha - a\beta)$$

$$M_{\alpha\,n+1} = M_{\alpha n} - m\mu_y \omega^2 (y - c\alpha + a\gamma)c + m\mu_z \omega^2 (z + b\alpha - a\beta)b + I_\alpha \mu_\alpha \omega^2 \alpha$$
$$M_{\beta\,n+1} = M_{\beta n} + m\mu_x \omega^2 (x + c\beta - b\gamma)c + m\mu_z \omega^2 (z + b\alpha - a\beta)a + I_\beta \mu_\beta \omega^2 \beta$$
$$M_{\gamma\,n+1} = M_{\gamma n} - m\mu_x \omega^2 (x + c\beta - b\gamma)b + m\mu_y \omega^2 (y - c\alpha + a\gamma)a + I_\gamma \mu_\gamma \omega^2 \gamma$$

These force expressions are shown in matrix form as the uncoupled sprung mass matrix on page 72.

Mass Matrix - Each concentrated mass rigidly attached to the fuselage structure is included in the analytical model by a mass matrix. The mass, with its associated inertial properties I_α, I_β, and I_γ, located at a, b, and c, longitudinal, lateral and vertical distances is accelerated by harmonic oscillation and produces inertia loads. As derived in Appendix A, the following expressions show the inertia load balance at the mass station.

$$F_{x\,n+1} = F_{xn} + m\omega^2 (x_n + c\beta_n - a\gamma_n)$$
$$F_{y\,n+1} = F_{yn} + m\omega^2 (y_n - c\alpha_n + b\gamma_n)$$
$$F_{z\,n+1} = F_{zn} + m\omega^2 (z_n + b\alpha_n - a\beta_n)$$
$$M_{\alpha\,n+1} = M_{\alpha n} - m\omega^2 (y_n - c\alpha_n + a\gamma_n)c + m\omega^2 (z_n + b\alpha_n - a\beta_n)b + I_\alpha \omega^2 \alpha_n$$
$$M_{\beta\,n+1} = M_{\beta n} + m\omega^2 (x_n + c\beta_n - b\gamma_n)c - m\omega^2 (z_n + b\alpha_n - a\beta_n)a + I_\beta \omega^2 \beta_n$$
$$M_{\gamma\,n+1} = M_{\gamma n} - m\omega^2 (x_n + c\beta_n - b\gamma_n)b + m\omega^2 (y_n - c\alpha_n + a\beta_n)a + I_\gamma \omega^2 \gamma_n$$

These fuselage load equations, together with the unchanged fuselage deflections at the station, are expressed in matrix form to produce the mass matrix shown on page 61.

Ground Spring Matrix - External spring restraints such as used in the ground shake test for suspension of the aircraft from the roof trusses of a hangar building are simulated in an analytical model by the inclusion of a ground spring matrix at each support point. If a beam station is restrained by springs, additional loads are induced on the structure in proportion to the motion in the direction of each spring. In matrix form the force expression shown in Appendix A, combined with the constant fuselage directions, results in the ground spring matrix illustrated on page 63.

Concentrated Spring Matrix - Concentrated springs between adjacent beam sections are necessary in the analytical representation for simulating localized flexibility of the structure, such as the attachment between the rotor transmission and the fuselage structure. Since no inertia loads are involved, the only changes across the joint are deflections resulting from the action of the loads on the spring. Therefore, the loads can be equated to the spring rate multiplied by the deflection change as shown below.

$$F_{xn} = +K_x (x_{n+1} - x_n), \qquad x_{n+1} = x_n + \frac{F_{xn}}{K_x}$$
$$F_{yn} = +K_y (y_{n+1} - y_n), \qquad y_{n+1} = y_n + \frac{F_{yn}}{K_y}$$

$$F_{zn} = +K_z(Z_{n+1} - Z_n), \quad Z_{n+1} = Z_n + F_{zn}/K_z$$
$$M_{\alpha n} = +K_\alpha(\alpha_{n+1} - \alpha_n), \quad \alpha_{n+1} = \alpha_n + M_{\alpha n}/K_\alpha$$
$$M_{\beta n} = +K_\beta(\beta_{n+1} - \beta_n), \quad \beta_{n+1} = \beta_n + M_{\beta n}/K_\beta$$
$$M_{\gamma n} = +K_\gamma(\gamma_{n+1} - \gamma_n), \quad \gamma_{n+1} = \gamma_n + M_{\gamma n}/K_\gamma$$

The concentrated spring matrix on page 65 is obtained using these displacement expressions together with the condition of no load change across the joint.

<u>Vertical Bend Matrix</u> - A general matrix program for elastic structures must permit a change in direction of the elastic axis such as used for a "U" beam representation of the H-21 fuselage. In progressing from station n to n+1 the loads and deflections are oriented from the original position to a direction corresponding to the new elastic axis location. The general procedure is illustrated below for the longitudinal Fx and vertical Fz forces.

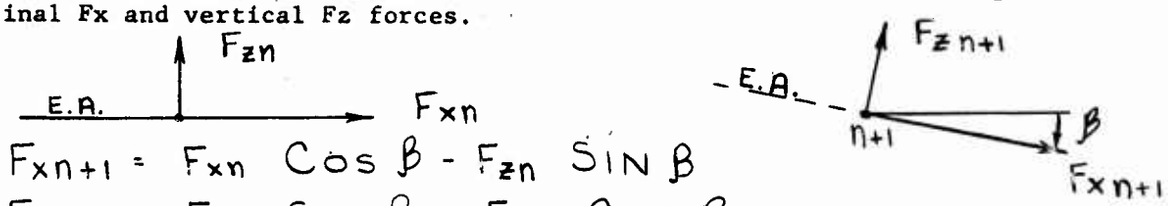

$$F_{xn+1} = F_{xn}\cos\beta - F_{zn}\sin\beta$$
$$F_{zn+1} = F_{xn}\sin\beta + F_{zn}\cos\beta$$

Using the same procedure for the additional loads and deflections and considering only rotation in the vertical plane, the vertical bend matrix on page 69 is obtained.

<u>Shift Matrix</u> - Inclusion of the engine suspension in the matrix program requires a transformation of loads and deflections from station 521, the point of fuselage attachment, to the engine C.G. at which the engine natural modes are defined. Considering a station (n+1) located a, longitudinally, b, laterally and c, vertically from the original station, the transformation equations shown below define the loads and deflections at the new position.

$$F_{xn+1} = F_{xn} \quad \text{——} \quad \alpha_{n+1} = \alpha_n$$
$$F_{yn+1} = F_{yn} \quad \text{——} \quad \beta_{n+1} = \beta_n$$
$$F_{zn+1} = F_{zn} \quad \text{——} \quad \gamma_{n+1} = \gamma_n$$
$$M_{\alpha n+1} = M_{\alpha n} - b_o F_{zn} + C_o F_{yn}, \quad X_{n+1} = X_n - b_o\gamma_n + C_o\beta_n$$
$$M_{\beta n+1} = M_{\beta n} - C_o F_{xn} + a_o F_{zn}, \quad y_{n+1} = y_n - C_o\alpha_n + a_o\gamma_n$$
$$M_{\gamma n+1} = M_{\gamma n} + b_o F_{xn} - a_o F_{yn}, \quad Z_{n+1} = Z_n + b_o\alpha_n - a_o\beta_n$$

In matrix form, these expressions are shown as the shift matrix on page 67.

Forced Matrix - In addition to the beam matrices necessary for a natural mode analysis, the forced solution requires one additional matrix which permits a forcing function to be inserted at any position on the structure. Considering that external loads are applied to a beam station n, the loads acting at station n+1 are shown below as derived in Appendix A.

$$F_{x\,n+1} = F_{xn} + \bar{F}_x$$
$$F_{y\,n+1} = F_{yn} + \bar{F}_y$$
$$F_{z\,n+1} = F_{zn} + \bar{F}_z$$
$$M_{x\,n+1} = M_{\alpha n} - c\bar{F}_y + b\bar{F}_z + \bar{M}_\alpha$$
$$M_{\beta\,n+1} = M_{\beta n} + c\bar{F}_x - a\bar{F}_z + \bar{M}_\beta$$
$$M_{\gamma\,n+1} = M_{\gamma n} - b\bar{F}_x + aF_y + \bar{M}_\gamma$$

In the forced frequency solution, the forcing functions are constant loads which are added to the inertia and elastic loads. To add the constant values, the analysis is expanded to a 13 x 13 matrix, and thus, permits the addition of a constant at any beam station. Expressing the forcing function as

$$\bar{F} = F_o + F_1 \cos\psi_n + F_2 \sin\psi_n$$

Where, ψ_n = Harmonic Azimuth

The forced matrix can be written as shown on page 79.

Effective Wing Mass - For extending the coupled matrix program to include the floating fuel wings an additional matrix is required to represent the modes and frequencies.

Fuselage - Wing Station

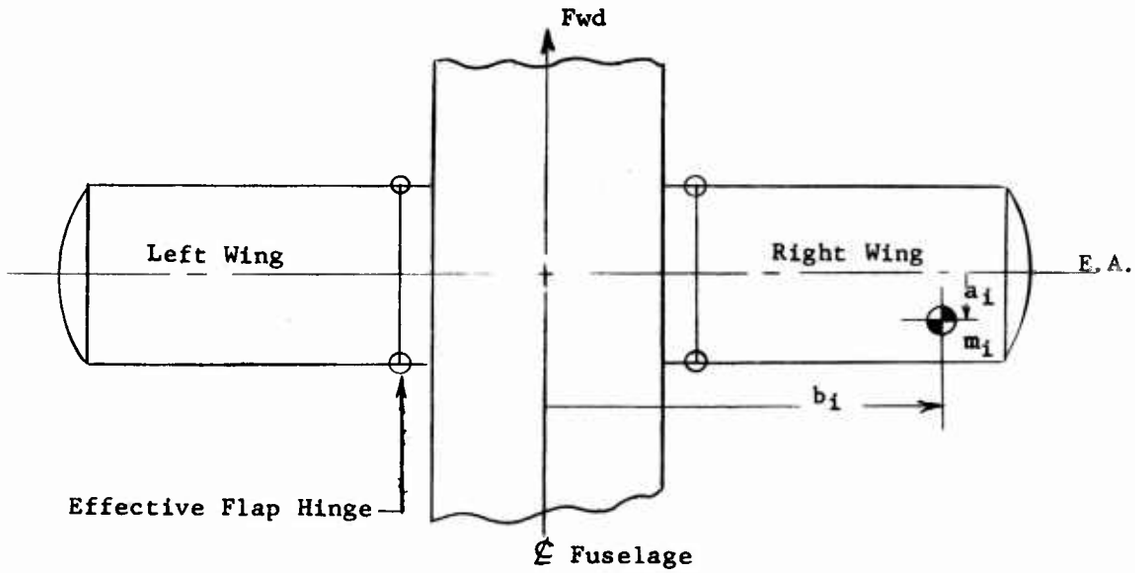

Considering the fuselage-wing schematic shown above, the right wing elemental mass motion as derived in Appendix A is,

$$\bar{X}_i = x - b_i\gamma$$

$$\bar{Y}_i = y + a_i\gamma$$

$$\bar{Z}_i = z = b_i\alpha - a_i\beta + z_i - a_i\beta_i$$

where, Z_i, α_i Wing Displacements

$x, y, z, \alpha, \beta, \gamma$ Fuselage Displacements

Summing along the wing, the total kinetic of the right wing is

$$T = \frac{1}{2}\sum m_i \begin{bmatrix} (\dot{x} - b_i\dot{\gamma})^2 \\ +(\dot{y} + a_i\dot{\gamma}) \\ +(\dot{z} + b_i\dot{\alpha} - a_i\dot{\beta} + z_i - a_i\dot{\beta}_i)^2 \end{bmatrix}$$

$$+\frac{1}{2}\sum\left[I_{\alpha_i}(\dot{\alpha} + \dot{\alpha}_i)^2 + I_{\beta_i}(\dot{\beta} + \dot{\beta}_i)^2 + I_{\gamma_i}(\dot{\gamma} + \dot{\gamma}_i)^2\right]$$

Applying Lagrange's Equations, the right wing equations of motion are:

$$x \qquad \left(\sum_i m_i\right)\ddot{x} + \left(-\sum_i m_i b_i\right)\ddot{\gamma} = F_x$$

$$y \qquad \left(\sum_i m_i\right)\ddot{y} + \left(\sum_i m_i a_i\right)\ddot{\gamma} = F_y$$

$$z \qquad \left(\sum_i m_i\right)\ddot{z} + \left(\sum_i m_i b_i\right)\ddot{\alpha} + \left(-\sum_i m_i a_i\right)\ddot{\beta} + \left[\sum_i m_i \left(z_i^{(s)} - a_i \beta_i^{(s)}\right)\right]\ddot{H}_s = F_z$$

$$\alpha \qquad \left[\sum_i \left(m_i b_i^2 + I_{\alpha i}\right)\right]\ddot{\alpha} + \left(\sum_i m_i b_i\right)\ddot{z} + \left(-\sum_i m_i a_i b_i\right)\ddot{\beta} + \left[\sum_i m_i b_i \left(z_i^{(s)} - a_i \beta_i^{(s)}\right) + \sum_i I_{\alpha i}\, \alpha_i^{(s)}\right]\ddot{H}_s = M_\alpha$$

$$\beta \qquad \left[\sum_i \left(m_i a_i^2 + I_{\beta i}\right)\right]\ddot{\beta} + \left(-\sum_i m_i a_i\right)\ddot{z} + \left(-\sum_i m_i a_i b_i\right)\ddot{\alpha} + \left[-\sum_i m_i a_i \left(z_i^{(s)} - a_i \beta_i^{(s)}\right) + \sum_i I_{\beta i}\, \beta_i^{(s)}\right]\ddot{H}_s = M_\beta$$

$$\gamma \qquad \left[\sum_i \left(m_i a_i^2 + m_i b_i^2 + I_{\gamma i}\right)\right]\ddot{\gamma} + \left(-\sum_i m_i b_i\right)\ddot{x} + \left(\sum_i m_i a_i\right)\ddot{y} = M_\gamma$$

$$H_s \qquad \left[\sum_i m_i \left(z_i^{(s)} - a_i \beta_i^{(s)}\right)^2 + I_{\alpha i}\, \alpha_i^{(s)2} + I_{\beta i}\, \beta_i^{(s)2}\right]\ddot{H}_s + K_s H_s$$
$$\left[\sum_i m_i \left(z_i^{(s)} - a_i \beta_i^{(s)}\right)\right]\ddot{z} + \left[\sum_i m_i b_i \left(z_i^{(s)} - a_i \beta_i^{(s)}\right) + \sum_i I_{\alpha i}\, \alpha_i^{(s)}\right]\ddot{\alpha}$$
$$+ \left[-\sum_i m_i a_i \left(z_i^{(s)} - a_i \beta_i^{(s)}\right) + \sum_i I_\beta\, \beta_i^{(s)}\right]\ddot{\beta} = 0$$

Assuming harmonic motion and solving for H_s

$$H_s = \frac{\left(\sigma_{zs} z + \sigma_{\alpha s} \alpha + \sigma_{\beta s} \beta\right)\omega^2}{\omega^2 I_s - \omega_s^2 I_s}$$

where,

$$\sigma_{\beta s} = -\sum_i m_i a_i \left(z_i^{(s)} - a_i \beta_i^{(s)} \right) + \sum_i I_{\beta i} \beta_i^{(s)}$$

$$\sigma_{\alpha s} = \sum_i m_i b_i \left(z_i^{(s)} - a_i \beta_i^{(s)} \right) + \sum_i I_{\alpha i} \alpha_i^{(s)}$$

$$I_s = \sum_i m_i \left(z_i^{(s)} - a_i \beta_i^{(s)} \right)^2 + \sum_i I_{\beta i} \beta_i^{(s)2} + \sum_i I_{\alpha i} \alpha_i^{(s)2}$$

$$\sigma_{zs} = \sum_i m_i \left(z_i^{(s)} - a_i \beta_i^{(s)} \right)$$

Substituting H_s in the equations of fuselage motion the right wing inertial loads can be expressed in matrix form as shown on page 92.

In a similar manner, the left wing inertial loads are obtained and added to the right wing resulting in the expressions shown on page 93. Expanding to the general matrix form, the effective wing matrix is illustrated on page 94.

SECTION III

WING-FUSELAGE FORCED RESPONSE

A. GENERAL

Forced response of the H-21 helicopter equipped with floating fuel wings is calculated using measured hub load data from Reference 7. These loads were measured on an H-21 helicopter and are applied to the analytical representation of the H-21 fuselage-wing combination so as to provide reasonable prediction of the forced response. Inclusion of the floating fuel wings, unlike the configuration used in the load measurement program introduces some error in regard to applied loads. However, this effect becomes significant only if a resonant condition exists with the forcing frequency, which could be evident in the undamped response.

As in the three-bladed H-21 helicopter without fuel wings, third harmonic vibration levels are usually a dominant portion of the vibration environment; therefore, calculations are performed using only the fixed system third harmonic loads. Hub load data in Reference 7 was determined in two forms; fixed system shaft loads which include rotor inertia and damping effects, and fixed system aerodynamic loads which are the shaft loads adjusted for inertia loads resulting from fuselage induced rotor hub-motion. In this analysis, the rotor shaft loads are used, thereby eliminating the complexity of the rotor system dynamics in the analytical representation.

Forced response of the H-21 fuselage-wing combination is investigated at maximum cruise speed of 90 knots for three rotor speeds within the operating rotor speed band. The analysis considers third harmonic loads corresponding to rotor speeds of 250, 258 and 268 RPM. In addition, the two extremes of the wing are considered, which are 0% fuel and 100% fuel corresponding to approximate weights of 1000 lbs. per wing and 8000 lbs. per wing respectively. Considering the extreme weight limits of the wing, the forced modes provide reasonable approximations of the third harmonic vibration environment which the H-21 helicopter-wing combination would experience under normal flight conditions.

B. ANALYTICAL MODEL

Fuselage - Previous theoretical studies performed under Reference 8, 9, and 10 showed the requirement for and subsequent development of an analytical representation of the H-21 fuselage which included vertical-lateral coupling. Figure 6 illustrates the final representation of the H-21 fuselage. In the forward fuselage, each elastic section is typified by a frame racking matrix which in addition to normal beam bending includes frame distortion. Figure 7 presents the complex elastic properties for each forward fuselage section. The adequacy of the forward fuselage representation is demonstrated by Figure 8 which compared the calculated forward fuselage deflection under a 3600 lb. vertical load to the deflection data obtained in the fuselage load test.

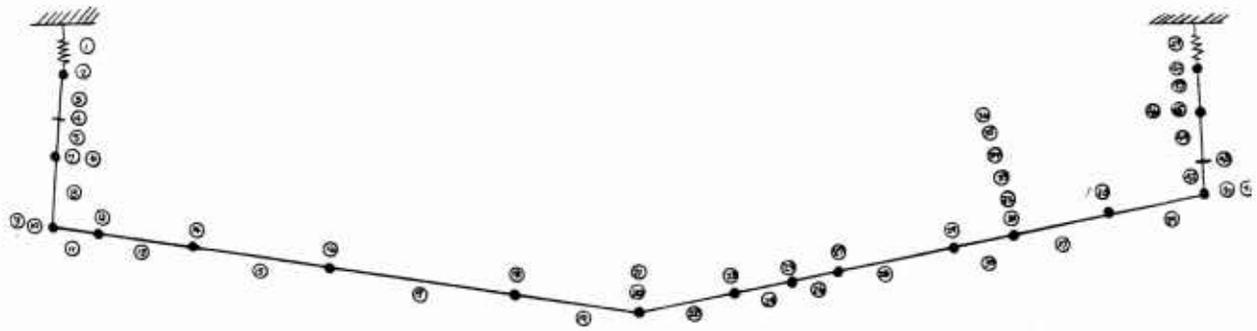

Item	Description	m	I_α	I_β	I_γ	a	b	c	L	A_x	A_y	A_z	$G J_x$	$E I_y$	$E I_z$	K_x	K_y	K_z	K_α	K_β	K_γ
		lb sec²/in	lb in sec²	lb in sec²	lb in sec²	in	in	in	in	in²	in²	in²	10^8 lb in²	10^8 lb in²	10^8 lb/in²	lb/in	10^3 lb/in	lb/in	lb/in	10^7 in lb rad	10^7 in lb/rad
1	Fwd. Rotor Bungee															154	.053	.053	0	0	0
2	Fwd. Rotor Mass	1.9559	0	0	0	5	0	0													
3	Rotor Shaft								19.7	14.3	13.8	13.8	2.85	3.96	3.96						
4	Rotor Shaft Spring																			2.5	2.5
5	Transmission Elastic Bay								15.6												
6	Transmission Mass	1.0549	56	61	61	-3	0	0													
7	Transmission Spring																350	23		4.0	7.0
8	Fwd. Pylon Elastic Bay								30.5												
9	Bend, Fwd. Pylon																				
10	Mass Station 100	4.5516	1962.1	3465.4	2259.4	-12.04	0	-8.23													
11	Frame Racking Bay								23	4.86	1.55	.91		407	1500						
12	Mass Station 119.5	0.80	0	0	0	18	0	-1.0													
13	Frame Racking Bay								40	4.86	1.55	.91		407	1500						
14	Mass Station 159.5	1.2674	181.99	335.22	318.87	3.46	11.05	-19.58													
15	Frame Racking Bay								60	4.63	1.21	2.43		657	669						
16	Mass Station 219.5	.8759	208.9	262.3	425.95	-9.46	6.28	-14.65													
17	Frame Racking Bay								80	5.29	2.15	1.48		617	755						
18	Mass Station 299-5	3.8563	605.3	1492.9	1443.9	18.53	8.11	-10.													
19	Frame Racking Bay								54.5	5.62	1.98	2.13		796	755						
20	Mass at Bend	1.047	89.49	96.30	6.77	-8.30	0	-12.19													
21	Fuselage Bend																				
22	Elastic Bay								38.5	5.71	2.39	3.13	552	670	514						
23	Mass Station 395	7.408	7044.2	3487.3	440.66	-5.24	0	-21.8													
24	Elastic Bay								31.0	5.76	2.39	3.13	552	670	514						
25	Mass Station 423	.599	0	0	0	-4.5	0	-8.0													
26	Elastic Bay								21.0	5.81	2.39	3.13	552	670	514						
27	Mass Station 445	.523	0	0	0	13.5	0	-12.0													
28	Elastic Bay								49.0	5.81	1.69	2.64	96	638	1000						
29	Mass Station 494	.597	0	0	0	6.5	0	-5.0													
30	Elastic Bay								26.0	5.90	1.69	2.64	96	638	1000						
31	Shift to Engine Axis																				
32	Rot. to Engine Axis																				
33	Engine Mass	4.76	1009	995	959																
34	Rot. from Engine Axis																				
35	Shift from Engine Axis																				
36	Mass Station 521	.6405	40.27	1.71	39.25	19.42	-6.20	-10.84													
37	Elastic Bay								40.5	5.83	2.19	1.52	64	740	204						
38	Mass Station 562	.415	0	0	0	24	0	5.5													
39	Elastic Bay								51.5	4.57	1.23	1.88	36	378	86						
40	Mass Station 604	1.0539	1461.9	203.5	1567.2	10.03	0	2.08													
41	Bend, Aft Pylon																				
42	Aft Pylon Elastic Bay								14.0												
43	Transmission Spring																130	139		3.8	3.0
44	Transmission Elastic Bay	1.015	103	76	76	9.5	0	1.5													
45	Transmission Mass								22.4												
46	Rotor Shaft Spring																			2.5	2.5
47	Rotor Shaft								19.7	14.3	13.8	13.8	2.85	3.95	3.95						
48	Aft Rotor Mass	1.705	0	0	0	-6.0	0	0													
49	Aft Rotor Bungee															154	.053	.053			

FIGURE 6 H-21 VERTICAL-LATERAL MATRIX REPRESENTATION

SECTION III

WING-FUSELAGE FORCED RESPONSE

A. GENERAL

Forced response of the H-21 helicopter equipped with floating fuel wings is calculated using measured hub load data from Reference 7. These loads were measured on an H-21 helicopter and are applied to the analytical representation of the H-21 fuselage-wing combination so as to provide reasonable prediction of the forced response. Inclusion of the floating fuel wings, unlike the configuration used in the load measurement program introduces some error in regard to applied loads. However, this effect becomes significant only if a resonant condition exists with the forcing frequency, which could be evident in the undamped response.

As in the three-bladed H-21 helicopter without fuel wings, third harmonic vibration levels are usually a dominant portion of the vibration environment; therefore, calculations are performed using only the fixed system third harmonic loads. Hub load data in Reference 7 was determined in two forms; fixed system shaft loads which include rotor inertia and damping effects, and fixed system aerodynamic loads which are the shaft loads adjusted for inertia loads resulting from fuselage induced rotor hub-motion. In this analysis, the rotor shaft loads are used, thereby eliminating the complexity of the rotor system dynamics in the analytical representation.

Forced response of the H-21 fuselage-wing combination is investigated at maximum cruise speed of 90 knots for three rotor speeds within the operating rotor speed band. The analysis considers third harmonic loads corresponding to rotor speeds of 250, 258 and 268 RPM. In addition, the two extremes of the wing are considered, which are 0% fuel and 100% fuel corresponding to approximate weights of 1000 lbs. per wing and 8000 lbs. per wing respectively. Considering the extreme weight limits of the wing, the forced modes provide reasonable approximations of the third harmonic vibration environment which the H-21 helicopter-wing combination would experience under normal flight conditions.

B. ANALYTICAL MODEL

Fuselage - Previous theoretical studies performed under Reference 8, 9, and 10 showed the requirement for and subsequent development of an analytical representation of the H-21 fuselage which included vertical-lateral coupling. Figure 6 illustrates the final representation of the H-21 fuselage. In the forward fuselage, each elastic section is typified by a frame racking matrix which in addition to normal beam bending includes frame distortion. Figure 7 presents the complex elastic properties for each forward fuselage section. The adequacy of the forward fuselage representation is demonstrated by Figure 8 which compared the calculated forward fuselage deflection under a 3600 lb. vertical load to the deflection data obtained in the fuselage load test.

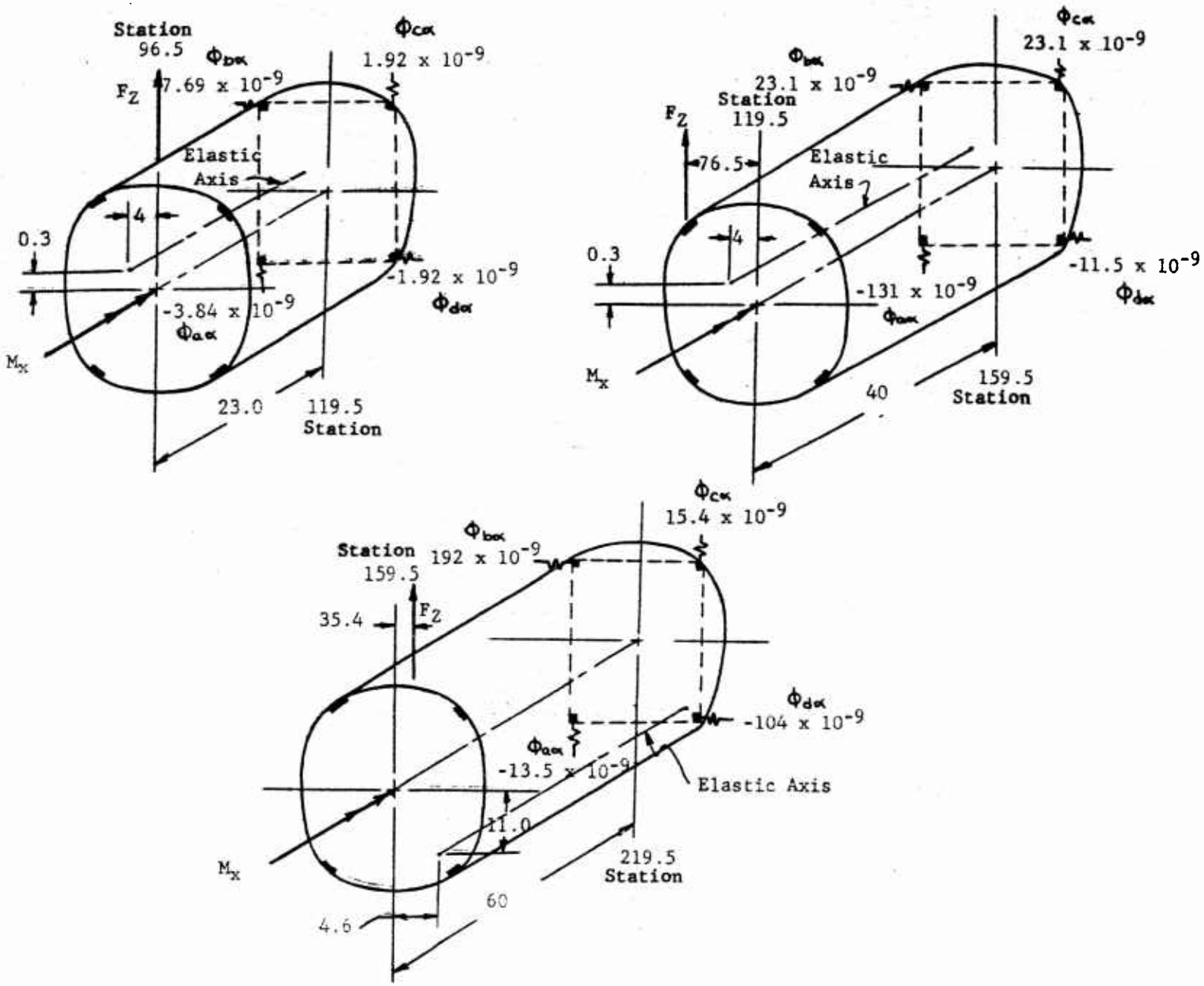

FIGURE 7 H-21 FORWARD FUSELAGE ELASTIC PROPERTIES

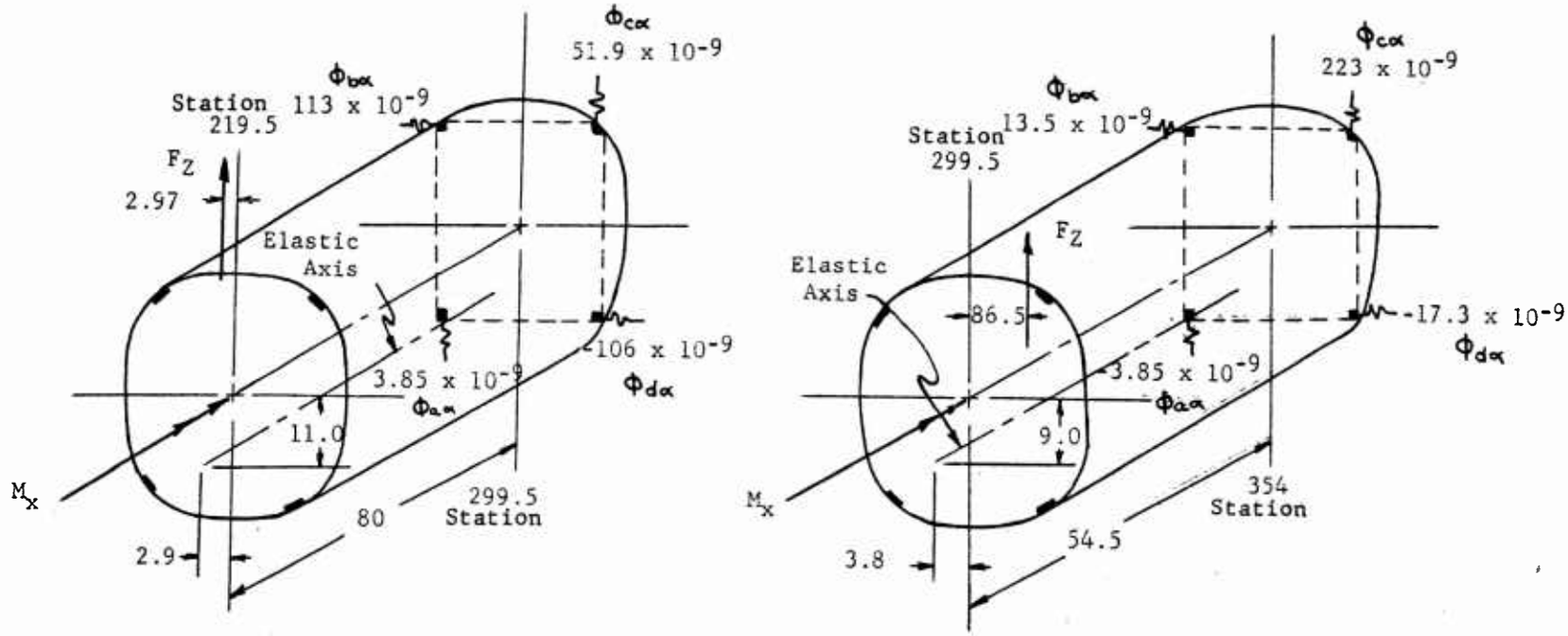

FIGURE 7 (CONT) H-21 FORWARD FUSELAGE ELASTIC PROPERTIES

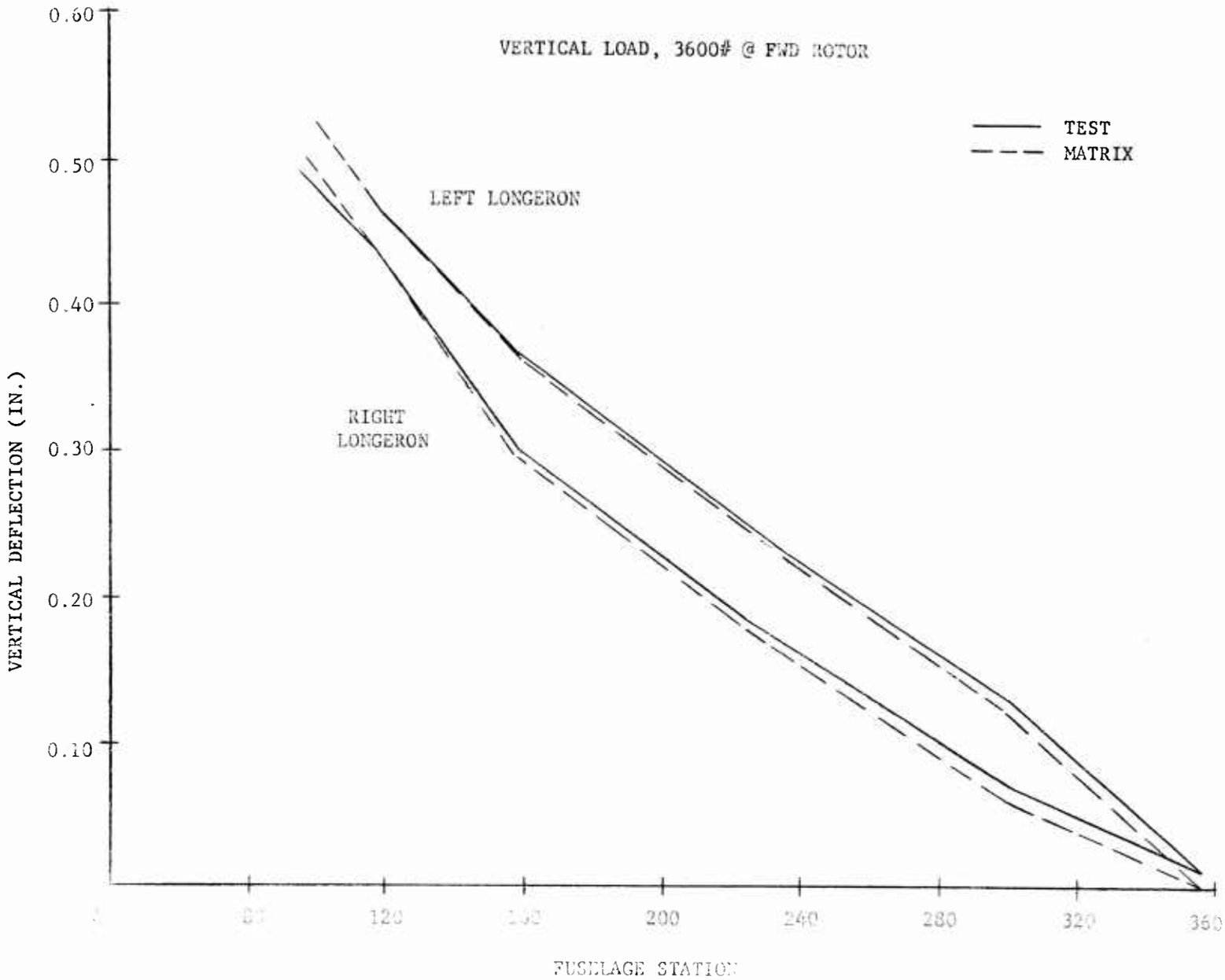

FIGURE 3 H-21 FORWARD FUSELAGE SIMULATED DEFLECTION

Figure 9 shows the elastic sections used for representing the aft fuselage. Weight distribution for the dynamic model of the fuselage is shown in Figure 10, together with the fuselage reference axis.

As a relatively important dynamic element, the fuselage model includes the engine as an elastically supported mass. An engine shake test, reported in Reference 8, was used to obtain the coupled modes and frequencies illustrated as Figure 11, for use in the analytical fuselage representation.

Floating Fuel Wings - Each floating fuel wing is attached to the helicopter through a skewed hinge so as to eliminate the bending moment applied at the fuselage by a conventional wing. The analytical representation of each wing includes rigid body motion to simulate rotation about the hinge and all natural modes up to and including the natural in the vicinity of 3Ω excitation. Using the stiffness and mass properties shown in Figure 12, calculations are performed to obtain the wing natural frequencies and modes. Figure 13 illustrates the wing modes for the 0% fuel configuration similarly, Figure 14 presents the wing modes for the 100% fuel configuration. The illustrated wing modes show only the semi-span shapes, but as a result of the coupled vertical-lateral motions, both symmetrical and anti-symmetrical modes exist at the indicated natural frequencies. Representing each of the uncoupled wing modes as generalized coordinates, the dynamic wing loads are transmitted to the fuselage in the coupled wing-fuselage analysis using the effective wing matrix.

C. FORCED RESPONSE

Forced Mode Solution - Using the analytical representation of the H-21 helicopter equipped with floating fuel wings, the forced responses are obtained from the coupled matrix analysis programmed for the Univac 1103A digital computer. A force matrix at each rotor applies the measured loads, and the matrix array is collapsed using the forcing frequency to apply acceleration to each mass and inertia item, resulting in an applied load and moment distribution. Applying the free-free boundary, the fuselage matrix collapses to a 6 x 6 boundary determinant which is solved for the forward rotor deflection. For each forcing frequency and the corresponding measured loads, the forced response is obtained by a detailed listing of intermediate results of each matrix multiplication starting with the forward rotor boundaries and continuing along the reference axis to the aft rotor.

Forced Mode Calculations - Using the analytical representation of the H-21 equipped with floating fuel wings and the measured third harmonic loads illustrated in Figure 15, matrix calculations are performed, and the results presented in Figures 16 to 18, and 20 to 22, as shown below.

WING FUEL	AIRSPEED, KNOTS	ROTOR SPEED, RPM	FIGURE
0%	90	250	16
0%	90	258	17
0%	90	268	18
100%	90	250	20
100%	90	258	21
100%	90	268	22

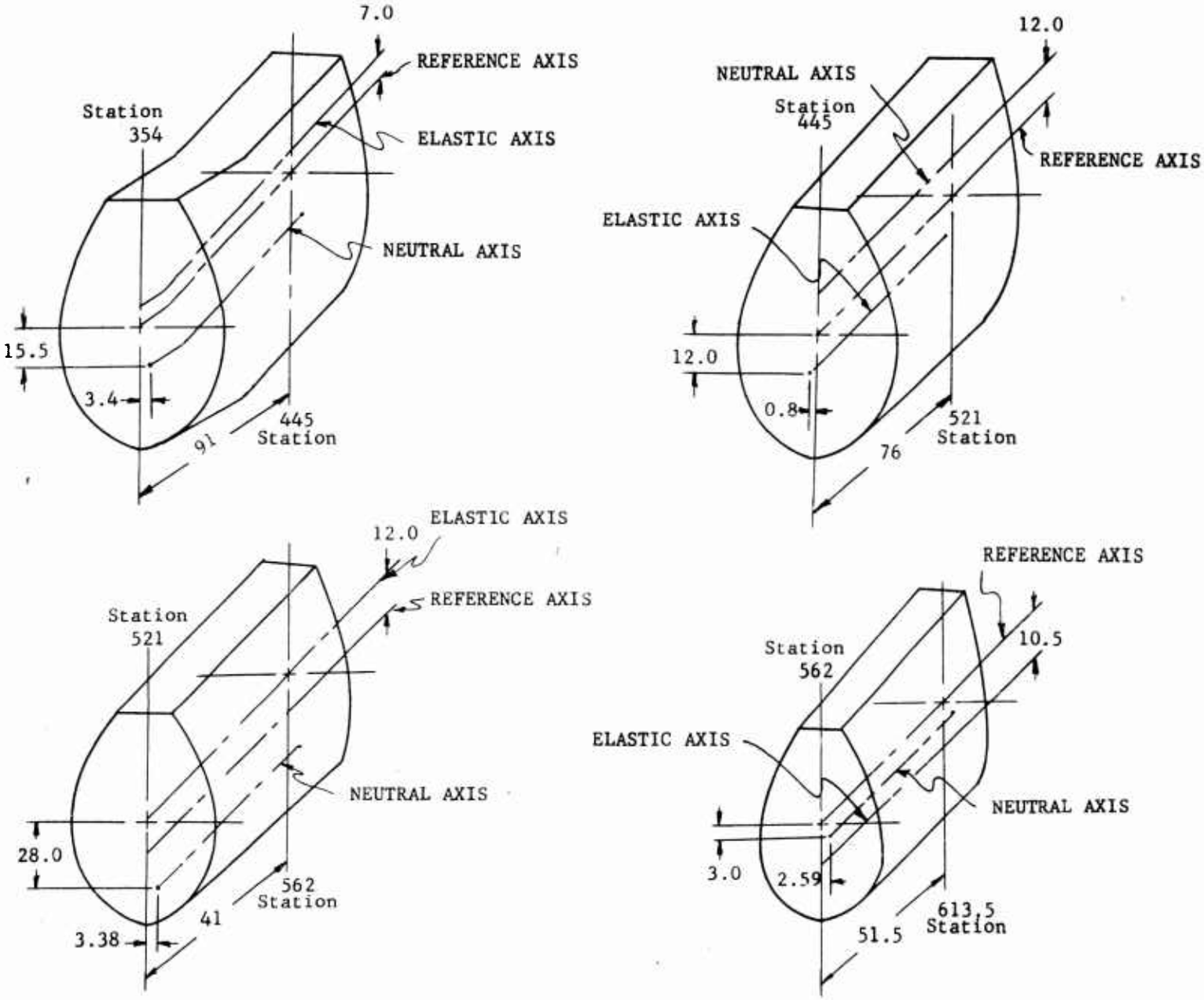

FIGURE 9 H-21 AFT FUSELAGE ELASTIC PROPERTIES

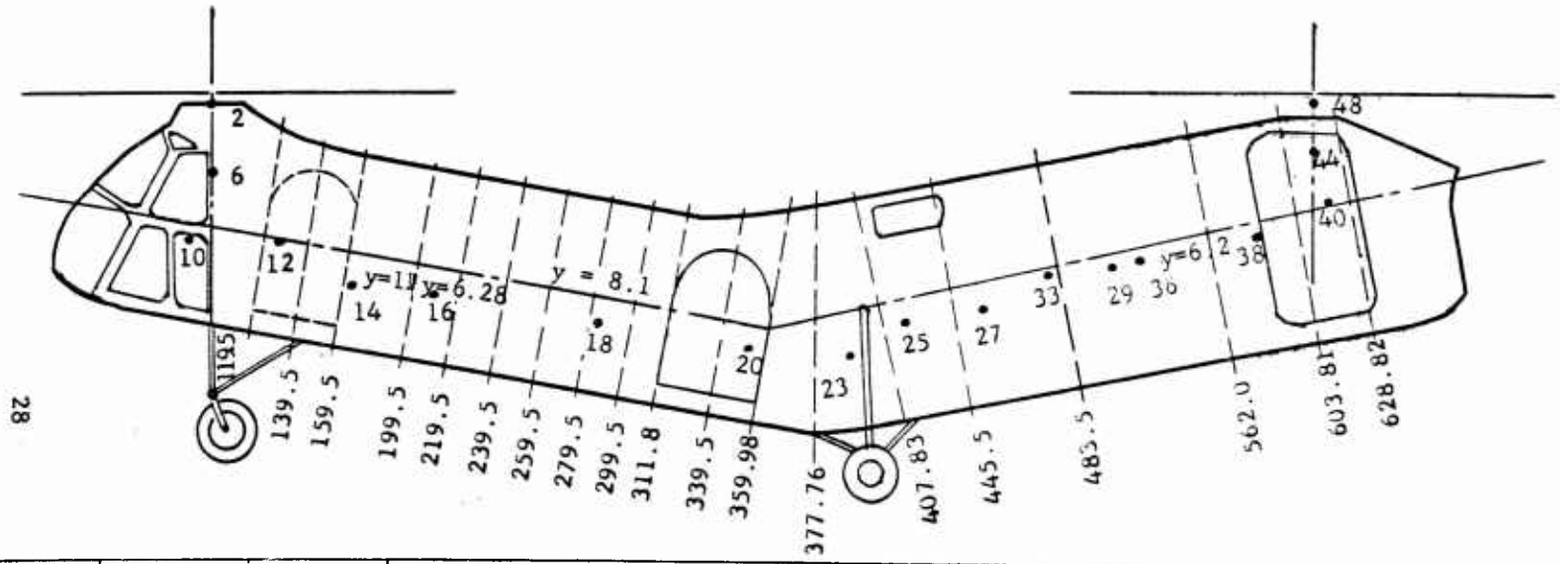

Matrix No.	Mass Lb-Sec^2/in.	Weight Lbs.	Inertia Lb-Sec^2-In. I_α Roll	I_β Pitch	I_γ Yaw	Matrix No.	Mass Lb-Sec^2/In.	Weight Lbs.	Inertia Lb-Sec^2-In. I_α Roll	I_β Pitch	I_γ Yaw
2	1.9513	154				25	.5978	231			
6	1.0533	407	56	61	61	27	.5228	202			
10	2.4793	958	1069.1	1888.3	1231.1	29	5952	230			
12	.6444	249				33	4.7567	1838	1009	995	959
14	1.1077	428	159.6	293.9	279.6	36	.6392	247	40.27	1.71	39.25
16	.7195	278	171.8	215.7	350.3	38	.4141	160			
18	1.4959	578	235.1	580.1	561.6	40	1.0533	407	1461.3	2035.0	1567.2
20	.8903	344	76.2	82.0	5.8	44	1.0145	392	103	76	76
23	6.6253	2560	6305.3	3121.5	3944.5	48	1.7029	658			

FIGURE 10 - H-21 REFERENCE AXIS LOCATION AND WEIGHT DISTRIBUTION

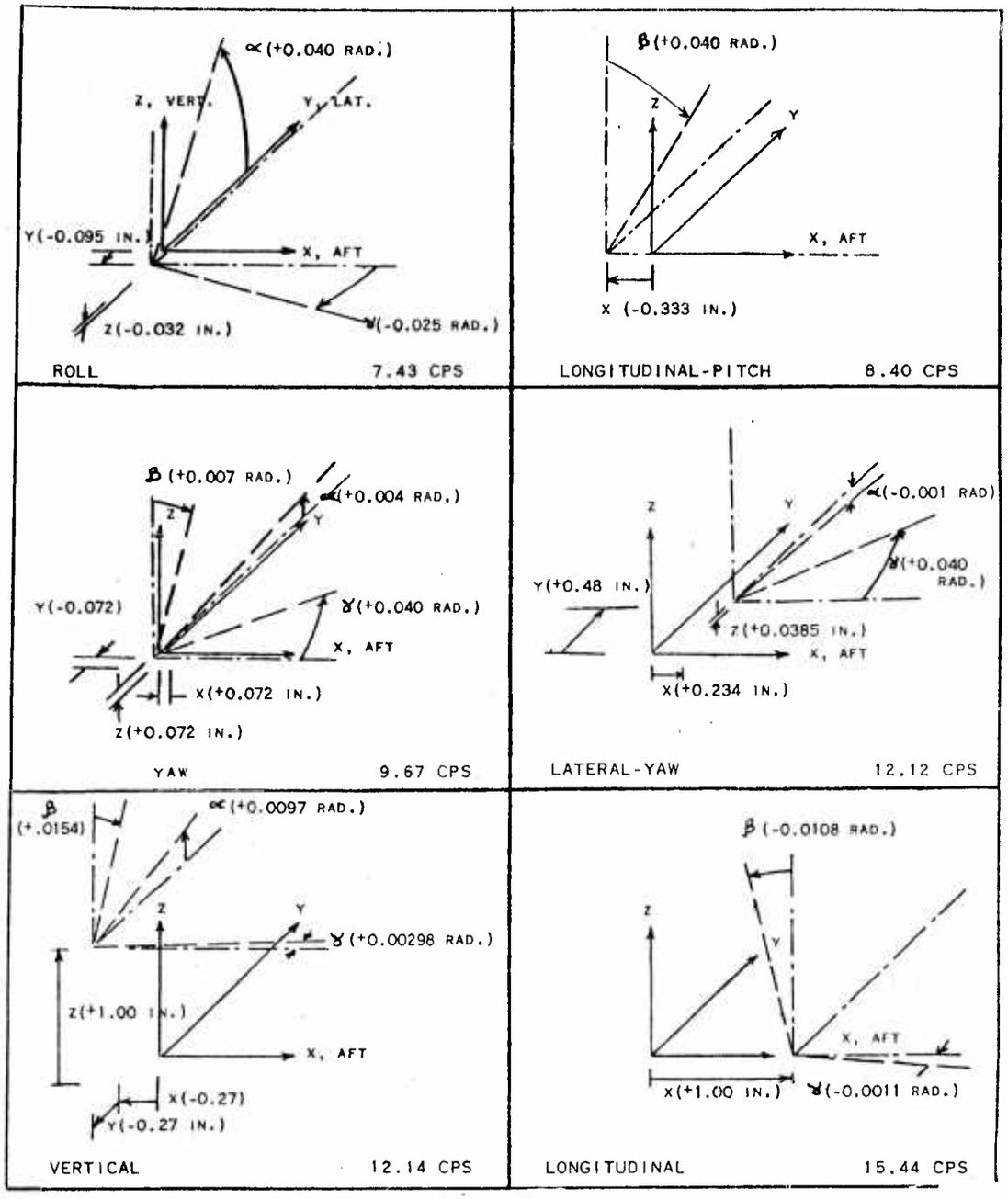

Modes where angles dominate have those angles normalized to 0.04 radians; 0.04 radians = 1" deflection at 25" radius. Where displacements dominate the displacements are normalized to one inch.

Figure 11. Normalized Engine Modes, H-21C-96 Engine Shake Test

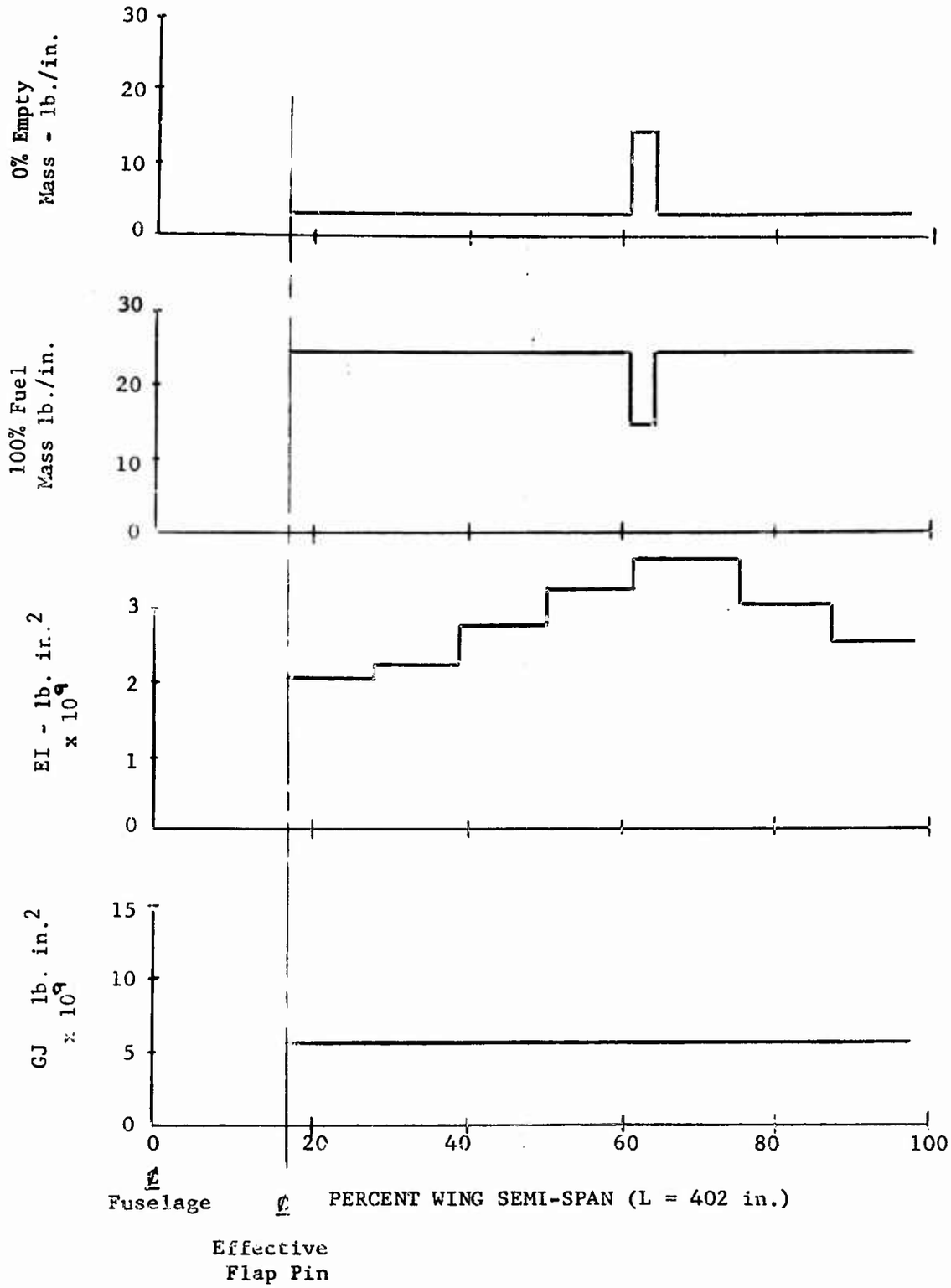

FIGURE 12 WING MASS AND STIFFNESS PROPERTIES

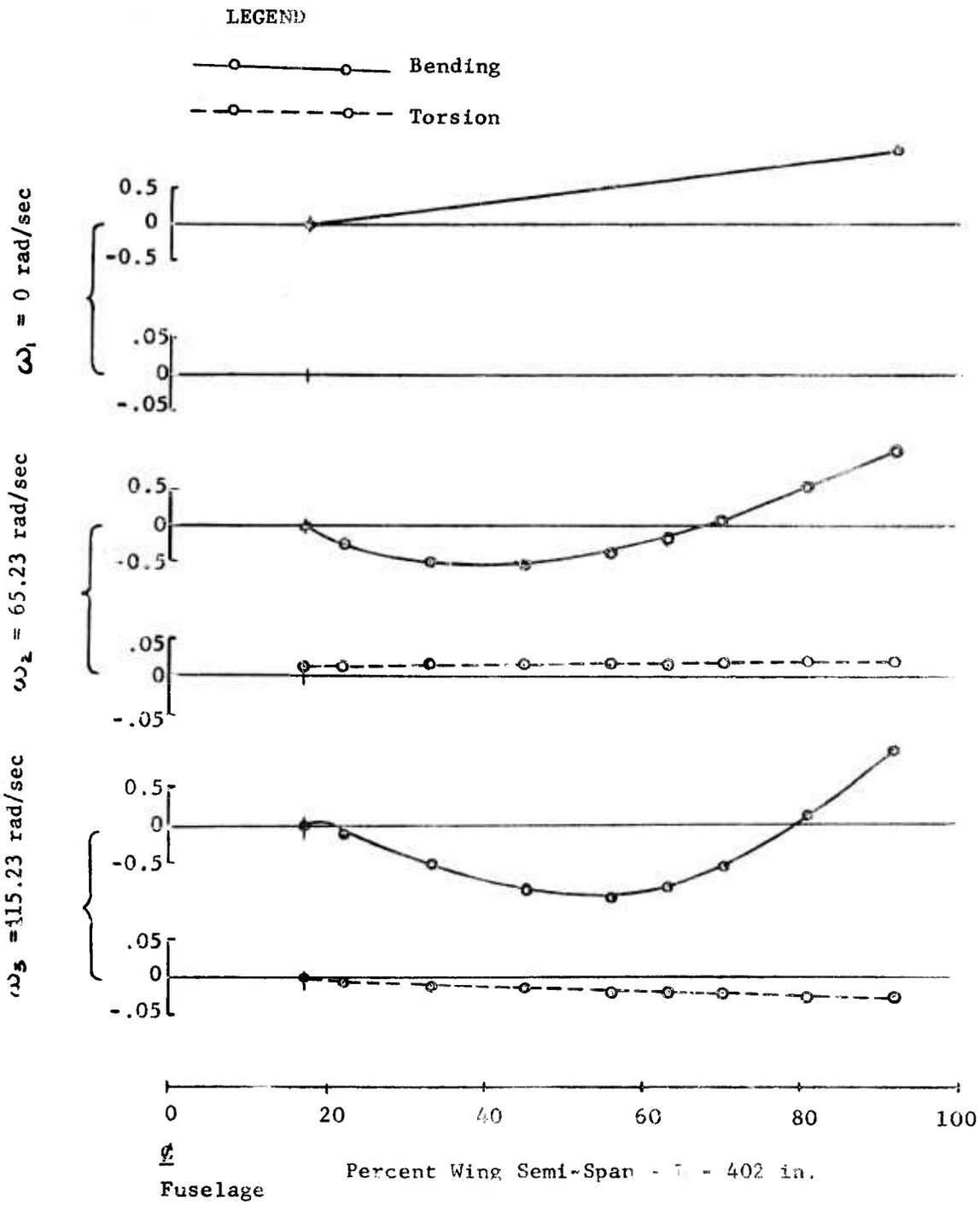

FIGURE 13 WING, FLAP BENDING AND TORSION MODES - 0%

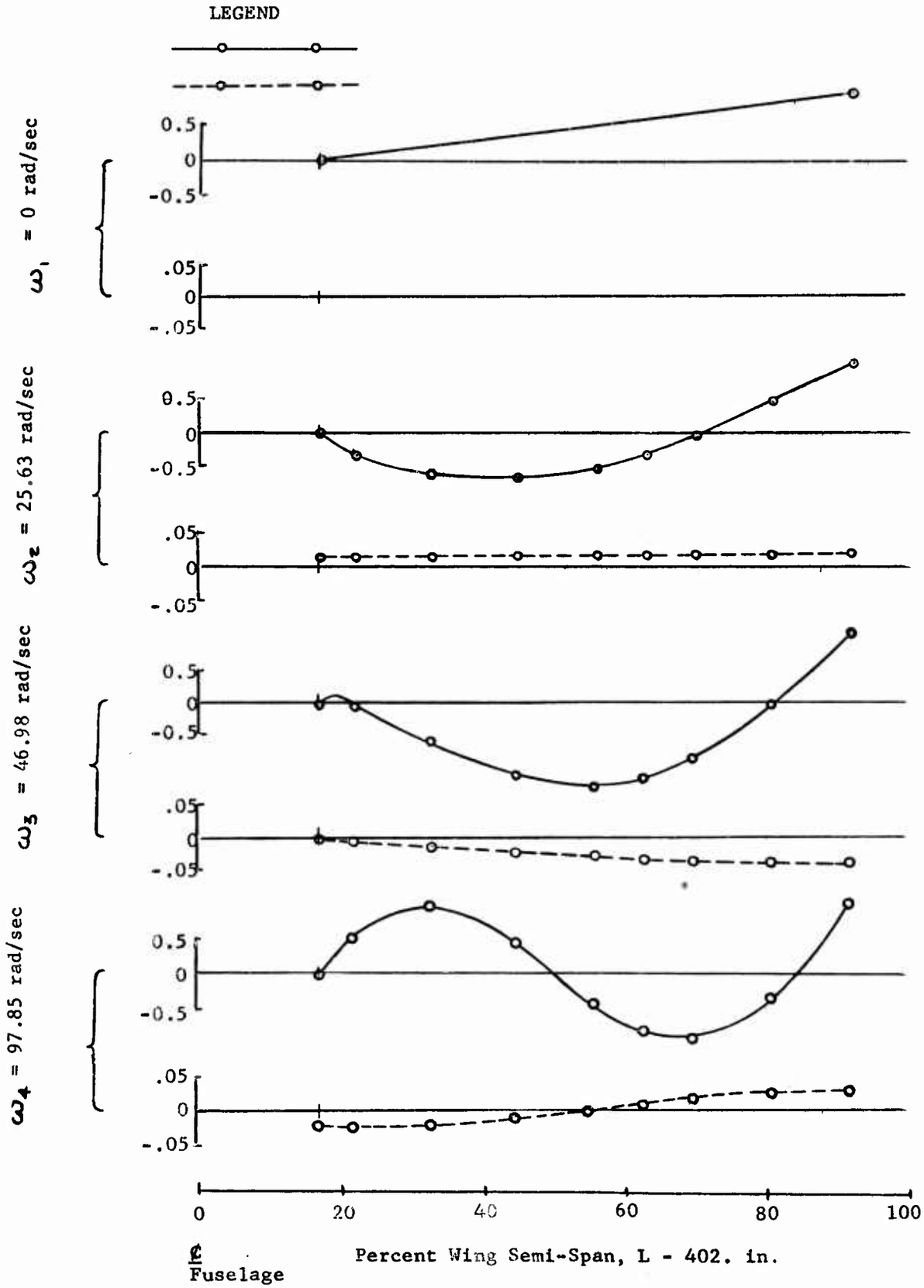

FIGURE 14 WING, FLAP BENDING AND TORSION MODES - 100%

THIRD HARMONIC FIXED SYSTEM SHAFT LOADS

90 KNOTS - RPM SWEEP

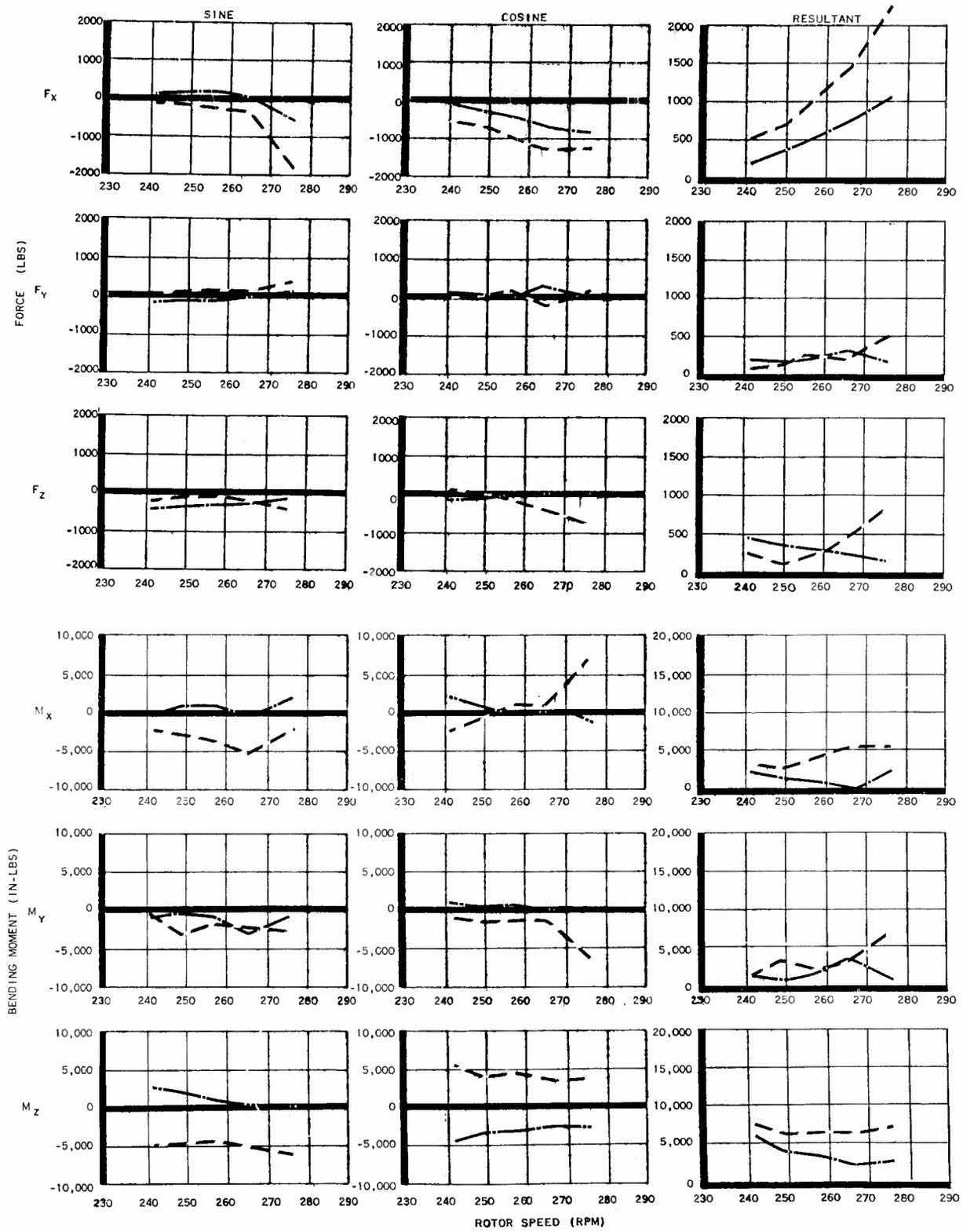

FIGURE 15

Third Harmonic Forced Response - 0% Wing Fuel

For the 0% wing fuel case, time histories of third harmonic forced response are illustrated in Figures 16, 17 and 18 during an RPM sweep at 90 knots. Each figure presents the instantaneous fuselage and engine amplitudes at four discrete time positions during a half cycle of third harmonic oscillation. The harmonic azimuth positions shown are at 0, 45, 90 and 135 degrees. The corresponding azimuth positions between 180 and 360 degrees repeat the original response in the opposite direction.

As shown in the vertical bending plots, the forward and aft pylon longitudinal deflections are normally in-phase, i.e., motions occur simultaneously in the same direction. The longitudinal magnitudes increase with RPM, reaching peaks of 0.08 inches at the forward rotor and 0.12 inches at the aft rotor at 268 RPM. In the vertical direction, the peak response occurs for fuselage station 603 at a rotor speed of 258 RPM with a 180 degree phase shift from the amplitude at 250 RPM and then, decreases to a negligible vertical response at 268 RPM.

Laterally, at 250 RPM, the fuselage response is small. However, when the rotor speed is increased to 258 RPM, the fuselage responds predominantly in rigid yaw which progresses to the first lateral bending mode at 268 RPM. Maximum lateral amplitudes of 0.09 and 0.10 inches occur near Station 100 and at the maximum rotor speed. Generally, the torsional response of the fuselage is small, although the aft fuselage shows some frequency sensitive response that increases with rotor speed.

Also, during the RPM sweep at 90 knots, the engine exhibits significant changes in amplitude. In the lateral direction, the engine response is negligible at 250 RPM, but increases with RPM, generally out-of-phase with the fuselage lateral motion, to a maximum of 0.08 inch at 268 RPM. Yaw motion of the engine shows an apparent phase reversal between 250 and 258 RPM, but relative to the aft fuselage vertical motion the phase is constant. Similarly, the vertical motion is out-of-phase with the fuselage and follows the vertical amplitude trend of the aft fuselage with a peak response of 0.20 inch at 258 RPM. It is of interest to note that at 258 RPM the longitudinal engine motion is in-phase with the pylons, but out-of-phase with the pylons at the higher and lower operating speeds.

The fuselage responses shown are influenced by the natural frequencies of the wing-fuselage combination, illustrated for the fuselage without wings in the matrix residual curve of Figure 19. Inclusion of the 0% fuel wing frequency at 10.39 CPS would influence the residual curve by producing an additional crossing corresponding to the wing mode and shifting the fuselage frequencies to include wing coupling. However, as shown in the mode plots the wing does not significantly restrain the motion of the forward fuselage because of its light weight relative to the fuselage alone. Therefore, it is reasonable to consider that the wing mode does not appreciably influence the fuselage forced response in the 0% fuel configuration.

THIRD HARMONIC FORCED RESPONSE

0% WING FUEL, 90 KNOTS, 250 RPM

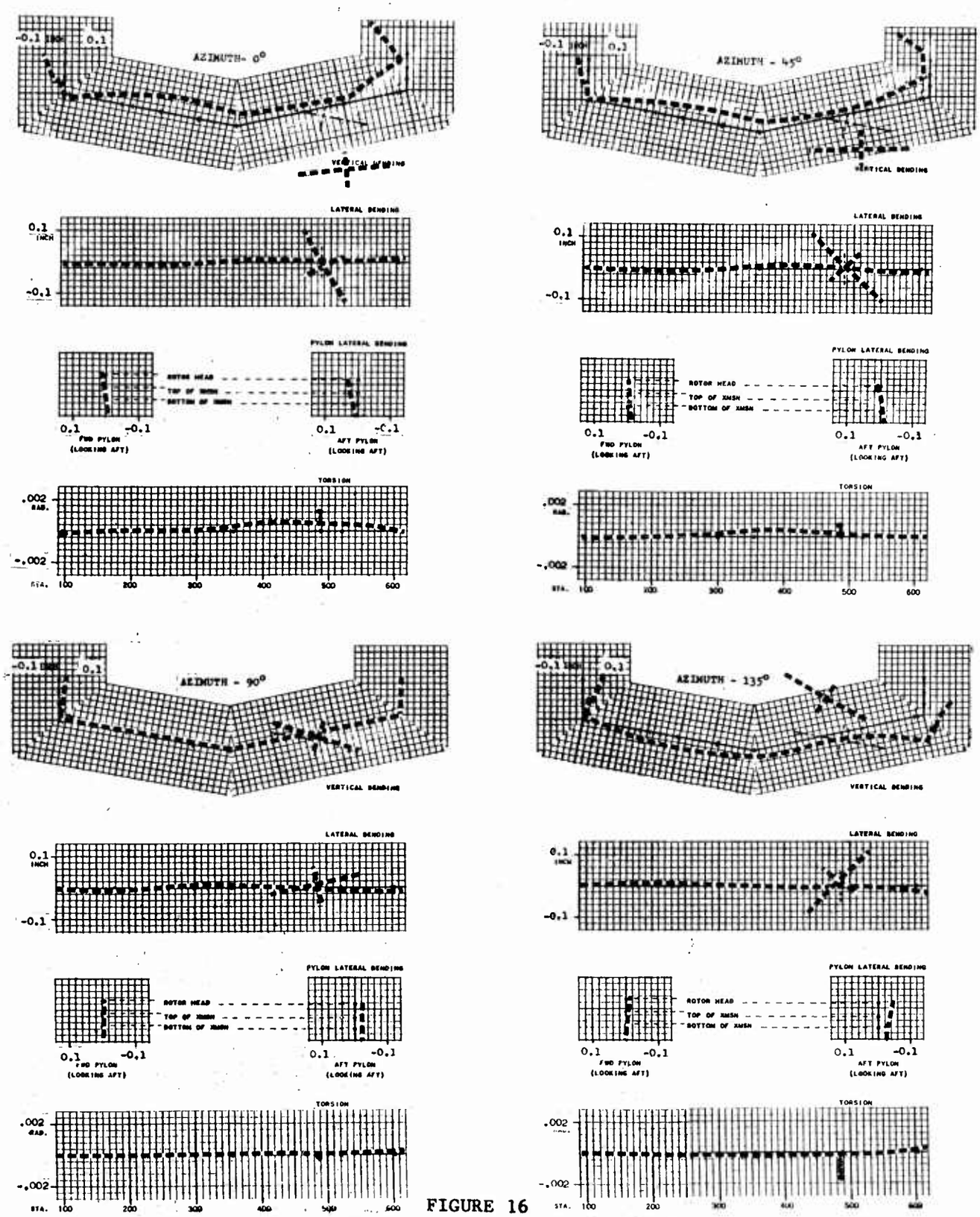

FIGURE 16

THIRD HARMONIC FORCED RESPONSE
0% WING FUEL, 90 KNOTS, 258 RPM

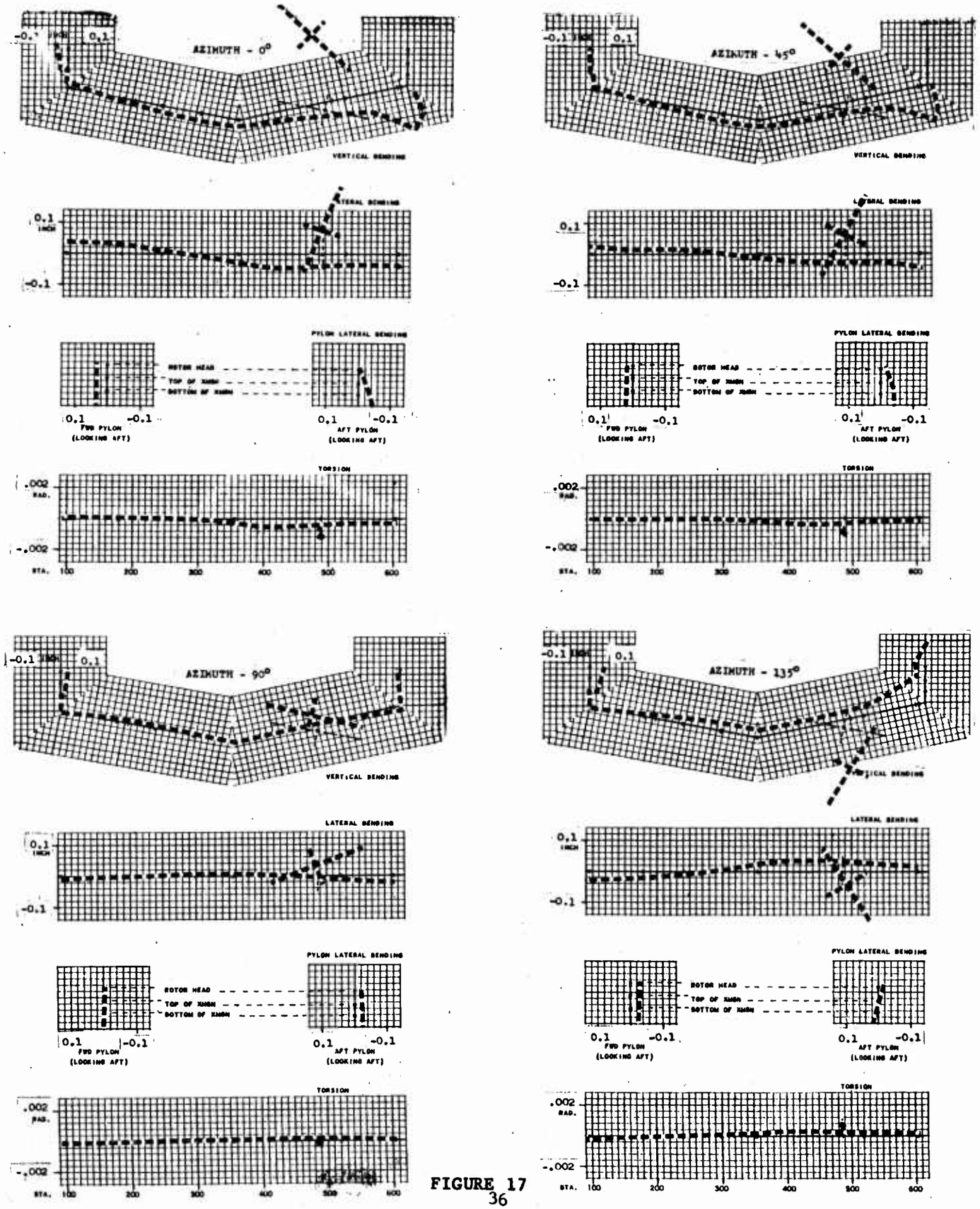

FIGURE 17

THIRD HARMONIC FORCED RESPONSE

0% WING FUEL, 90 KNOTS, 268 RPM

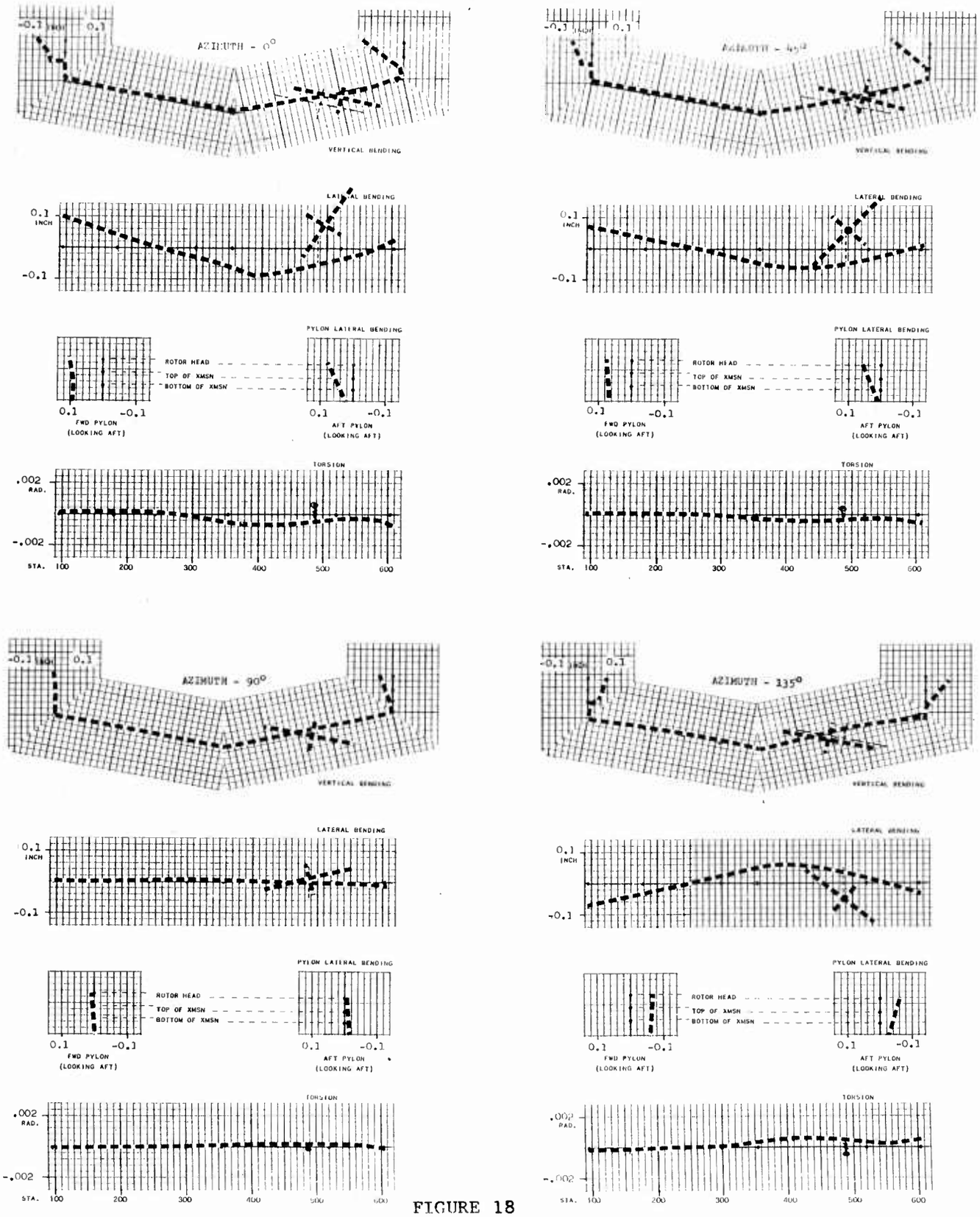

FIGURE 18

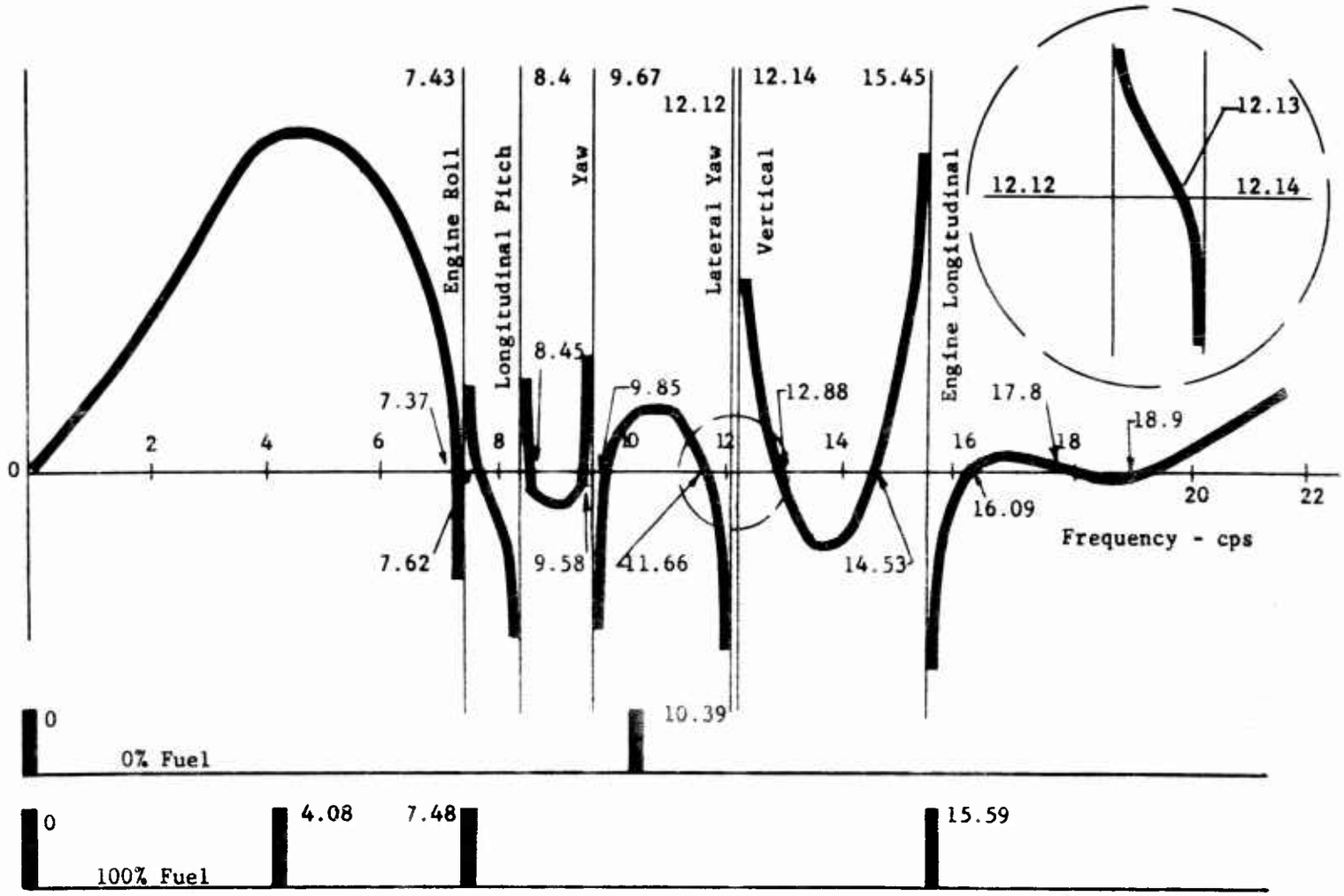

FIGURE 19 MATRIX RESIDUAL PLOT

Third Harmonic Forced Response - 100% Wing Fuel

Figures 20, 21 and 22 illustrate the third harmonic forced response during an RPM sweep at a cruise speed of 90 knots. Presented in the same format as the previous response plots, the instantaneous fuselage and engine amplitudes are shown for harmonic azimuth positions of 0, 45, 90, and 135 degrees.

At 250 RPM in Figure 20, longitudinal pylons in phase response is seen to occur, but the amplitude relative to lateral fuselage motion is much smaller than it was during the 0% fuel condition. Lateral motion is very large, with lateral forward fuselage motions of $\pm$ 0.5 inches at 3Ω, and correspondingly large torsional amplitudes. Note that the scales in Figure 20 differ from the other figures because of the large lateral amplitudes. The fully fueled wing is not easily excited because of its large mass so that the wing point at Station 259 is a node, with the fuselage bending about this point as though it were a pivot magnifying the cockpit floor lateral motion. This large response is indicative of a natural frequency of the coupled fuselage-wing system.

Natural modes of the helicopter without wings are represented by the zero crossings in the Figure 19 residual curve. Introduction of the wing natural modes of Figure 14 as asymptotes would modify the residual plot and produce additional coupled natural frequencies. Inasmuch as the residual curve was calculated for a gross weight of 11,100 lb whereas the helicopter wing system with 100% fuel has a gross weight of 27,100 lb the natural modes shown on the residual curve provide no definite verification of the predicted resonance.

However, the previous matrix calculations without the fuel wings as represented on the residual curve show a lateral fuselage mode at 18.9 CPS with maximum amplitude in the vicinity of the wing attachment. Using the frequency correction as the square root of the gross weights, $\left[\frac{(11,100)}{(27,100)}\right]^{\frac{1}{2}} \times 18.9$, the corresponding natural frequency of the fuselage-wing system is 12.1 CPS. Therefore, it is probable that this natural mode near 3Ω results from the 18.9 CPS lateral fuselage mode

Increasing RPM reduces the lateral response amplitude as shown in the Figure 21 plot at 258 normal RPM. Vertical amplitudes are now of about the same order as the laterals, with rotor pylon peaks near $\pm$ 0.1 inches. The scales in Figure 21 are enlarged back to their previous values, but the plots of course represent smaller amplitudes. The highest RPM considered, 268 RPM in Figure 22 exhibits similar vertical amplitudes, but lateral-torsion amplitudes are further reduced.

100% WING FUEL, 90 KNOTS, 250 RPM

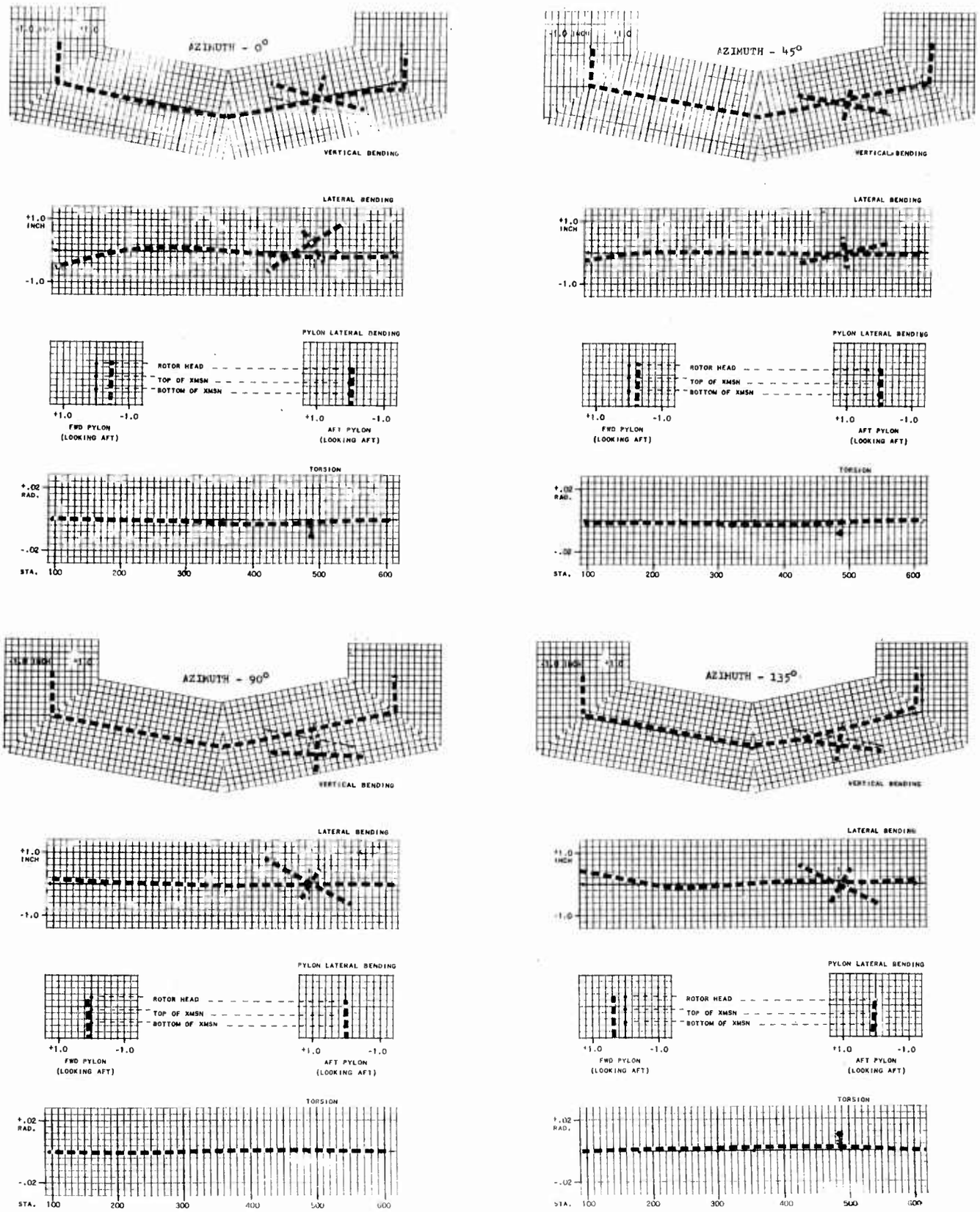

FIGURE 20

THIRD HARMONIC FORCED RESPONSE

100% WING FUEL, 90 KNOTS, 258 RPM

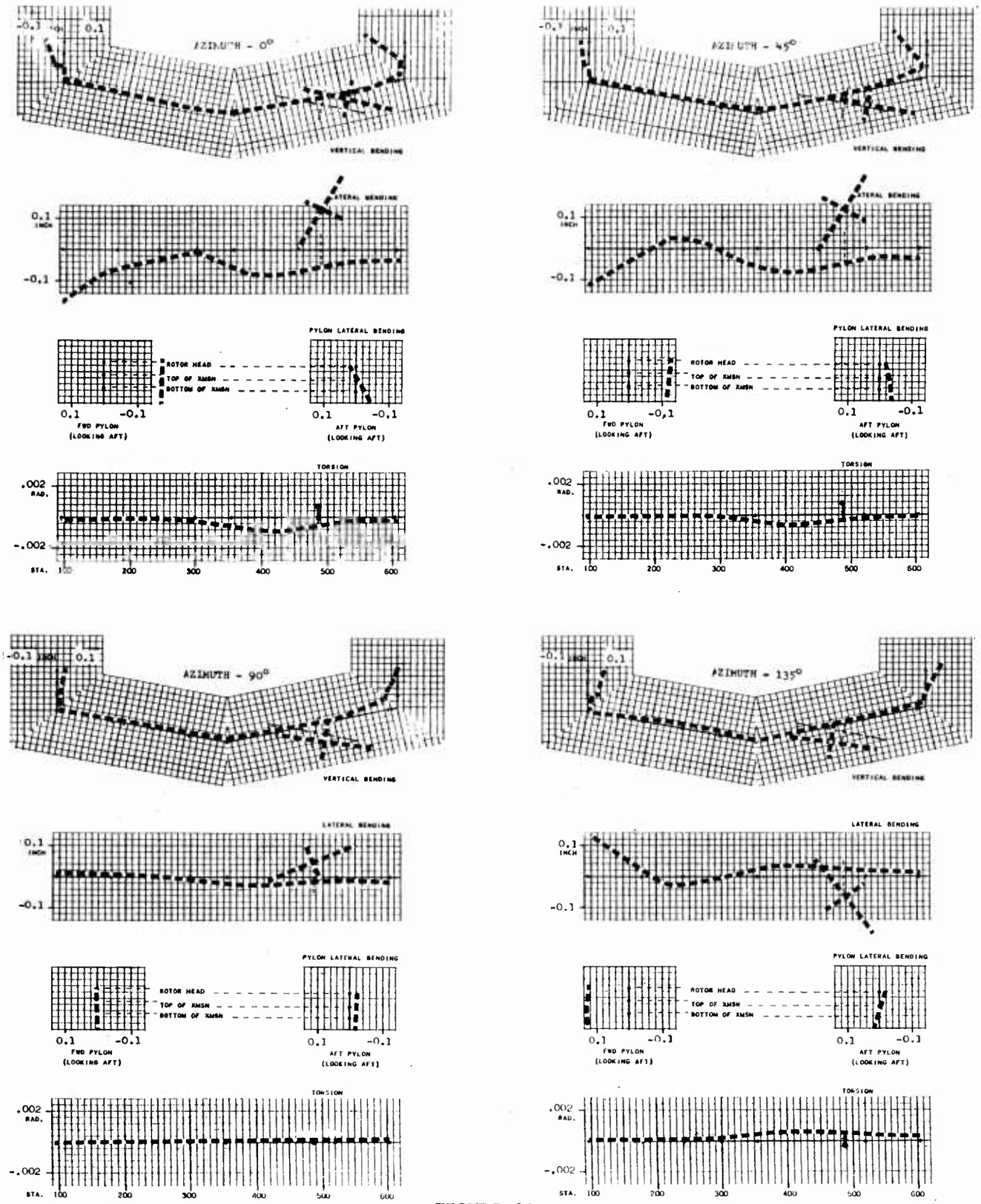

FIGURE 21

THIRD HARMONIC FORCED RESPONSE

100% WING FUEL, 90 KNOTS, 268 RPM

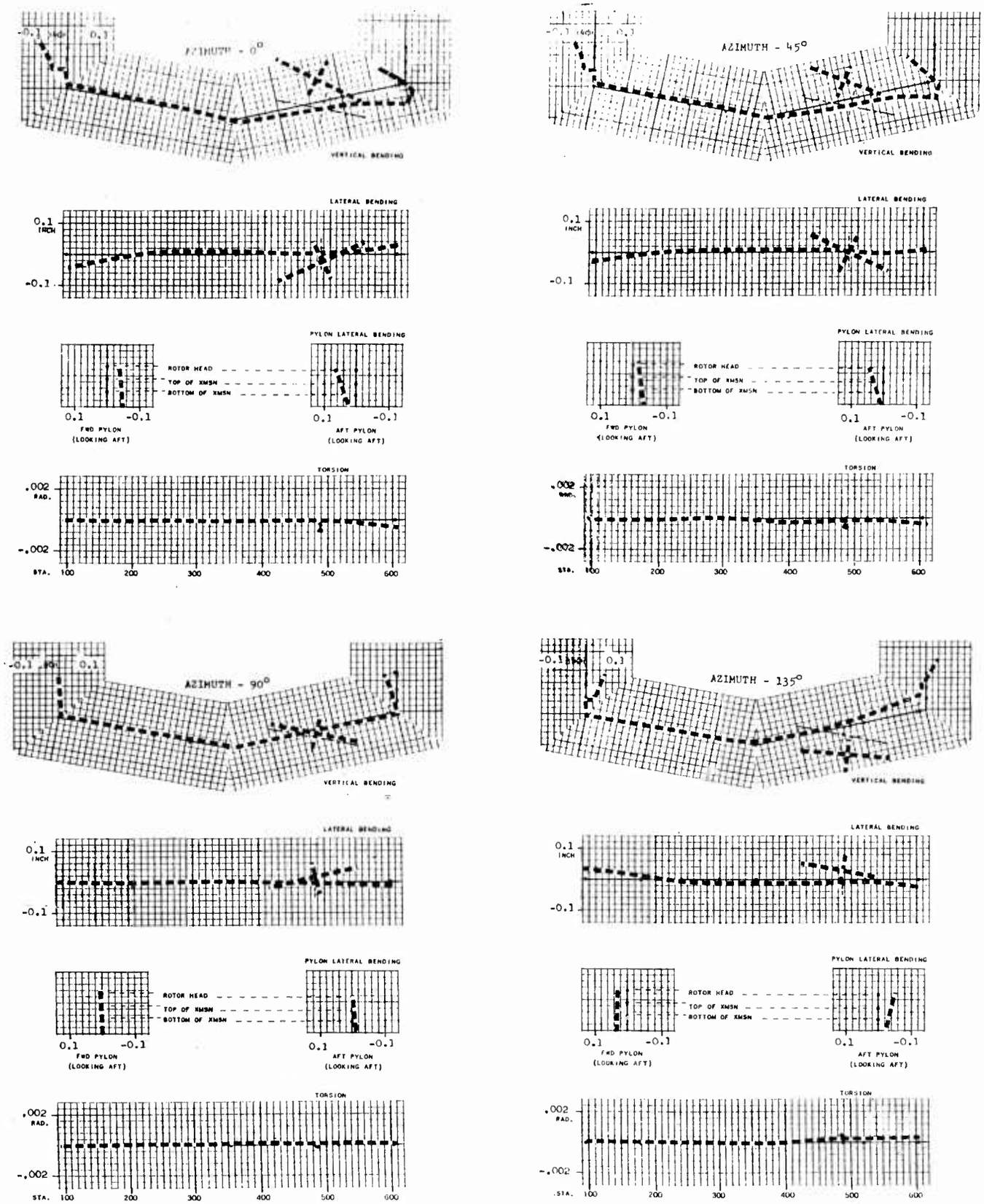

FIGURE 22

Third Harmonic Cockpit Floor Motion

Calculated cockpit floor responses for the standard fuselage without wings are compared in Figure 23 with measured flight amplitudes. This figure, taken from Reference 8 , presents calculated amplitudes as solid lines and measured amplitudes as dashed lines. Vertical calculated amplitudes compare very well with measured amplitudes. Lateral amplitude is satisfactory at 240, 250 and 278 RPM, but compare poorly at 260 and 270 RPM.

Figure 24 presents similar cockpit floor calculated amplitudes for the helicopter with wings. In the vertical direction with 0% wing fuel, the amplitude at each operating speed is nearly identical to those calculated for the helicopter without wings. Laterally for the same configuration, at 250 RPM, the responses are again nearly identical with an amplitude of .002 inch, but with increasing rotor speed the response of the helicopter with wings increases above that of the standard helicopter. Calculations show a peak response of 0.10 inch at 268 RPM approximately five times the response of the helicopter without floating fuel wings.

For the 100% fuel configuration, the maximum undamped cockpit floor response occurs in the lateral direction at 250 RPM. From a calculated peak amplitude of 0.764 inch, the lateral response decreases as the rotor speed increases reaching 0.17 inch at 258 RPM and then, at 268 RPM a minimum value of 0.005 inch close to the calculated response of the helicopter without wings. Corresponding to the near resonant condition in the lateral direction, the .035 inch vertical peak occur at 250 RPM. As the rotor speed is increased, the vertical response appears similar to that calculated for the helicopter without wings.

The very large amplitudes calculated here at low RPM indicate the rapid buildup of amplitude for an undamped resonance. From past experience, although large vibration levels can occur, amplitude increases as large as that in Figure 24 are unlikely in the real damped case. The results do indicate that the heavy fueled wing will tend to induce higher than normal fuselage vibration levels during the early part of a ferry mission, until the fuel quantity is somewhat reduced. It is also clear that there is a strong tendency toward higher levels with reduced rotor RPM, but from performance studies the RPM will tend to be closer to or slightly above normal for best range.

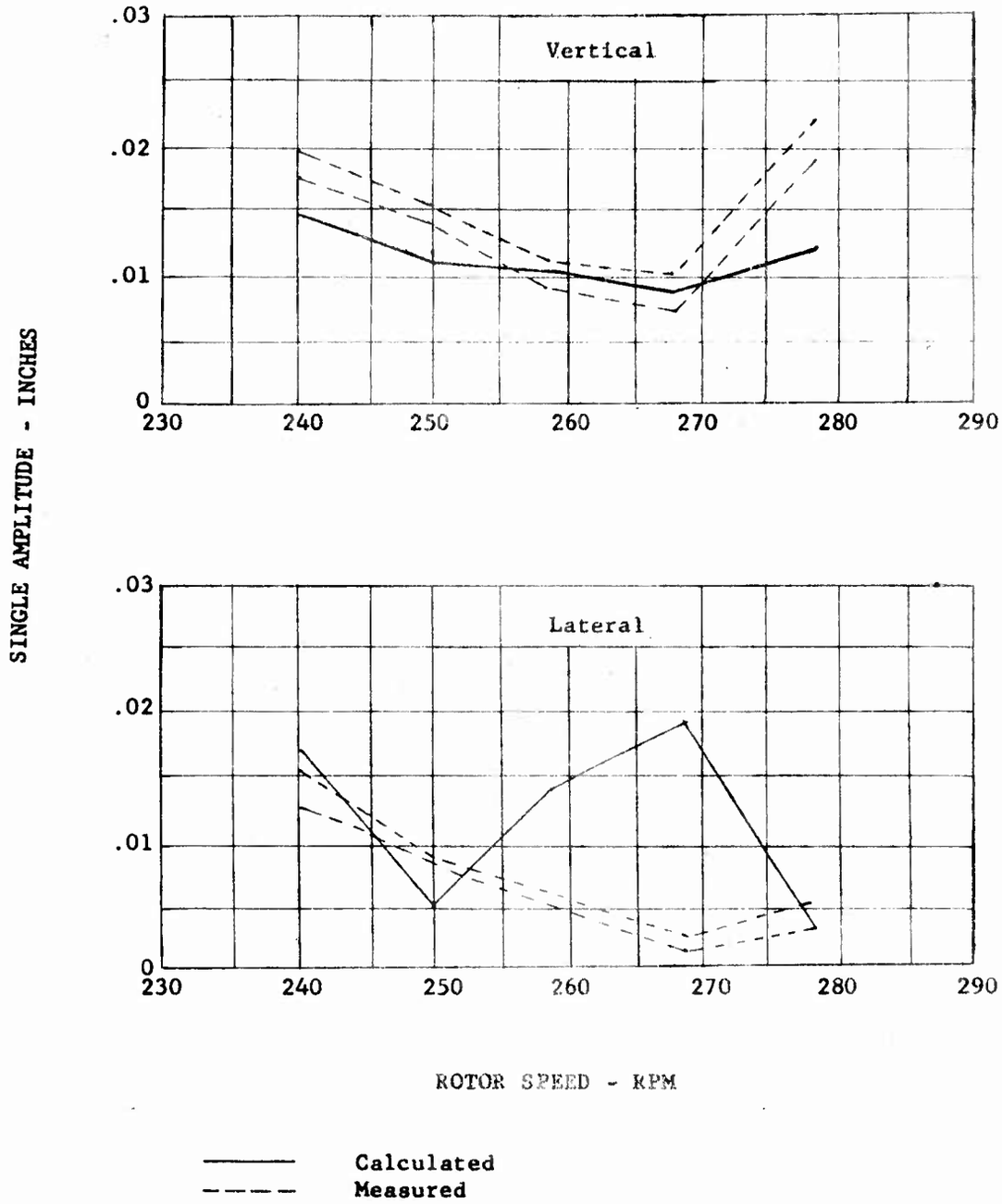

Figure 23. Cockpit Floor Response, 90 Knot RPM Sweep Without Floating Fuel Wings

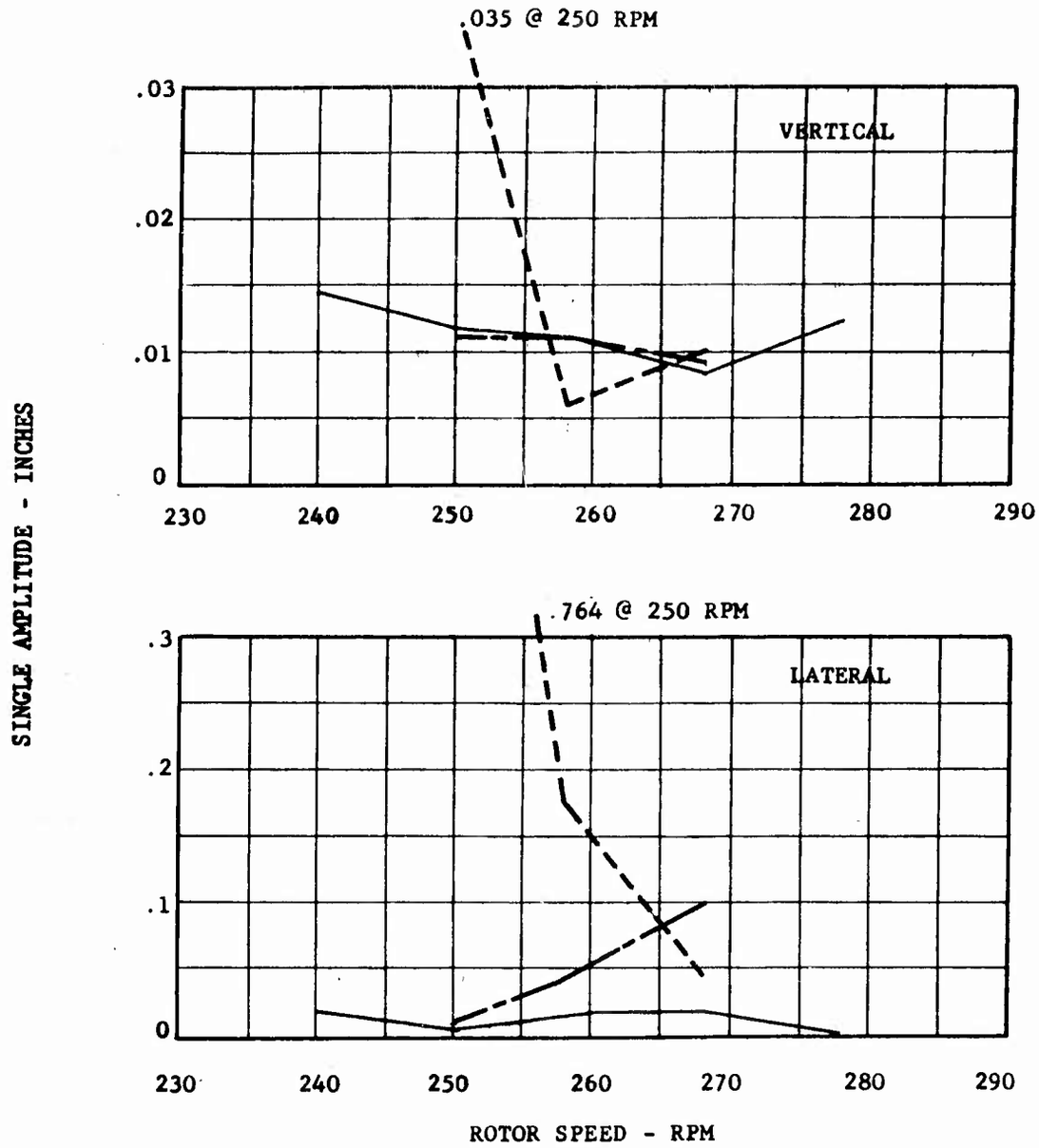

WITHOUT WING

WING - 0% FUEL

WING - 100% FUEL

FIGURE 24 COCKPIT FLOOR RESPONSE - 90 KNOT, RPM SWEEP

SECTION IV

CONCLUSIONS

The H-21 helicopter equipped with floating fuel tanks for ferry range extension has been investigated for fuselage vibratory response characteristics.

Third harmonic response of the H-21 equipped with floating fuel tanks was investigated for the two extremes of wing loading, 0% and 100% wing fuel, and compared to the cockpit floor vibration of the helicopter without fuel wings. Calculated using measured third harmonic loads, the forced modes corresponding to 0% wing fuel are strongly coupled lateral-vertical modes with significant fuselage motion. Cockpit floor motion compares favorably in the vertical direction with that calculated for the helicopter without fuel wings, but laterally, the fuselage response increases with rotor speed to a maximum of 0.10 inch at 268 RPM. Therefore, the acceptable cockpit 3Ω vibration environment associated with the helicopter without wings is maintained during the lower rotor speeds when the fuel tanks are nearly empty. At the higher rotor speed, the calculated 3Ω vibration is at a high level, but damping should reduce these amplitudes to a nearly satisfactory level.

In the 100% fuel configuration, the calculated 3Ω vibration level appears high at the lower rotor speeds, but satisfactory at 268 RPM. Fuselage mode plots show the same trends with RPM and further, indicate the presence of a lateral fuselage mode in the vicinity of, but below the 3Ω excitation at 250 RPM. Laterally, at 250 RPM the cockpit floor motion peaks at 0.76 inch reflecting the undamped natural mode, and then decreases rapidly to an amplitude of .005 inch at 268 RPM. Reflecting the near lateral resonance, the vertical cockpit floor motion at 250 RPM shows an undamped response of .035 inch. However, above 258 RPM, the third harmonic vertical vibration level is nearly equal to, or less than those calculated for the helicopter without fuel wings. Therefore, with full fuel tanks, the undamped calculations show a satisfactory vibration environment would exist in the aircraft at the maximum rotor speed. At the lower rotor speeds, the calculated amplitudes are high reflecting the undamped lateral resonance. Past experience has shown that amplitude increases as large as those calculated are very unlikely in the real damped case.

It is recommended that prior to flight, a simplified ground shake test be performed on the H-21 fuselage-wing combination to substantiate the theoretical calculations. In addition to providing a check on the calculated resonance below the 3Ω excitation at 250 RPM with 100% fuel, the test would provide reasonable prediction of the fuel and structural damping. Further, the proposed shake test may provide advantageous partial fuel arrangements and a sequence for emptying the fuel tanks which by controlling the important natural frequencies and increasing fuel damping would improve the vibration characteristics.

SECTION V

REFERENCES

1. Army Contract DA-44-177-TC-550, "Wind Tunnel Test and Further Study of the Floating Wing Fuel Tanks for Helicopter Range Extension."

2. Transportation Research and Engineering Command, Project No. 9-38-01-000 ST801, Contract DA44-177-TC-478, 1958.

3. C. B. Fay, "Feasibility Study of Helicopter Range Extension using Floating Wing Fuel Tanks", Boeing-Vertol Report R-156, September 28, 1958, ASTIA No. AD203262.

4. "Proposal for Wind Tunnel Test and Further Study of the Floating Wing Fuel Tanks for Helicopter Range Extension", Boeing-Vertol, Report PR-275, March 1959.

5. V. Capurso, R. Ricks, R. Gabel, "Wind Tunnel Tests and Further Analysis of the Floating Wing Fuel Tanks for Helicopter Range Extension", Volume 2, "Ground and Air Mechanical Instability Analysis", Boeing-Vertol, Report No. R197, March 1960.

6. R. Ricks, V. Capurso, R. Gabel, "Wind Tunnel Tests and Further Analysis of the Floating Wing Fuel Tanks for Helicopter Range Extension", Volume 3, "Wing Flutter Analysis", Boeing-Vertol, Report No. R-228, August 1961.

7. R. T. Yntema, R. Gabel, R. Ricks, "A Study of Tandem Helicopter Fuselage Vibration; Phase III, In-Flight Measurement of Steady and Oscillatory Rotor Shaft Loads", Boeing-Vertol, Report R-238, February 1961.

8. R. T. Yntema, R. Gabel, R. Ricks, "A Study of Tandem Helicopter Fuselage Vibration; Phase IIc and IV, A Method for the Prediction of Coupled Vertical-Lateral Natural and Forced Modes", Boeing-Vertol, Report R-246, April 1961.

9. R. T. Yntema, I. Manger, "A Study of Tandem Helicopter Fuselage Vibration; Phase IIb, Load Deflection Tests on an H-21 Helicopter Fuselage to Determine Stiffness Characteristics", Boeing-Vertol, Report R-180, April 1959.

10. R. G. Loewy, R. T. Yntema, R. Gabel, "A Study of Tandem Helicopter Fuselage Vibration; Phase IIa, A Method for the Prediction of Natural Modes and Frequencies from Design Mass and Stiffness Data", Boeing-Vertol, Report No. R-181, February 1960.

APPENDIX A

COUPLED MODE ASSOCIATED MATRIX DERIVATION

Associated Matrix Procedure

For fuselage vertical-lateral bending modes, six degrees of freedom are described by the matrix terms; longitudinal, lateral and vertical displacement, roll, pitch and yaw rotation. The structure is separated into lumped parameter form and a matrix representation prepared for each property. The matrices are assembled into an array to simulate a progression from one end of the fuselage beam to the other. Starting with a set of load and deflection boundary conditions at one end of the beam, the top of the forward rotor; successive multiplication of numerical matrices is performed to reach the other end of the beam. For this operation, a trial frequency, ω, is used, which, by the conventional harmonic motion assumption, applies an acceleration to each mass and inertia item, resulting in an applied load and moment distribution on the beam. At the other end of the beam, a second set of boundary conditions are enforced; by successive trials, frequencies are found which satisfy the boundaries and are, therefore, the natural frequencies being sought. Each trial matrix multiplication produces a non-zero residual; when this value is at or very near zero, the natural frequency is established.

When the natural frequency, ω_n, is determined, one further matrix multiplication of the system is required; this ω_n value and an assumed unit deflection at one boundary is used to obtain a detailed listing of the intermediate results of each matrix multiplication, thus providing the natural mode shapes corresponding to ω_n. This listing contains displacements, rotations, forces and moments at each station along the structure. In practice, the extensive matrix multiplications are performed on a digital computer and lead to rapid solution.

Elastic Matrix

The general elastic matrix for a weightless beam element undergoing deflections in the vertical plane was derived in Appendix A, Reference 10

$$\begin{bmatrix} F_z \\ M_\beta \\ F_x \\ X \\ \beta \\ Z \end{bmatrix}_{n+1} = \begin{bmatrix} 1 & 0 & 0 & 0 & 0 & 0 \\ l_i & 1 & 0 & 0 & Q_{li} & 0 \\ & 0 & 1 & 0 & 0 & 0 \\ 0 & 0 & -li/AE & 1 & 0 & 0 \\ -li^2/2GI_y & -li/EI_y & 0 & 0 & 1 & 0 \\ li^3/6EI_y - li/AG & li^2/2EI_y & 0 & 0 & -li & 1 \end{bmatrix} \begin{bmatrix} F_z \\ M_\beta \\ F_x \\ X \\ \beta \\ Z \end{bmatrix}_n .$$

The elastic matrix for a weightless beam element undergoing deflections in the lateral plane was also derived in Appendix A, Reference 10

$$\begin{bmatrix} F_y \\ M_\gamma \\ M_\alpha \\ \alpha \\ \gamma \\ Y \end{bmatrix}_{n+1} = \begin{bmatrix} 1 & 0 & 0 & 0 & 0 & 0 \\ -li & 1 & 0 & 0 & -Q_{li} & 0 \\ 0 & 0 & 1 & 0 & 0 & 0 \\ 0 & 0 & -li/GI_x & 1 & 0 & 0 \\ li^2/2EI_z & -li/EI_z & 0 & 0 & 1 & 0 \\ li^3/6EI_z - li/AG & -li^2/2EI_z & 0 & 0 & li & 1 \end{bmatrix} \begin{bmatrix} F_y \\ M_\gamma \\ M_\alpha \\ \alpha \\ \gamma \\ Y \end{bmatrix}_n$$

The effect of the axial force Q in the above matrices will be neglected in the formation of the coupled elastic matrix because experience has proved it to have little effect. The first step in forming the coupled matrix is the writing of a twelfth order matrix containing both the above uncoupled components in their proper diagonal positions.

$$[E_3]$$

$$
\begin{bmatrix} F_z \\ M_\beta \\ F_x \\ x \\ \beta \\ z \\ F_y \\ M_\gamma \\ M_\alpha \\ \alpha \\ \gamma \\ y \end{bmatrix}_{n+1}
\begin{bmatrix}
1 & & & & & & & & & & & \\
L & 1 & & & & & & & & & & \\
 & & 1 & & & & & & & & & \\
 & & -\frac{L}{A_x E} & 1 & & & & & & & & \\
-\frac{L^2}{2EI_y} & -\frac{L}{EI_y} & & & 1 & & & & & & & \\
\frac{L^3}{6EI_y} - \frac{L}{A_z G} & \frac{L^2}{2EI_y} & & & -L & 1 & & & & & & \\
 & & & & & & 1 & & & & & \\
 & & & & & & -L & 1 & & & & \\
 & & & & & & & & 1 & & & \\
 & & & & & & & & -\frac{L}{GJ_x} & 1 & & \\
 & & & & & & \frac{L^2}{2EI_y} & -\frac{L}{EI_z} & & & 1 & \\
 & & & & & & \frac{L^3}{6EI_z} - \frac{L}{A_z G} & -\frac{L^2}{2EI_z} & & & L & 1
\end{bmatrix}
\begin{bmatrix} F_z \\ M_\beta \\ F_x \\ x \\ \beta \\ z \\ F_y \\ M_\gamma \\ M_\alpha \\ \alpha \\ \gamma \\ y \end{bmatrix}_{n}
$$

WHERE

A_x = LONGITUDINAL AREA

A_z = VERTICAL SHEAR AREA

A_y = LATERAL SHEAR AREA

Pitching moment, yawing moment, and axial longitudinal load are shifted from the reference axis system through the distances b_n, c_n to the neutral axis prior to calculation of the resulting deflections in the elastic matrix. Similarly, vertical and lateral loads and rolling moment (fuselage torsion) are shifted from the reference axes to the shear center axis b_e, c_e as shown below:

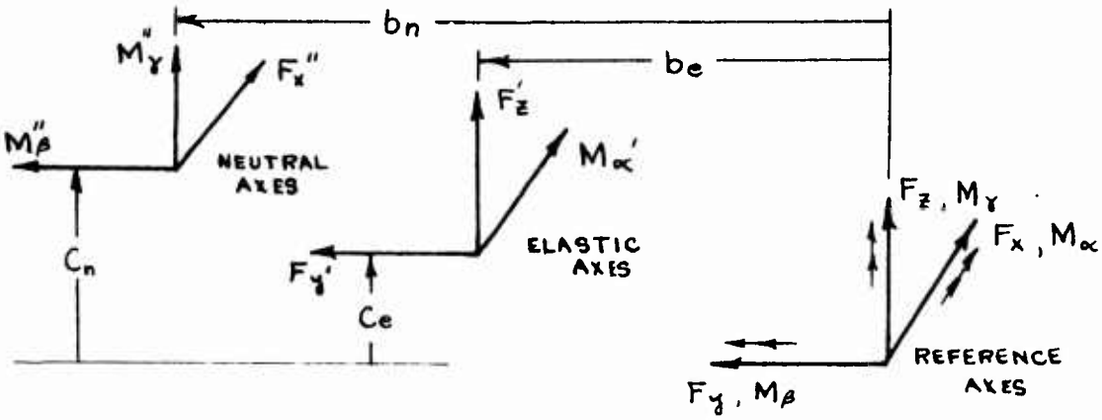

Therefore $F'_y = F_y$ $\qquad$ $F''_x = F_x$

$F'_z = F_z$ $\qquad$ $M''_\gamma = M_\gamma + b_n F_x$

$M'_\alpha = M_\alpha - b_e F_z + C_e F_y$ $\qquad$ $M''_\beta = M_\beta - C_n F_x$

Similarly the linear and angular deflections are transformed to their respective Set of axes

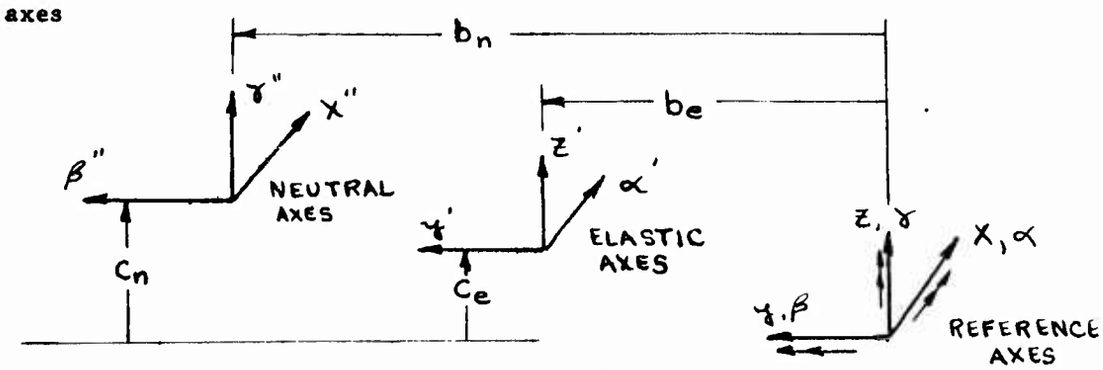

$\alpha' = \alpha$ $\qquad$ $x'' = x - b_n \gamma + C_n \beta$

$\beta'' = \beta$ $\qquad$ $y' = y - C_e \alpha$

$\gamma'' = \gamma$ $\qquad$ $z' = z + b_e \alpha$

Thus, the transfer matrix of forces and displacements from the reference axes to the shear center and neutral axes is $[E_1]$

$$
\begin{bmatrix} F_z' \\ M_\beta'' \\ F_x'' \\ x'' \\ \beta'' \\ z' \\ F_y' \\ M_\gamma'' \\ M_\alpha' \\ \alpha' \\ \gamma'' \\ y' \end{bmatrix}_{n',n''}
=
\begin{bmatrix}
1 & & & & & & & & & & & \\
 & 1 & -c_n & & & & & & & & & \\
 & & 1 & & & & & & & & & \\
 & & & 1 & c_n & & & & & & -b_n & \\
 & & & & 1 & & & & & & & \\
 & & & & & 1 & & & & b_e & & \\
 & & & & & & 1 & & & & & \\
 & & & & & & & 1 & & & & \\
 & & b_n & & & & & & 1 & & & \\
-b_e & & & & & & & c_e & & 1 & & \\
 & & & & & & & & & & 1 & \\
 & & & & & & & & & -c_e & & 1
\end{bmatrix}
\begin{bmatrix} F_z \\ M_\beta \\ F_x \\ x \\ \beta \\ z \\ F_y \\ M_\gamma \\ M_\alpha \\ \alpha \\ \gamma \\ y \end{bmatrix}_{n}
$$

In order to write the bending equations without considering additional stiffness coupling terms, the axis system is oriented to the principal axes.

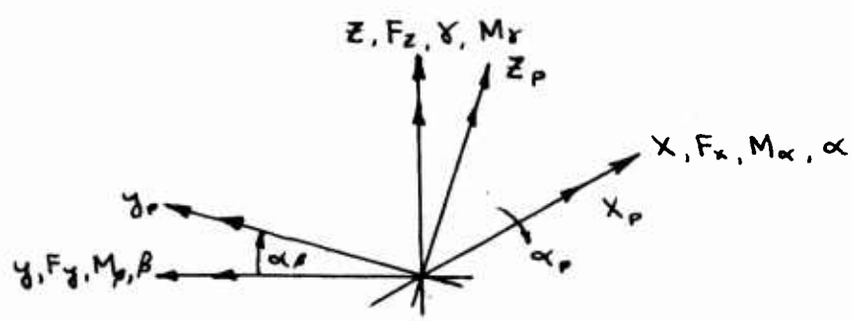

$$x_p = x \qquad \alpha_p = \alpha$$

$$y_p = y \cos\alpha_p + z \sin\alpha_p \qquad \beta_p = \beta \cos\alpha_p + \gamma \sin\alpha_p$$

$$z_p = -y \sin\alpha_p + z \cos\alpha_p \qquad \gamma_p = -\beta \sin\alpha_p + \gamma \cos\alpha_p$$

$$F_{x_p} = F_x \qquad M_{\alpha_p} = M_\alpha$$

$$F_{y_p} = F_y \cos\alpha_p + F_z \sin\alpha_p \qquad M_{\beta_p} = M_\beta \cos\alpha_p + M_\gamma \sin\alpha_p$$

$$F_{z_p} = -F_y \sin\alpha_p + F_z \cos\alpha_p \qquad M_{\gamma_p} = -M_\beta \sin\alpha_p + M_\gamma \cos\alpha_p$$

WRITING THE MATRIX $\left[E_2\right]$ REPRESENTING THESE EQUATIONS,

$$
\begin{bmatrix} F_z \\ M_\beta \\ F_x \\ X \\ \beta \\ Z \\ F_y \\ M_\gamma \\ M_\alpha \\ \alpha \\ \gamma \\ y \end{bmatrix}_n
\begin{bmatrix}
\cos\alpha_p & & & & & & -\sin\alpha_p & & & & & \\
 & \cos\alpha_p & & & & & & \sin\alpha_p & & & & \\
 & & 1 & & & & & & & & & \\
 & & & 1 & & & & & & & & \\
 & & & & \cos\alpha_p & & & & & & \sin\alpha_p & \\
 & & & & & \cos\alpha_p & & & & & & -\sin\alpha_p \\
\sin\alpha_p & & & & & & \cos\alpha_p & & & & & \\
 & -\sin\alpha_p & & & & & & \cos\alpha_p & & & & \\
 & & & & & & & & 1 & & & \\
 & & & & & & & & & 1 & & \\
 & & & & -\sin\alpha_p & & & & & & \cos\alpha_p & \\
 & & & & & \sin\alpha_p & & & & & & \cos\alpha_p
\end{bmatrix}
\begin{bmatrix} F_z \\ M_\beta \\ F_x \\ X \\ \beta \\ Z \\ F_y \\ M_\gamma \\ M_\alpha \\ \alpha \\ \gamma \\ y \end{bmatrix}_n
$$

Thus, the triple matrix product,

$$[E_3][E_2][E_1] = \begin{bmatrix}\text{Elastic}\\ \text{Matrix}\end{bmatrix} \begin{bmatrix}\text{Rotation}\\ \text{Matrix}\end{bmatrix} \begin{bmatrix}\text{Translation}\\ \text{Matrix}\end{bmatrix}$$

will relate the forces and displacements at station n with those at $(n + 1)$ with respect to the principal - neutral and principal - elastic axes of the elastic beam. Since the forces and displacements must be with respect to the reference axes in order to continue with the associated matrix method, a rotation and translation opposite to those derived previously are required. Thus $[E_5]\ [E_4]\ [E_3]\ [E_2]\ [E_1] =$

$$= \begin{bmatrix}\text{Return}\\ \text{Trans-}\\ \text{lation}\\ \text{Matrix}\end{bmatrix} \begin{bmatrix}\text{Return}\\ \text{Rotation}\\ \text{Matrix}\\ \\ \end{bmatrix} \begin{bmatrix}\text{Elastic}\\ \text{Matrix}\\ \\ \\ \end{bmatrix} \begin{bmatrix}\text{Rotation}\\ \text{Matrix}\\ \\ \\ \end{bmatrix} \begin{bmatrix}\text{Translation}\\ \text{Matrix}\\ \\ \\ \end{bmatrix}$$

will relate the forces and displacements at station n with those at station $(n + 1)$ with respect to the reference axes.

The required matrices to return to the reference axes are as follows:

$$
\begin{bmatrix} F_z \\ M_\beta \\ F_x \\ X \\ \beta \\ Z \\ F_\gamma \\ M_\gamma \\ M_\alpha \\ \alpha \\ \gamma \\ y \end{bmatrix}_{n+1}
\begin{bmatrix}
\cos\alpha_p & & & & & & \sin\alpha_p & & & & & \\
 & \cos\alpha_p & & & & & & -\sin\alpha_p & & & & \\
 & & 1 & & & & & & & & & \\
 & & & 1 & & & & & & & & \\
 & & & & \cos\alpha_p & & & & & & -\sin\alpha_p & \\
 & & & & & \cos\alpha_p & & & & & & \sin\alpha_p \\
-\sin\alpha_p & & & & & & \cos\alpha_p & & & & & \\
 & \sin\alpha_p & & & & & & \cos\alpha_p & & & & \\
 & & & & & & & & 1 & & & \\
 & & & & & & & & & 1 & & \\
 & & & & \sin\alpha_p & & & & & & \cos\alpha_p & \\
 & & & & & -\sin\alpha_p & & & & & & \cos\alpha_p
\end{bmatrix}
\begin{bmatrix} F_z \\ M_\beta \\ F_x \\ X \\ \beta \\ Z \\ F_\gamma \\ M_\gamma \\ M_\alpha \\ \alpha \\ \gamma \\ y \end{bmatrix}_{n',n''}
$$

$$
\begin{bmatrix} F_z \\ M_\beta \\ F_x \\ X \\ \beta \\ Z \\ F_\gamma \\ M_\gamma \\ M_\alpha \\ \alpha \\ \gamma \\ y \end{bmatrix}_{n+1}
=
\begin{bmatrix}
1 & & & & & & & & & & & \\
 & 1 & C_N & & & & & & & & & \\
 & & 1 & & & & & & & & & \\
 & & & 1 & -C_N & & & & & & b_N & \\
 & & & & 1 & & & & & & & \\
 & & & & & 1 & & & & -b_E & & \\
 & & & & & & 1 & & & & & \\
 & & -b_N & & & & & 1 & & & & \\
b_E & & & & & & -C_E & & 1 & & & \\
 & & & & & & & & & 1 & & \\
 & & & & & & & & & & 1 & \\
 & & & & & & & & & C_E & & 1
\end{bmatrix}
\begin{bmatrix} F_z \\ M_\beta \\ F_x \\ X \\ \beta \\ Z \\ F_\gamma \\ M_\gamma \\ M_\alpha \\ \alpha \\ \gamma \\ y \end{bmatrix}_{n}
$$

ELASTIC MATRIX (COLLAPSED)

1												
L	1											
		1										
$\frac{C_N L^2}{2EI_y}$	$\frac{C_N L}{EI_y}$	$-\frac{C_N^2 L}{EI_y}-\frac{b_N^2 L}{EI_z}-\frac{L}{EA_x}$	1			$\frac{b_N L^2}{2EI_z}$	$-\frac{b_N L}{EI_z}$					
$-\frac{L^2}{2EI_y}$	$-\frac{L}{EI_y}$	$\frac{C_N L}{EI_y}$		1								
$\frac{L^3}{6EI_y}-\frac{L}{A_z G}-\frac{b_E^2 L}{GJ_x}$	$\frac{L^2}{2EI_y}$	$-\frac{C_N L^2}{2EI_y}$		-L	1	$\frac{b_E C_E L}{GJ_x}$		$\frac{b_E L}{GJ_x}$				
						1						
						-L	1					
								1				
$\frac{b_E L}{GJ_x}$						$-\frac{C_E L}{GJ_x}$		$-\frac{L}{GJ_x}$	1			
		$-\frac{b_N L}{EI_z}$				$\frac{L^2}{2EI_z}$	$\frac{L}{EI_z}$			1		
$\frac{b_E C_E L}{GJ_x}$		$-\frac{b_N L^2}{2EI_z}$				$\frac{L^3}{6EI_z}-\frac{L}{A_y G}-\frac{C_E^2 L}{GJ_x}$	$-\frac{L^2}{2EI_z}$	$-\frac{C_E L}{GJ_x}$		L	1	
												1

Mass Matrix

Consider a mass M whose position is known with respect to the reference axes of an arbitrary section, n associated with the mass are the inertial properties I_α, I_β and I_γ about its centroid. These masses and inertias, accelerated by harmonic occillations, produce inertial loads on the beam structure.

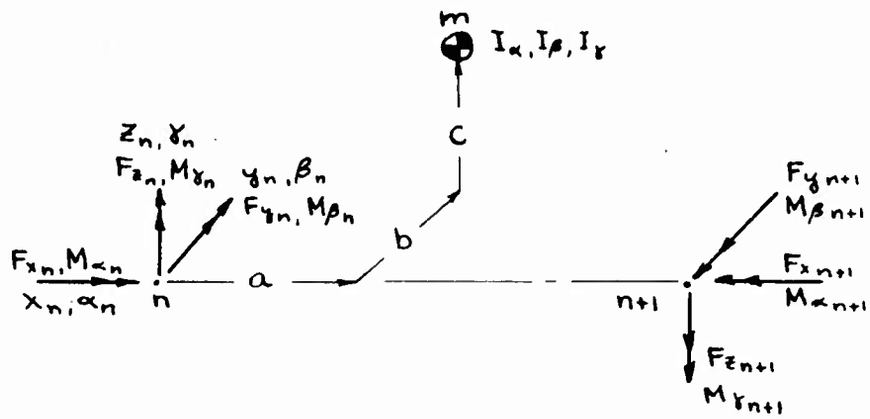

$$\sum F_x = 0 = F_{x_n} + m\omega^2(x_n + c\beta_n - b\gamma_n) - F_{x_{n+1}}$$

$$\sum F_y = 0 = F_{y_n} + m\omega^2(y_n - c\alpha_n + a\gamma_n) - F_{y_{n+1}}$$

$$\sum F_z = 0 = F_{z_n} + m\omega^2(z_n + b\alpha_n - a\beta_n) - F_{z_{n+1}}$$

$$\sum M_\alpha = 0 = M_{\alpha_n} - m\omega^2(y_n - c\alpha_n + a\gamma_n)c + m\omega^2(z_n + b\alpha_n - a\beta_n)b + I_\alpha\omega^2\alpha_n - M_{\alpha_{n+1}}$$

$$\sum M_\beta = 0 = M_{\beta_n} + m\omega^2(x_n + c\beta_n - b\gamma_n)c - m\omega^2(z_n + b\alpha_n - a\beta_n)a + I_\beta\omega^2\beta_n - M_{\beta_{n+1}}$$

$$\sum M_\gamma = 0 = M_{\gamma_n} - m\omega^2(x_n + c\beta_n - b\gamma_n)b + m\omega^2(y_n - c\alpha_n + a\gamma_n)a + I_\gamma\omega^2\gamma_n - M_{\gamma_{n+1}}$$

Deflections are unchanged across the mass stations. The final matrix form is

MASS MATRIX

$$
\begin{bmatrix} F_z \\ M_\beta \\ F_x \\ X \\ \beta \\ Z \\ F_y \\ M_\gamma \\ M_\alpha \\ \alpha \\ \gamma \\ y \end{bmatrix}_{n+1}
=
\begin{bmatrix}
1 & & & & -ma\omega^2 & m\omega^2 & & & & mb\omega^2 & & \\
 & 1 & & mc\omega^2 & m(a^2+c^2)\omega^2 + I_\beta\omega^2 & -ma\omega^2 & & & & -mab\omega^2 & -mbc\omega^2 & \\
 & & 1 & m\omega^2 & mc\omega^2 & & & & & & -mb\omega^2 & \\
 & & & 1 & & & & & & & & \\
 & & & & 1 & & & & & & & \\
 & & & & & 1 & & & & & & \\
 & & & & & & 1 & & & -mc\omega^2 & ma\omega^2 & m\omega^2 \\
 & & & -mb\omega^2 & -mbc\omega^2 & & & 1 & & -mac\omega^2 & m(a^2+b^2)\omega^2 + I_\gamma\omega^2 & ma\omega^2 \\
 & & & & -mab\omega^2 & mb\omega^2 & & & 1 & m(b^2+c^2)\omega^2 + I_\alpha\omega^2 & -mac\omega^2 & -mc\omega^2 \\
 & & & & & & & & & 1 & & \\
 & & & & & & & & & & 1 & \\
 & & & & & & & & & & & 1
\end{bmatrix}
\begin{bmatrix} F_z \\ M_\beta \\ F_x \\ X \\ \beta \\ Z \\ F_y \\ M_\gamma \\ M_\alpha \\ \alpha \\ \gamma \\ y \end{bmatrix}_{n}
$$

Ground Spring Matrix

A mathematical device which permits simulation of ground shake tests, in which the aircraft is suspended from the roof trusses of a hangar building, is the ground spring matrix. Suppose a station, n, has its six degrees of freedom partially restrained by springs, then these external springs induce additional loads on the vibrating structure in proportion to the motion amplitude and spring rates.

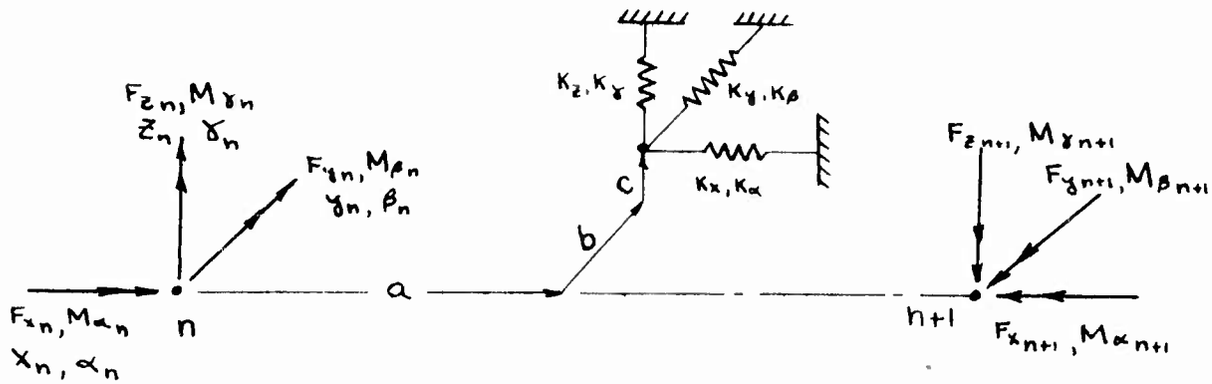

$$F_x = 0 = F_{x_n} - K_x(x_n + c\beta_n - b\gamma_n) - F_{x_{n+1}}$$

$$F_y = 0 = F_{y_n} - K_y(y_n - c\alpha_n + a\gamma_n) - F_{y_{n+1}}$$

$$F_z = 0 = F_{z_n} - K_z(z_n + b\alpha_n - a\beta_n) - F_{z_{n+1}}$$

$$M_\alpha = 0 = M_{\alpha_n} + K_y(y_n - c\alpha_n + a\gamma_n)c - K_z(z_n + b\alpha_n - a\beta_n)b - K_\alpha\alpha_n - M_{\alpha_{n+1}}$$

$$M_\beta = 0 = M_{\beta_n} - K_x(x_n + c\beta_n - b\gamma_n)c + K_z(z_n + b\alpha_n - a\beta_n)a - K_\beta\beta_n - M_{\beta_{n+1}}$$

$$M_\gamma = 0 = M_{\gamma_n} + K_x(x_n + c\beta_n - b\gamma_n)b - K_y(y_n - c\alpha_n + a\gamma_n) - K_\gamma\gamma_n - M_{\gamma_{n+1}}$$

GROUND SPRING MATRIX

$$
\begin{bmatrix} F_z \\ M_\beta \\ F_x \\ X \\ \beta \\ Z \\ F_y \\ M_\gamma \\ M_\alpha \\ \alpha \\ \gamma \\ y \end{bmatrix}_{n+1}
=
\begin{bmatrix}
1 & & & & k_z a & -k_z & & & & -k_z b & & \\
 & 1 & & -k_x c & \begin{matrix} -k_x c^2 \\ -k_z a^2 \\ -k_\beta \end{matrix} & k_z a & & & & k_z ab & k_x bc & \\
 & & 1 & -k_x & -k_x c & & & & & & k_x b & \\
 & & & 1 & & & & & & & & \\
 & & & & 1 & & & & & & & \\
 & & & & & 1 & & & & & & \\
 & & & & & & 1 & & & k_y c & -k_y a & -k_y \\
 & & & k_x b & k_x bc & & & 1 & & k_y ac & \begin{matrix} -k_x b^2 \\ -k_x a^2 \\ -k_\gamma \end{matrix} & -k_y a \\
 & & & & k_z ab & -k_z b & & & 1 & \begin{matrix} -k_y c^2 \\ -k_z b^2 \\ -k_\alpha \end{matrix} & k_y ac & k_y c \\
 & & & & & & & & & 1 & & \\
 & & & & & & & & & & 1 & \\
 & & & & & & & & & & & 1
\end{bmatrix}
\begin{bmatrix} F_z \\ M_\beta \\ F_x \\ X \\ \beta \\ Z \\ F_y \\ M_\gamma \\ M_\alpha \\ \alpha \\ \gamma \\ y \end{bmatrix}_{n}
$$

Concentrated Spring Matrix

Concentrated springs between adjacent fuselage beam sections, such as the attachment of a rotor transmission to the fuselage structure, are handled by a matrix. Consider the following joint,

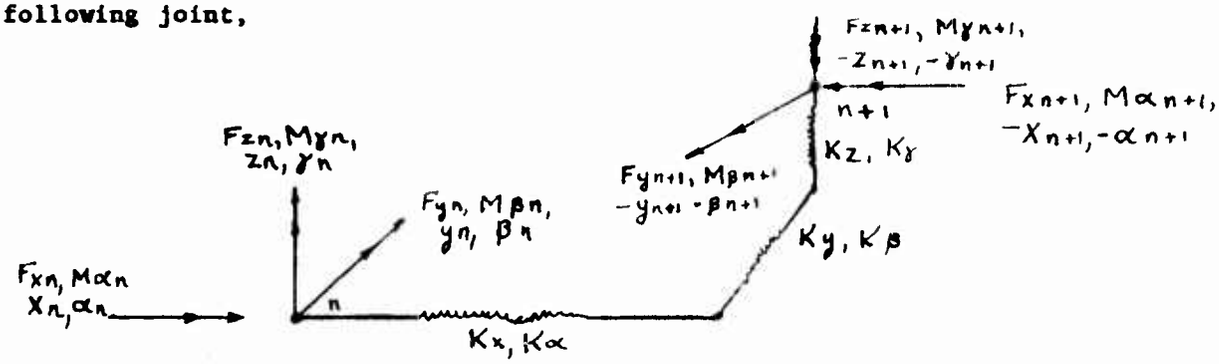

Since no force generation occurs across the spring joint, the forces at stations n and n = 1 are equal. Deflections change because of the action of forces on the springs. At joint n,

$$\sum F_x = 0 = F_{xn} - K_x(x_n - x_{n+1})$$

$$\sum F_y = 0 = F_{yn} - K_y(y_n - y_{n+1})$$

$$\sum F_z = 0 = F_{zn} - K_z(Z_n - Z_{n+1})$$

$$\sum M_\alpha = 0 = M_{\alpha n} - K_\alpha(\alpha_n - \alpha_{n+1})$$

$$\sum M_\beta = 0 = M_{\beta n} - K_\beta(\beta_n - \beta_{n+1})$$

$$\sum M_\gamma = 0 = M_{\gamma n} - K_\gamma(\gamma_n - \gamma_{n+1})$$

Solving these equations for the displacements at station n + 1, the concentrated spring matrix is,

CONCENTRATED SPRING MATRIX

$$
\begin{bmatrix} F_z \\ M_\beta \\ F_x \\ X \\ \beta \\ Z \\ F_y \\ M_\gamma \\ M_\alpha \\ \alpha \\ \gamma \\ y \end{bmatrix}_{n+1}
=
\begin{bmatrix}
1 & & & & & & & & & & & \\
 & 1 & & & & & & & & & & \\
 & & 1 & & & & & & & & & \\
 & & -\frac{1}{k_x} & 1 & & & & & & & & \\
 & -\frac{1}{k_\beta} & & & 1 & & & & & & & \\
-\frac{1}{k_z} & & & & & 1 & & & & & & \\
 & & & & & & 1 & & & & & \\
 & & & & & & & 1 & & & & \\
 & & & & & & & & 1 & & & \\
 & & & & & & & & -\frac{1}{k_\alpha} & 1 & & \\
 & & & & & & & -\frac{1}{k_\gamma} & & & 1 & \\
 & & & & & & -\frac{1}{k_y} & & & & & 1
\end{bmatrix}
\cdot
\begin{bmatrix} F_z \\ M_\beta \\ F_x \\ X \\ \beta \\ Z \\ F_y \\ M_\gamma \\ M_\alpha \\ \alpha \\ \gamma \\ y \end{bmatrix}_{n}
$$

Shift Matrix

To permit a change of position of the reference axes, a shift matrix is employed to convert loads and deflections from one axis orientation to another

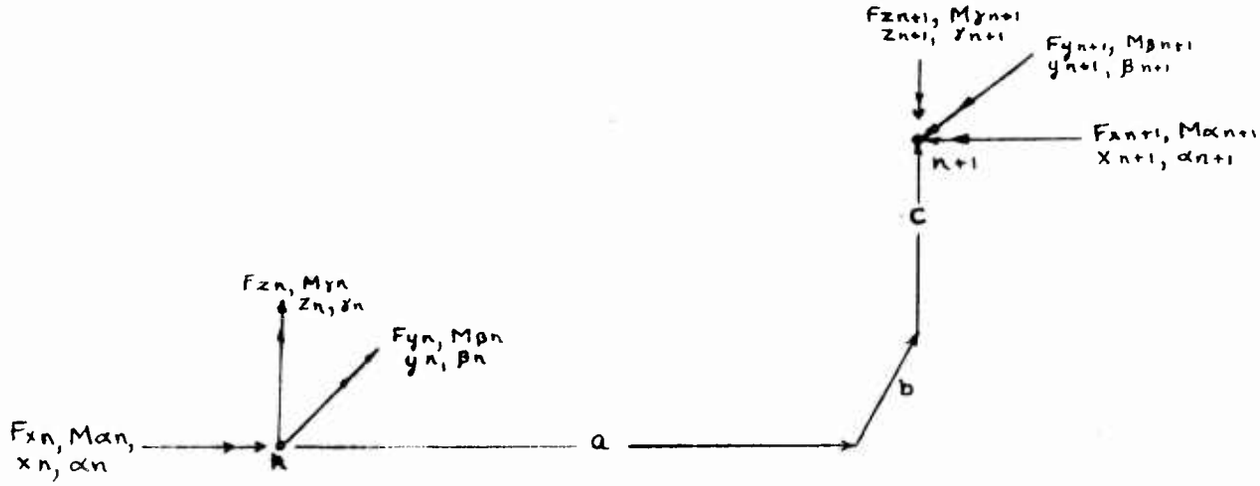

$$F_{x_{n+1}} = F_{x_n} \qquad \alpha_{n+1} = \alpha_n$$

$$F_{y_{n+1}} = F_{y_n} \qquad \beta_{n+1} = \beta_n$$

$$F_{z_{n+1}} = F_{z_n} \qquad \gamma_{n+1} = \gamma_n$$

$$M_{\alpha_{n+1}} = M_{\alpha_n} - b_o F_{z_n} + c_o F_{y_n} \qquad X_{n+1} = X_n - b_o \gamma_n + c_o \beta_n$$

$$M_{\beta_{n+1}} = M_{\beta_n} - c_o F_{x_n} + a_o F_{z_n} \qquad Y_{n+1} = Y_n - c_o \alpha_n + a_o \gamma_n$$

$$M_{\gamma_{n+1}} = M_{\gamma_n} + b_o F_{x_n} - a_o F_{y_n} \qquad Z_{n+1} = Z_n + b_o \alpha_n - a_o \beta$$

Thus the shift matrix

SHIFT MATRIX

$$
\begin{bmatrix} F_z \\ M_\beta \\ F_x \\ X \\ \beta \\ Z \\ F_y \\ M_\gamma \\ M_\alpha \\ \alpha \\ \gamma \\ y \end{bmatrix}_{n+1}
=
\begin{bmatrix}
1 & & & & & & & & & & & \\
a & 1 & -c & & & & & & & & & \\
 & & 1 & & & & & & & & & \\
 & & & 1 & c & & & & & & -b & \\
 & & & & 1 & & & & & & & \\
 & & & & -a & 1 & & & & b & & \\
 & & & & & & 1 & & & & & \\
 & & b & & & & -a & 1 & & & & \\
-b & & & & & & c & & 1 & & & \\
 & & & & & & & & & 1 & & \\
 & & & & & & & & & & 1 & \\
 & & & & & & & & & -c & a & 1
\end{bmatrix}
\begin{bmatrix} F_z \\ M_\beta \\ F_x \\ X \\ \beta \\ Z \\ F_y \\ M_\gamma \\ M_\alpha \\ \alpha \\ \gamma \\ y \end{bmatrix}_{n}
$$

Bend Matrix

To permit a change of direction of the elastic axis, a bend matrix is employed to convert loads and deflections from one axis orientation to another

In progressing from left to right, the bend angle β is defined as clockwise from an extension of the initial reference axis past the bend.

$$X_{n+1} = X_n \cos(2\pi - \beta_p) + Z_n \sin(2\pi - \beta_p)$$
$$Z_{n+1} = Z_n \cos(2\pi - \beta_p) - X_n \sin(2\pi - \beta_p)$$
$$y_{n+1} = y_n$$

$$\alpha_{n+1} = \alpha_n \cos(2\pi - \beta_p) + \gamma_n \sin(2\pi - \beta_p)$$
$$\gamma_{n+1} = \gamma_n \cos(2\pi - \beta_p) - \alpha_n \sin(2\pi - \beta_p)$$
$$\beta_{n+1} = \beta_n$$

$$F_{xn+1} = F_{xn} \cos(2\pi - \beta_p) + F_{zn} \sin(2\pi - \beta_p)$$
$$F_{zn+1} = F_{zn} \cos(2\pi - \beta_p) - F_{xn} \sin(2\pi - \beta_p)$$
$$F_{yn+1} = F_{yn}$$

$$M_{\alpha n+1} = M_{\alpha n} \cos(2\pi - \beta_p) + M_{\gamma n} \sin(2\pi - \beta_p)$$
$$M_{\gamma n+1} = M_{\gamma n} \cos(2\pi - \beta_p) - M_{\alpha n} \sin(2\pi - \beta_p)$$
$$M_{\beta n+1} = M_{\beta n}$$

VERTICAL BEND MATRIX

$$
\begin{bmatrix} F_z \\ M_\beta \\ F_x \\ X \\ \beta \\ Z \\ F_y \\ M_\gamma \\ M_\alpha \\ \alpha \\ \gamma \\ y \end{bmatrix}_{n+1}
=
\begin{bmatrix}
\cos\beta_p & & \sin\beta_p & & & & & & & & & \\
 & 1 & & & & & & & & & & \\
-\sin\beta_p & & \cos\beta_p & & & & & & & & & \\
 & & & \cos\beta_p & & -\sin\beta_p & & & & & & \\
 & & & & 1 & & & & & & & \\
 & & & \sin\beta_p & & \cos\beta_p & & & & & & \\
 & & & & & & 1 & & & & & \\
 & & & & & & & \cos\beta_p & \sin\beta_p & & & \\
 & & & & & & & -\sin\beta_p & \cos\beta_p & & & \\
 & & & & & & & & & \cos\beta_p & -\sin\beta_p & \\
 & & & & & & & & & \sin\beta_p & \cos\beta_p & \\
 & & & & & & & & & & & 1
\end{bmatrix}
\begin{bmatrix} F_z \\ M_\beta \\ F_x \\ X \\ \beta \\ Z \\ F_y \\ M_\gamma \\ M_\alpha \\ \alpha \\ \gamma \\ y \end{bmatrix}_{n}
$$

Sprung Mass Matrices

Consider a mass, m, whose position is known with respect to the axes at an arbitrary station, n. Associated with the mass are the inertial properties I_α, I_β, I_γ about its centroid. In addition, the mass is mounted on six simple springs which act in the same directions as the general displacements. These masses and inertias, accelerated by harmonic oscillations, produce inertial loads on the beam structure.

(a) Uncoupled system

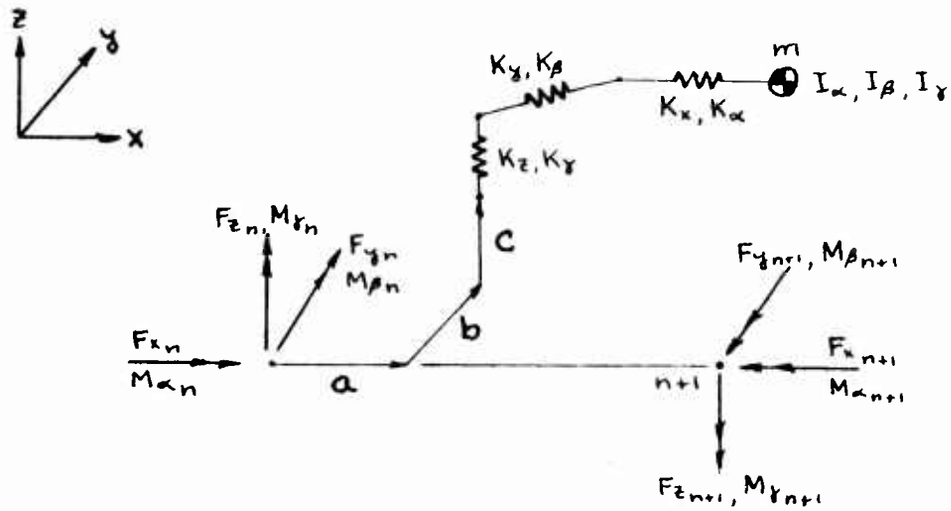

$$\sum F_x = 0 = F_{x_n} + m\mu_x\omega^2(x + c\beta - b\gamma) - F_{x_{n+1}}$$

$$\sum F_y = 0 = F_{y_n} + m\mu_y\omega^2(y - c\alpha + a\gamma) - F_{y_{n+1}}$$

$$\sum F_z = 0 = F_{z_n} + m\mu_z\omega^2(z + b\alpha - a\beta) - F_{z_{n+1}}$$

$$\sum M_\alpha = 0 = M_{\alpha_n} - m\mu_y\omega^2(y - c\alpha + a\gamma)c + m\mu_z\omega^2(z + b\alpha - a\beta)b + I_\alpha\mu_\alpha\omega^2\alpha - M_{\alpha_{n+1}}$$

$$\sum M_\beta = 0 = M_{\beta_n} + m\mu_x\omega^2(x + c\beta - b\gamma)c - m\mu_z\omega^2(z + b\alpha - a\beta)a + I_\beta\mu_\beta\omega^2\beta - M_{\beta_{n+1}}$$

$$\sum M_\gamma = 0 = M_{\gamma_n} - m\mu_x\omega^2(x + c\beta - b\gamma)b + m\mu_y\omega^2(y - c\alpha + a\gamma)a + I_\gamma\mu_\gamma\omega^2\gamma - M_{\gamma_{n+1}}$$

where from simple spring-mass theory, μ represents the amplification factors of the system

$$\mu_x = \frac{1}{1-\left(\frac{\omega}{\omega_x}\right)^2} \qquad \mu_\alpha = \frac{1}{1-\left(\frac{\omega}{\omega_\alpha}\right)^2}$$

$$\mu_Y = \frac{1}{1-\left(\frac{\omega}{\omega_Y}\right)^2} \qquad \mu_\beta = \frac{1}{1-\left(\frac{\omega}{\omega_\beta}\right)^2}$$

$$\mu_z = \frac{1}{1-\left(\frac{\omega}{\omega_z}\right)^2} \qquad \mu_\gamma = \frac{1}{1-\left(\frac{\omega}{\omega_\gamma}\right)^2}$$

and

$$\omega_x^2 = \frac{K_x}{m} \qquad \omega_\alpha^2 = \frac{K_\alpha}{I_\alpha}$$

$$\omega_y^2 = \frac{K_Y}{m} \qquad \omega_\beta^2 = \frac{K_\beta}{I_\beta}$$

$$\omega_z^2 \quad \frac{K_z}{m} \qquad \omega_\gamma^2 = \frac{K_\gamma}{I_\gamma}$$

Thus, since the displacements and stations n and n + 1 are equal the matrix is:

UNCOUPLED SPRUNG MASS MATRIX

$$
\begin{bmatrix} F_z \\ M_\beta \\ F_x \\ X \\ \beta \\ Z \\ F_y \\ M_\gamma \\ M_\alpha \\ \alpha \\ \gamma \\ y \end{bmatrix}_{n+1}
=
\begin{bmatrix}
1 & & & & -m\mu_z a\omega^2 & m\mu_z\omega^2 & & & & m\mu_z b\omega^2 & & \\
 & 1 & & m\mu_x c\omega^2 & m(\mu_z a^2+\mu_x c^2)\omega^2 + I_\beta\mu_\beta\omega^2 & -m\mu_z a\omega^2 & & & & -m\mu_z ab\omega^2 & -m\mu_x bc\omega^2 & \\
 & & 1 & m\mu_x\omega^2 & m\mu_x c\omega^2 & & & & & & -m\mu_x b\omega^2 & \\
 & & & 1 & & & & & & & & \\
 & & & & 1 & & & & & & & \\
 & & & & & 1 & & & & & & \\
 & & & & & & 1 & & & -m\mu_y c\omega^2 & m\mu_y a\omega^2 & m\mu_y\omega^2 \\
 & & & -m\mu_x b\omega^2 & -m\mu_x bc\omega^2 & & & 1 & & -m\mu_y ac\omega^2 & m(\mu_y a^2+\mu_x b^2)\omega^2 + I_\gamma\mu_\gamma\omega^2 & m\mu_y a\omega^2 \\
 & & & & -m\mu_z ab\omega^2 & m\mu_z b\omega^2 & & & 1 & m(\mu_z b^2+\mu_y c^2)\omega^2 + I_\alpha\mu_\alpha\omega^2 & -m\mu_y ac\omega^2 & -m\mu_y c\omega^2 \\
 & & & & & & & & & 1 & & \\
 & & & & & & & & & & 1 & \\
 & & & & & & & & & & & 1
\end{bmatrix}
\cdot
\begin{bmatrix} F_z \\ M_\beta \\ F_x \\ X \\ \beta \\ Z \\ F_y \\ M_\gamma \\ M_\alpha \\ \alpha \\ \gamma \\ y \end{bmatrix}_{n}
$$

where

$$\mu_i = \frac{1}{1 - \frac{\omega^2}{\omega_i^2}} \qquad i = x, y, z, \alpha, \beta, \gamma$$

(b) The coupled force relationship (effective mass matrix), let mass properties be denoted as follows:

$$M = m_1$$
$$I_\beta = m_2$$
$$M = m_3$$
$$M = m_4$$
$$I_\gamma = m_5$$
$$I_\alpha = m_6$$

Let mass motion be denoted as follows (with respect to fuselage):

$$Z_e = e_1$$
$$\beta_e = e_2$$
$$X_e = e_3$$
$$y_e = e_4$$
$$\gamma_e = e_5$$
$$\alpha_e = e_6$$

Let fuselage motion and external forces be denoted as follows:

$$Z = f_1 \qquad F_z = -Q_1$$
$$\beta = f_2 \qquad M_\beta = -Q_2$$
$$X = f_3 \qquad F_X = -Q_3$$
$$y = f_4 \qquad F_Y = -Q_4$$
$$\gamma = f_5 \qquad F_\gamma = -Q_5$$
$$\alpha = f_6 \qquad F_\alpha = -Q_6$$

Let mass frequencies and modes be denoted as follows:

$$\omega_r \begin{cases} e_1^{(r)} \\ e_2^{(r)} \\ e_3^{(r)} \\ e_4^{(r)} \\ e_5^{(r)} \\ e_6^{(r)} \end{cases} \qquad r^{TH} \text{ MODE } (r = 1, 2, 3, 4, 5, 6.)$$

Let the mass motion with respect to fuselage be represented as the sum of all normal modes

$$e_r = \sum_{r=1}^{6} e_r^{(r)} H_r$$

Where H_r is the generalized coordinate in the r^{TH} mode.

The total knetic energy of mass for fuselage and displacements due to external forces and moments is,

$$T = \frac{1}{2} \sum_{i=1}^{6} m_i (\dot{f}_i + \dot{e}_i)^2$$

By substitution, the kinetic energy becomes

$$T = \frac{1}{2} \sum_{i=1}^{6} m_i (\dot{f}_i + \sum_{r=1}^{6} e_i^{(r)} \dot{H}_r)^2$$

or

$$T = \frac{1}{2} \sum_{i=1}^{6} m_i (\dot{f}_i^2 + 2 \dot{f}_i \sum_{r=1}^{6} e_i^{(r)} \dot{H}_r + \sum_{r=1}^{6} e_i^{(r)^2} H_r^2)$$

The total potential energy of system is

$$V = \frac{1}{2} \sum_{r=1}^{6} K_r H_r^2$$

where

K_r = EFFECTIVE SPRING IN r^{TH} MODE

since by orthogonality of normal modes

$$\sum_{i=1}^{6} m_i e_i^{(r)} e_i^{(s)} = 0 \quad \text{FOR } r \neq s$$

The Lagrange equations of motion are as follows:

$$f_i: \quad m_i \ddot{f}_i + \sum_{r=1}^{6} m_i e_i^{(r)} \ddot{H}_r = -Q_i$$

$$H_r: \quad M_r \ddot{H}_r + K_r H_r + \sum_{j=1}^{6} m_j e_j^{(r)} \ddot{f}_j = 0$$

where

$$M_r = \sum_{i=1}^{6} m_i e_i^{(r)^2}$$

Solving for $\ddot{H}_r$ in H_r equation and assuming $f_j = f_{j0} e^{i\omega t}$ (Harmonic Motion)

$$\ddot{H}_r = \frac{\sum_{j=1}^{6} m_j e_j^{(r)} \ddot{f}_j}{M_r \left(\frac{\omega_r^2}{\omega^2} - 1\right)}$$

Substituting in f_i equation ,

$$m_i \ddot{f}_i + \sum_{r=1}^{6} \frac{\sum_{j=1}^{6} m_i m_j e_i^{(r)} e_j^{(r)} \ddot{f}_j}{M_r \left(\frac{\omega_r^2}{\omega^2} - 1 \right)} = -Q_i$$

for simplicity the equation is written

$$m_i \ddot{f}_i + \Delta m_{ij} \ddot{f}_j = -Q_i$$

Since harmonic motion is assumed,

$$m_i f_i \omega^2 + \Delta m_{ij} f_j \omega^2 = Q_i$$

A schematic free body diagram of the effective mass - fuselage combination between stations n and n + 1

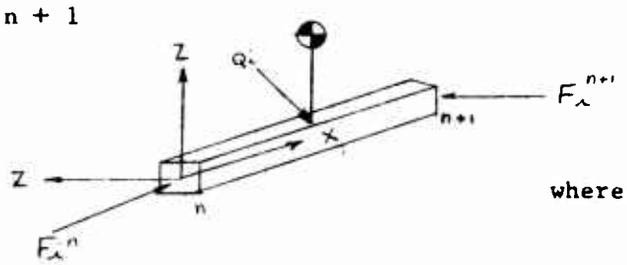

where F_i^n AND F_i^{n+1} are the six components of force at station n and n + 1 respectively

$$\Sigma F_i = 0 = F_i^n + Q_i - F_i^{n+1}$$

or

$$F_i^{n+1} = F_i^n + M_i f_i \omega^2 + \Delta m_{ij} f_j \omega^2$$

Since the position vector of station n + 1 with respect to station n is small, the six displacement components at the two stations are equal. Thus the "effective mass matrix" is written as follows:

COUPLED SPRUNG MASS MATRIX

$$
\begin{bmatrix} F_z \\ M_\beta \\ F_x \\ X \\ \beta \\ Z \\ F_y \\ M_\gamma \\ M_\alpha \\ \alpha \\ \gamma \\ y \end{bmatrix}_{n+1}
=
\begin{bmatrix}
1 & & & \Delta m_{13}\omega^2 & \Delta m_{12}\omega^2 & (m_1+\Delta m_{11})\omega^2 & & & & \Delta m_{16}\omega^2 & \Delta m_{15}\omega^2 & \Delta m_{14}\omega^2 \\
 & 1 & & \Delta m_{23}\omega^2 & (m_2+\Delta m_{22})\omega^2 & \Delta m_{21}\omega^2 & & & & \Delta m_{26}\omega^2 & \Delta m_{25}\omega^2 & \Delta m_{24}\omega^2 \\
 & & 1 & (m_3+\Delta m_{33})\omega^2 & \Delta m_{32}\omega^2 & \Delta m_{31}\omega^2 & & & & \Delta m_{36}\omega^2 & \Delta m_{35}\omega^2 & \Delta m_{34}\omega^2 \\
 & & & 1 & & & & & & & & \\
 & & & & 1 & & & & & & & \\
 & & & & & 1 & & & & & & \\
 & & & \Delta m_{43}\omega^2 & \Delta m_{42}\omega^2 & \Delta m_{41}\omega^2 & 1 & & & \Delta m_{46}\omega^2 & \Delta m_{45}\omega^2 & (m_4+\Delta m_{44})\omega^2 \\
 & & & \Delta m_{53}\omega^2 & \Delta m_{52}\omega^2 & \Delta m_{51}\omega^2 & & 1 & & \Delta m_{56}\omega^2 & (m_5+\Delta m_{55})\omega^2 & \Delta m_{54}\omega^2 \\
 & & & \Delta m_{63}\omega^2 & \Delta m_{62}\omega^2 & \Delta m_{61}\omega^2 & & & 1 & (m_6+\Delta m_{66})\omega^2 & \Delta m_{65}\omega^2 & \Delta m_{64}\omega^2 \\
 & & & & & & & & & 1 & & \\
 & & & & & & & & & & 1 & \\
 & & & & & & & & & & & 1
\end{bmatrix}
\cdot
\begin{bmatrix} F_z \\ M_\beta \\ F_x \\ X \\ \beta \\ Z \\ F_y \\ M_\gamma \\ M_\alpha \\ \alpha \\ \gamma \\ y \end{bmatrix}_{n}
$$

$$
\Delta m_{ij} = \sum_{r=1}^{6} \frac{m_i m_j e_i^{(r)} e_j^{(r)}}{M_r} \left[\frac{1}{\frac{\omega_r^2}{\omega^2} - 1} \right] \; ; \quad M_r = \sum_{i=1}^{6} m_i e_i^{(r)^2}
$$

Force Matrix

A mathematical device which permits simulation of a forcing function placed anywhere along the fuselage of an aircraft is the force matrix. Suppose a station, n, is subjected to a forcing function having six components, then these external forces induce additional loads on the vibrating structure.

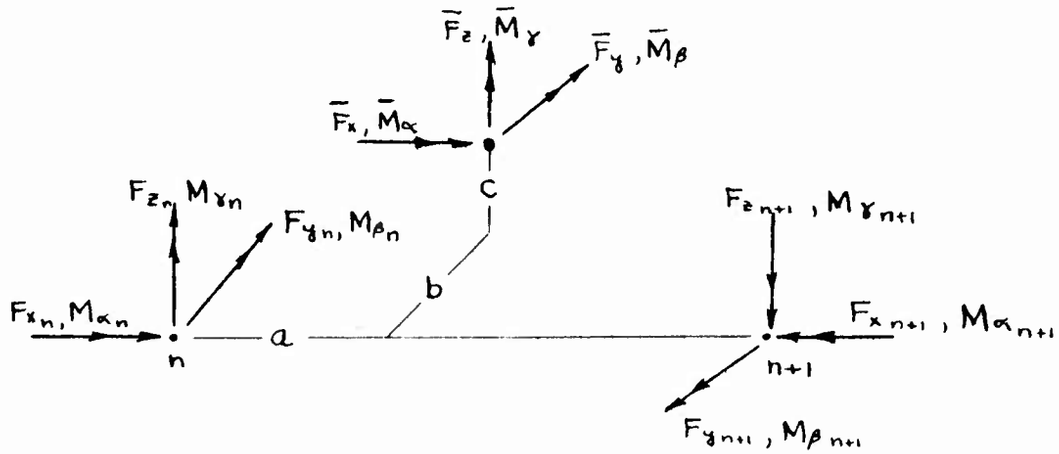

$$\sum F_x = 0 = F_{x_n} + \bar{F}_x - F_{x_{n+1}}$$

$$\sum F_y = 0 = F_{y_n} + \bar{F}_y - F_{y_{n+1}}$$

$$\sum F_z = 0 = F_{z_n} + \bar{F}_z - F_{z_{n+1}}$$

$$\sum M_\alpha = 0 = M_{\alpha_n} - c\bar{F}_y + b\bar{F}_z - M_{\alpha_{n+1}} + \bar{M}_\alpha$$

$$\sum M_\beta = 0 = M_{\beta_n} + c\bar{F}_x - a\bar{F}_z - M_{\beta_{n+1}} + \bar{M}_\beta$$

$$\sum M_\gamma = 0 = M_\gamma - b\bar{F}_x + a\bar{F}_y - M_{\gamma_{n+1}} + \bar{M}_\gamma$$

In general, the forcing function, $\bar{F}_{ij}$, is of the form

$$\bar{F} = F_0 + F_1 \cos \psi_n + F_2 \sin \psi_n$$

where ψ_n is harmonic azimuth angle

Since the forcing function must be added to the inertial and elastic forces applied to the fuselage, the forces are handled by adding a 13th row and column to the previous 12 x 12 matrix.

This 13 x 13 force matrix requires that all the previously derived matrices be padded from 12 x 12 matrices to 13 x 13.

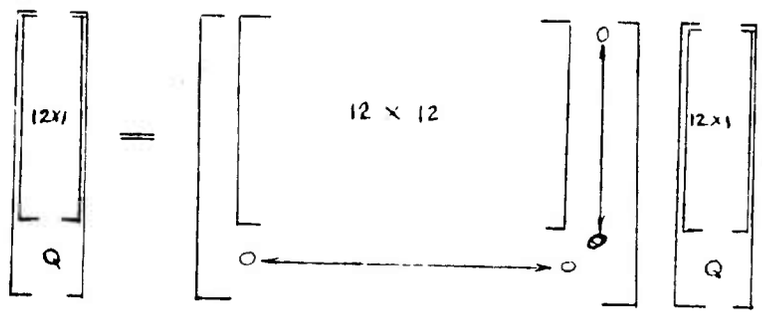

FORCE MATRIX

F_z	1												$F_{uz} + F_{cz}\cos\psi_n + F_{sz}\sin\psi_n$	F_z
M_β		1											$M_{u\beta} + C_F F_{ux} - a_F F_{uz} + (M_{c\beta} + C_F F_{cx} - a_F F_{cz})\cos\psi_n + (M_{s\beta} + C_F F_{sx} - a_F F_{sz})\sin\psi_n$	M_β
F_x			1										$F_{ux} + F_{cx}\cos\psi_n + F_{sx}\sin\psi_n$	F_x
X				1										X
β					1									β
Z						1								Z
F_y							1						$F_{uy} + F_{cy}\cos\psi_n + F_{sy}\sin\psi_n$	F_y
M_γ								1					$M_{u\gamma} + a_F F_{uy} - b_F F_{ux} + (M_{c\gamma} + a_F F_{cy} - b_F F_{cx})\cos\psi_n + (M_{s\alpha} - C_F F_{sy} + b_F F_{sz})\sin\psi_n$	M_γ
M_α									1				$M_{u\alpha} - C_F F_{uy} + b_F F_{uz} + (M_{c\alpha} - C_F F_{cy} + b_F F_{cz})\cos\psi_n + (M_{s\alpha} - C_F F_{sy} + b_F F_{sz})\sin\psi_n$	M_α
α										1				α
γ											1			γ
y												1		y
Q													1	Q

$n+1$ $\qquad$ n

F_{ux}, F_{uy}, F_{uz} Unit Forces (lb.)
$M_{u\alpha}, M_{u\beta}, M_{u\gamma}$ Unit Moments (In.#)
F_{cx}, F_{cy}, F_{cz} Cos Force Coefficients (#)
$M_{c\alpha}, M_{c\beta}, M_{c\gamma}$ Cos Moment Coefficients (In.#)

F_{sx}, F_{sy}, F_{sz} Sin Force Coefficients (#)
$M_{s\alpha}, M_{s\beta}, M_{s\gamma}$ Sin Moment Coefficients (In.#)
ψ_n Harmonic Azimuth (deg.)
a_F, b_F, c_F Long, Lat. & Vert. Force Locations (

General Matrix

The general matrix shown below was placed in the computer program to permit the formation of any additional matrices needed in the coupled vertical-lateral matrix analysis.

GENERAL MATRIX

$$
\begin{bmatrix} F_z \\ M_\beta \\ F_x \\ X \\ \beta \\ Z \\ F_y \\ M_\gamma \\ M_\alpha \\ \alpha \\ \gamma \\ y \\ Q \end{bmatrix}_{n+1}
=
\begin{bmatrix}
a_{1-1} & a_{1-2} & a_{1-3} & a_{1-4} & a_{1-5} & a_{1-6} & a_{1-7} & a_{1-8} & a_{1-9} & a_{1-10} & a_{1-11} & a_{1-12} & a_{1-13} \\
a_{2-1} & & & & & & & & & & & & \\
a_{3-1} & & & & & & & & & & & & \\
a_{4-1} & & & & & & & & & & & & \\
a_{5-1} & & & & & & & & & & & & \\
a_{6-1} & & & & & & & & & & & & \\
a_{7-1} & & & & & & & & & & & & \\
a_{8-1} & & & & & & & & & & & & \\
a_{9-1} & & & & & & & & & & & & \\
a_{10-1} & & & & & & & & & & & & \\
a_{11-1} & & & & & & & & & & & & \\
a_{12-1} & & & & & & & & & & & & \\
a_{13-1} & & & & & & & & & & & &
\end{bmatrix}
\begin{bmatrix} F_z \\ M\beta \\ F_x \\ X \\ \beta \\ Z \\ F_y \\ M_\gamma \\ M_\alpha \\ \alpha \\ \gamma \\ y \\ Q \end{bmatrix}_{n}
$$

Frame Racking Matrix

From deflection tests of the H-21 helicopter, it was noted that frame racking occurs in the vertical and lateral directions in the "constant section" portion of the fuselage. If elementary beam theory is used in conjunction with test data, an elastic matrix which describes the force-displacement relationship in the "constant section" may be derived.

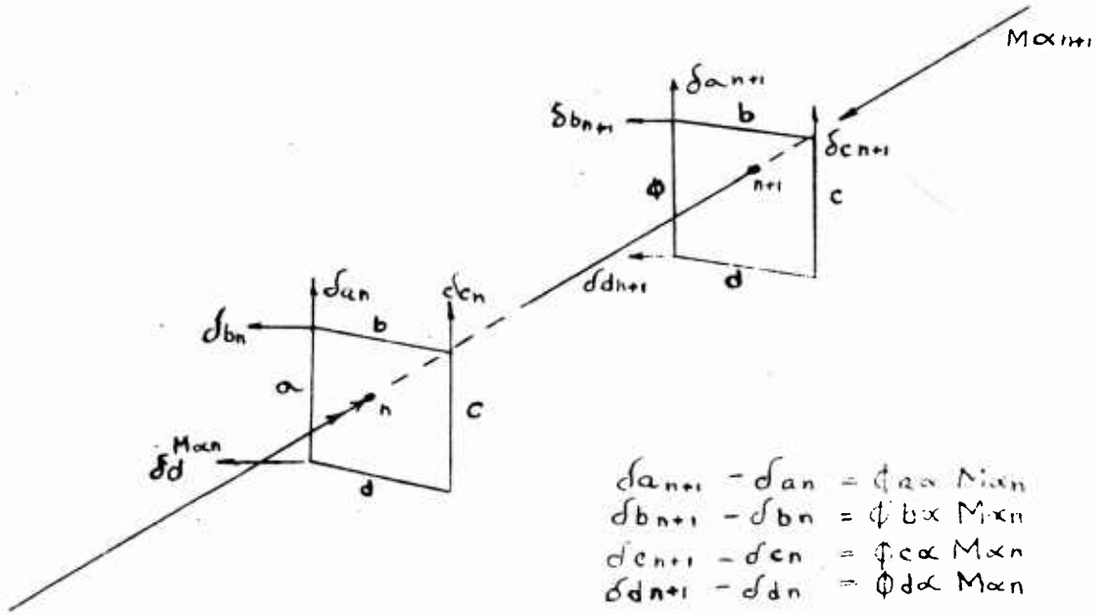

$$\delta a_{n+1} - \delta a_n = \phi_{a\alpha} M\alpha_n$$
$$\delta b_{n+1} - \delta b_n = \phi_{b\alpha} M\alpha_n$$
$$\delta c_{n+1} - \delta c_n = \phi_{c\alpha} M\alpha_n$$
$$\delta d_{n+1} - \delta d_n = \phi_{d\alpha} M\alpha_n$$

The deflections δa_n, δb_n, δc_n, δd_n, δa_{n+1}, δb_{n+1}, δc_{n+1} AND δd_{n+1} came from test data for a unit torsional moment, $M\alpha_n$ thus from the above equations the racking coefficients $\phi_{a\alpha}$, $\phi_{b\alpha}$ $\phi_{c\alpha}$, and $\phi_{d\alpha}$ were computed.

Having the racking coefficients for relative translations in the vertical direction, enables calculation of the relative vertical translation at any point in the fuselage and the relative rotation about the longitudinal axis

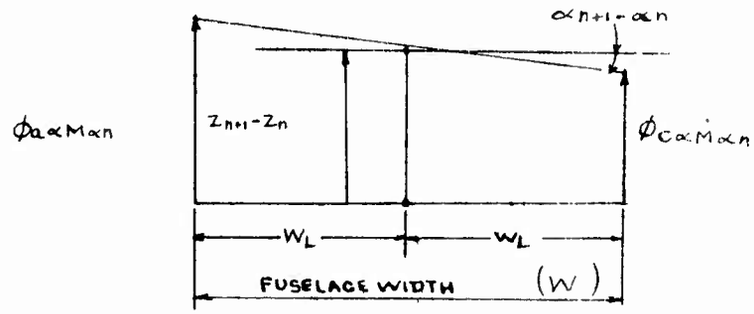

LOOKING AFT

Thus

$$\alpha_{n+1}-\alpha_n = \frac{(\phi_{\alpha a} - \phi_{c\alpha}) M_{\alpha n}}{W}$$

$$Z_{n+1}-Z_n = \phi_{c\alpha} M_{\alpha n} + (\alpha_{n+1}-\alpha_n) W_1$$

Replacing the relative rotation in the above equation

$$Z_{n+1}-Z_n = \left(1-\frac{W_1}{W}\right)\phi_{c\alpha} M_{\alpha n} + \frac{W_1}{W}\phi_{a\alpha} M$$

Likewise, using the lateral racking coefficients

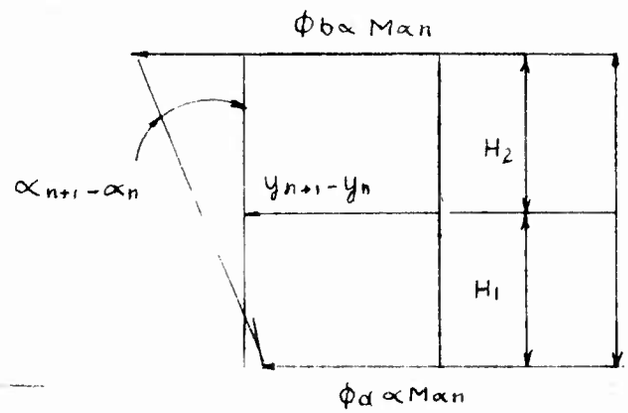

FUSELAGE HEIGHT (H)

$$\alpha_{n+1}-\alpha_n = \frac{(\phi_{b\alpha} - \phi_{d\alpha}) M_{\alpha n}}{H}$$

$$y_{n+1}-y_n = \phi_{b\alpha} M_{\alpha n} - (\alpha_{n+1}-\alpha_n) H_2$$

Placing the relative rotation in the above equating

$$Y_{n+1}-Y_n = \left(1-\frac{H_2}{H}\right)\phi_{b\alpha} M_{\alpha n} + \frac{H_2}{H}\phi_{d\alpha} M_{\alpha n}$$

Thus, if the equations for vertical and lateral translation and longitudinal rotation are added to the equations comprising the existing elastic matrix, the result is an elastic matrix which includes frame racking.

$$
\begin{bmatrix} F_z \\ M_\beta \\ F_x \\ X \\ \beta \\ Z \\ F_y \\ M_\gamma \\ M_\alpha \\ \alpha \\ \gamma \\ \gamma \\ Q \end{bmatrix}_{n+1}
=
\underbrace{\begin{bmatrix}
1 & & & & & & & & & & & & \\
L & 1 & & & & & & & & & & & \\
 & & 1 & & & & & & & & & & \\
 & & -\frac{L}{A_x E} & 1 & & & & & & & & & \\
-\frac{L^2}{2EI_y} & -\frac{L}{EI_y} & & & 1 & & & & & & & & \\
\frac{L^3}{6EI_y} - \frac{L}{A_z G} & \frac{L^2}{2EI_y} & & & -L & 1 & & & \phi_{c\alpha}\left[1 - \frac{W_1}{W}\right] + \phi_{a\alpha}\frac{W_1}{W} & & & & \\
 & & & & & & 1 & & & & & & \\
 & & & & & & -L & 1 & & & & & \\
 & & & & & & & & 1 & & & & \\
 & & & & & & & & A & 1 & & & \\
 & & & & & & \frac{L^2}{2EI_z} & -\frac{L}{EI_z} & & & 1 & & \\
 & & & & & & \frac{L^3}{6EI_z} - \frac{L}{A_y G} & -\frac{L^2}{2EI_z} & \phi_{b\alpha}\left[1 - \frac{H_2}{H}\right] + \phi_{d\alpha}\frac{H_2}{H} & & L & 1 & \\
 & & & & & & & & & & & & 1
\end{bmatrix}}_{E_2}
\cdot
\begin{bmatrix} F_z \\ M_\beta \\ F_x \\ X \\ \beta \\ Z \\ F_y \\ M_\gamma \\ M_\alpha \\ \alpha \\ \gamma \\ \gamma \\ Q \end{bmatrix}_{n}
$$

WHERE $A = \left[\frac{\phi_{a\alpha} - \phi_{c\alpha}}{W}\right]$ OR $\left[\frac{\phi_{d\alpha} - \phi_{b\alpha}}{H}\right]$

The frame racking matrix in the lateral and vertical direction is used with neutral axis and shear center axis shift matrices developed earlier. The subdivided elastic matrix can be written as,

$$\left[\overline{E}\right] = \left[\overline{E_3}\right]\left[\overline{E_2}\right]\left[\overline{E_1}\right]$$

Input required for E_1, E_2, E_3 matrices shown on the following pages.

b_n, Dist. from the ref. axis to the neutral axis in the y direction (in.)

C_n, Dist. from the ref. axis to the neutral axis in the z direction (in.)

A_x, Axial Compression area (in^2)

A_y, effective shear area in the y direction (in^2)

A_z, effective shear area in the z direction (in^2)

I_y, Bending stiffness about the y axis (in^4)

I_z, Bending stiffness about the z axis (in^4)

E, Bending modulus ($\#/in^2$)

G, Shear modulus ($\#/in^2$)

L, Elastic bay length (in)

$\phi_a \alpha$, Linear deflection at the right side of the frame from a unit moment (1/#)

$\phi_b \alpha$, Linear deflection at the top section of the frame from a unit moment (1/#)

$\phi_c \alpha$, Linear deflection at the left side of the frame from a unit moment (1/#)

$\phi_d \alpha$, Linear deflection at the bottom section of the frame from a unit moment (1/#)

W, Lateral distance between longerons (in.)

W_1, Lateral distance from the reference axis to the right longeron (in.)

H, Vertical distance between longerons (in.)

H_2, Vertical distance from the reference axis to the upper longeron (in.)

$$[E_1]$$

$$
\begin{bmatrix} F_z \\ M_\beta \\ F_x \\ x \\ \beta \\ z \\ F_y \\ M_\gamma \\ M_\alpha \\ \alpha \\ \gamma \\ y \\ Q \end{bmatrix}
=
\begin{bmatrix}
1 & & & & & & & & & & & & \\
 & 1 & -a_N & & & & & & & & & & \\
 & & 1 & & & & & & & & & & \\
 & & & 1 & a_N & & & & & & -b_N & & \\
 & & & & 1 & & & & & & & & \\
 & & & & & 1 & & & & & & & \\
 & & & & & & 1 & & & & & & \\
 & & b_N & & & & & 1 & & & & & \\
 & & & & & & & & 1 & & & & \\
 & & & & & & & & & 1 & & & \\
 & & & & & & & & & & 1 & & \\
 & & & & & & & & & & & 1 & \\
 & & & & & & & & & & & & 1
\end{bmatrix}
\cdot
\begin{bmatrix} F_z \\ M_\beta \\ F_x \\ x \\ \beta \\ z \\ F_y \\ M_\gamma \\ M_\alpha \\ \alpha \\ \gamma \\ y \\ Q \end{bmatrix}
$$

$$[E_3]$$

$$
\begin{bmatrix} F_z \\ M_\beta \\ F_\chi \\ X \\ \beta \\ Z \\ F_y \\ M_\gamma \\ M_\alpha \\ \alpha \\ \gamma \\ y \\ Q \end{bmatrix}_{n+1}
=
\begin{bmatrix}
1 & & & & & & & & & & & & \\
 & 1 & C_N & & & & & & & & & & \\
 & & 1 & & & & & & & & & & \\
 & & & 1 & -C_N & & & & & & b_N & & \\
 & & & & 1 & & & & & & & & \\
 & & & & & 1 & & & & & & & \\
 & & & & & & 1 & & & & & & \\
 & & -b_N & & & & & 1 & & & & & \\
 & & & & & & & & 1 & & & & \\
 & & & & & & & & & 1 & & & \\
 & & & & & & & & & & 1 & & \\
 & & & & & & & & & & & 1 & \\
 & & & & & & & & & & & & 1
\end{bmatrix}
\cdot
\begin{bmatrix} F_z \\ M_\beta \\ F_\chi \\ X \\ \beta \\ Z \\ F_y \\ M_\gamma \\ M_\alpha \\ \alpha \\ \gamma \\ y \\ Q \end{bmatrix}_{n}
$$

FRAME RACKING MATRIX (COLLAPSED)

1												
L	1											
		1										
$\frac{C_N L^2}{2EI_y}$	$\frac{C_N L}{EI_y}$	$-\frac{C_N^2 L}{EI_y} - \frac{L}{A_x E} - \frac{b_N^2 L}{EI_z}$	1			$\frac{b_N L^2}{2EI_z}$	$-\frac{b_N L}{EI_z}$					
$-\frac{L^2}{2EI_y}$	$-\frac{L}{EI_y}$	$\frac{C_N L}{EI_y}$		1								
$\frac{L^3}{6EI_y} - \frac{L}{A_z G}$	$\frac{L^2}{2EI_y}$	$-\frac{C_N L^2}{2EI_y}$		$-L$	1			$\phi_{c\alpha}\left[1-\frac{W_1}{W}\right] + \phi_{a\alpha}\frac{W_1}{W}$				
						1						
						$-L$	1					
								1				
								A	1			
		$-\frac{b_N L}{EI_z}$				$\frac{L^2}{2EI_z}$	$-\frac{L}{EI_z}$			1		
		$-\frac{b_N L^2}{2EI_z}$				$\frac{L^3}{6EI_z} - \frac{L}{A_y G}$	$-\frac{L^2}{2EI_z}$	$\phi_{b\alpha}\left[1-\frac{H_2}{H_1}\right] + \phi_{d\alpha}\frac{H_2}{H}$		L	1	
												1

Where, $A = \left[\frac{\phi_{a\alpha} - \phi_{c\alpha}}{W}\right]$ OR $\left[\frac{\phi_{d\alpha} - \phi_{b\alpha}}{H}\right]$

(The largest absolute value of "A" is to be used in this matrix)

EFFECTIVE WING MATRIX

Inclusion of the floating fuel wings in the representation requires an effective wing matrix which transmit the inertial loads of the wing to the fuselage beam station. Consider the plan view of the fuselage-wing as shown below.

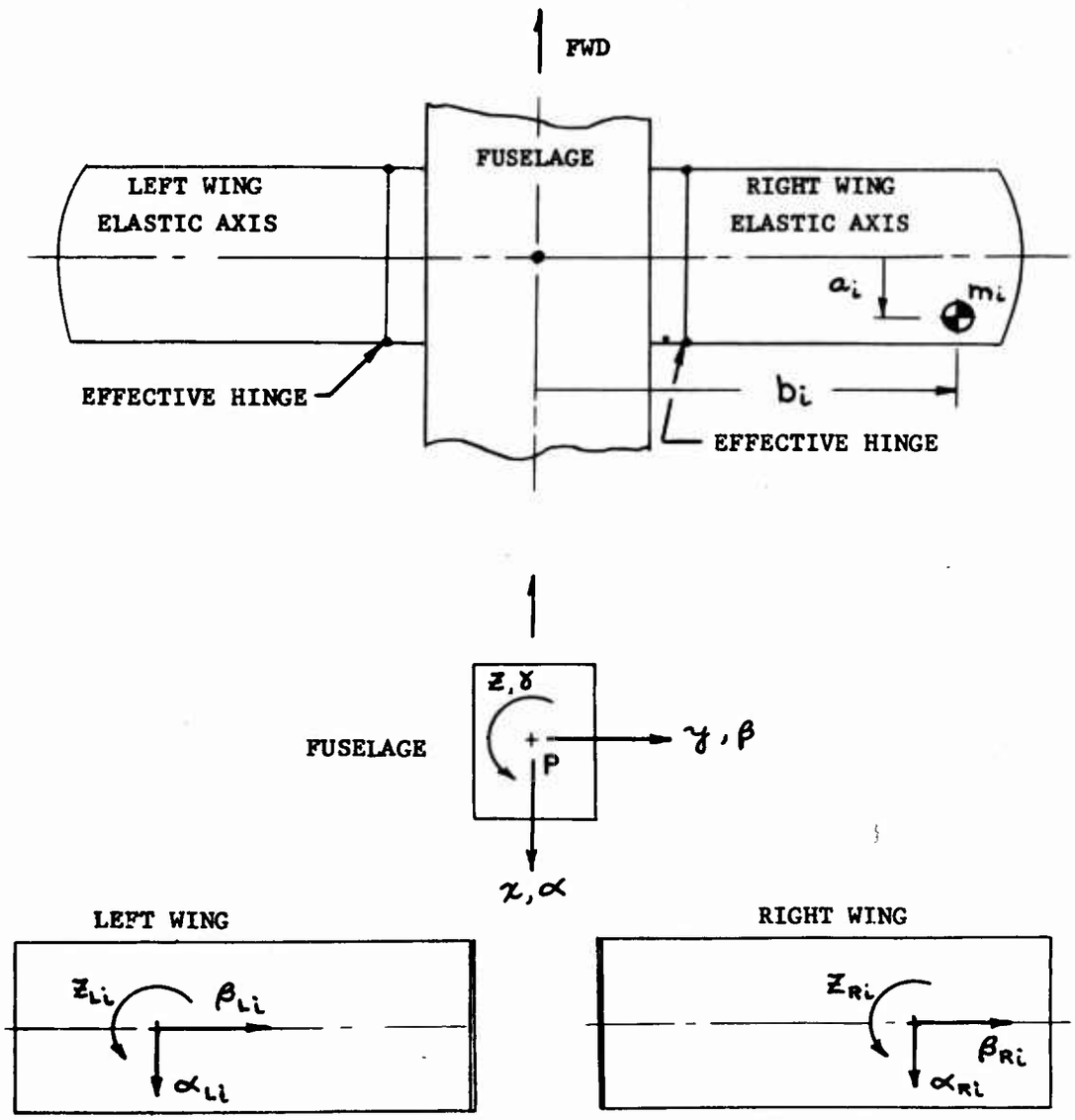

$x, y, z, \alpha, \beta, \gamma$ GENERAL DISPLACEMENTS OF FUSELAGE

$z_{Li}, \beta_{Li}, \alpha_{Li}$ Displacements of left wing

$z_{Ri}, \beta_{Ri}, \alpha_{Ri}$ Displacements of right wing

where,

$$z_{Li} = \sum_{S=1}^{S} z_L^{(S)} H_S \qquad z_{Ri} = \sum_{S=1}^{S} z_R^{(S)} H_S$$

$$\beta_{Li} = \sum_{S=1}^{S} \beta_L^{(S)} H_S \qquad \beta_{Ri} = \sum_{S=1}^{S} \beta_R^{(S)} H_S$$

$$\alpha_{Li} = \sum_{S=1}^{S} \alpha_L^{(S)} H_S \qquad \alpha_{Ri} = \sum_{S=1}^{S} \alpha_R^{(S)} H_S$$

and H_S, generalized coordinate in the "S"th wing mode

The right wing elemental mass motion is,

$$\bar{x}_i = x - b_i \gamma$$

$$\bar{y}_i = y + a_i \gamma$$

$$\bar{z}_i = z + b_i \alpha - a_i \beta + z_i - a_i \beta_i$$

Summing along the wing, the kinetic energy of the right wing is,

$$T = \frac{1}{2} \sum m_i \left\{ \begin{array}{l} (\dot{x} - b_i \dot{\gamma})^2 \\ + (\dot{y} + a_i \dot{\gamma})^2 \\ + (\dot{z} + b_i \dot{\alpha} - a_i \dot{\beta} + z_i - a_i \dot{\beta}_i)^2 \end{array} \right\}$$

$$+ \frac{1}{2} \sum \left\{ I_{\alpha i} (\dot{\alpha} + \alpha_i)^2 + I_{\beta i} (\dot{\beta} + \dot{\beta}_i)^2 + I_{\gamma i} (\dot{\gamma} + \dot{\gamma}_i)^2 \right\}$$

Expressing the right wing generalized loads in matrix form as a function of displacement

$$
\begin{bmatrix} F_x \\ F_y \\ F_z \\ M_\alpha \\ M_\beta \\ M_\gamma \end{bmatrix}
=
\begin{bmatrix}
\omega^2\sum m_i & & & & & -\omega^2\sum m_i b_i \\
 & \omega^2\sum m_i & & & & \omega^2\sum m_i a_i \\
 & & \omega^2\sum m_i + \sum_s \frac{\sigma_z^2\,\omega^2}{I_s\left(\frac{\omega_s^2}{\omega^2}-1\right)} & \omega^2\sum m_i b_i + \sum_s \frac{\sigma_z\,\sigma_\alpha\,\omega^2}{I_s\left(\frac{\omega_s^2}{\omega^2}-1\right)} & -\omega^2\sum m_i a_i + \sum_s \frac{\sigma_z\,\sigma_\beta\,\omega^2}{I_s\left(\frac{\omega_s^2}{\omega^2}-1\right)} & \\
 & & \omega^2\sum m_i b_i + \sum_s \frac{\sigma_\alpha\,\sigma_z\,\omega^2}{I_s\left(\frac{\omega_s^2}{\omega^2}-1\right)} & \omega^2\sum(m_i b_i^2 + I_\alpha) + \sum_s \frac{\sigma_\alpha^2\,\omega^2}{I_s\left(\frac{\omega_s^2}{\omega^2}-1\right)} & -\omega^2\sum m_i a_i b_i + \sum_s \frac{\sigma_\alpha\,\sigma_\beta\,\omega^2}{I_s\left(\frac{\omega_s^2}{\omega^2}-1\right)} & \\
 & & -\omega^2\sum m_i a_i^2 + \sum_s \frac{\sigma_\beta\,\sigma_z\,\omega^2}{I_s\left(\frac{\omega_s^2}{\omega^2}-1\right)} & -\omega^2\sum m_i a_i b_i + \sum_s \frac{\sigma_\beta^2\,\omega^2}{I_s\left(\frac{\omega_s^2}{\omega^2}-1\right)} & \omega^2\sum(m_i a^2 + I_\beta) + & \\
\omega^2\sum m_i b_i & \omega^2\sum m_i a_i & & & & \omega^2\sum(m_i a_i^2 + m_i b_i^2 + I_\gamma)
\end{bmatrix}
\begin{bmatrix} x \\ y \\ z \\ \alpha \\ \beta \\ \gamma \end{bmatrix}
$$

In terms of the effective spring, K_e in each mode, the potential energy of the right wing is

$$V = \frac{1}{2}\sum_{s=1}^{6} K_e^{(s)} H_s$$

where,

$$K_e^{(s)} = I_s\,\omega_s^2$$

Applying Lagrange's equation, the right wing equations of motion are,

$$x \qquad \left(\sum_i m_i\right)\ddot{x} + \left(-\sum_i m_i b_i\right)\ddot{\gamma} = F_x$$

$$y \qquad \left(\sum_i m_i\right)\ddot{y} + \left(\sum_i m_i a_i\right)\ddot{\gamma} = F_y$$

$$z \qquad \left(\sum_i m_i\right)\ddot{z} + \left(\sum_i m_i b_i\right)\ddot{\alpha} + \left(-\sum m_i a_i\right)\ddot{\beta} + \left[\sum m_i\left(z_i^{(s)} - a_i\beta_i^{(s)}\right)\right]\ddot{H}_s = F_z$$

$$\alpha \quad \left[\sum_i (m_i b_i^2 + I_{\alpha i})\right]\ddot{\alpha} + \left(\sum_i m_i b_i\right)\ddot{z} + \left(-\sum m_i a_i b_i\right)\ddot{\beta}$$
$$+\left[\sum_i m_i b_i (z_i^{(s)} - a_i \beta_i^{(s)}) + \sum_i I_{\alpha i}\alpha_i^{(s)}\right]\ddot{H}_s = M_\alpha$$

$$\beta \quad \left[\sum_i (m_i a_i^2 + I_{\beta i})\right]\ddot{\beta} + \left(-\sum_i m_i a_i\right)\ddot{z} + \left(-\sum_i m_i a_i b_i\right)\ddot{\alpha}$$
$$+\left[-\sum_i m_i a_i (z_i^{(s)} - a_i \beta_i^{(s)}) + \sum_i I_{\beta i}\beta_i^{(s)}\right]\ddot{H}_s = M_\beta$$

$$\gamma \quad \left[\sum_i (m_i a_i^2 + m_i b_i^2 + I_{\gamma i})\right]\ddot{\gamma} + \left(-\sum_i m_i b_i\right)\ddot{x} + \left(\sum_i m_i a_i\right)\ddot{y} = M_\gamma$$

$$H_s \quad \left[\sum_i m_i (z_i^{(s)} - a_i \beta_i^{(s)})^2 + I_{\alpha i}\alpha_i^{(s)2} + I_{\beta i}\beta_i^{(s)2}\right]\ddot{H}_s + K_s H_s$$
$$+\left[\sum_i m_i (z_i^{(s)} - a_i \beta_i^{(s)})\right]\ddot{z} + \left[\sum_i m_i b_i (z_i^{(s)} - a_i \beta_i^{(s)}) + \sum_i I_\alpha \alpha_i^{(s)}\right]\ddot{\alpha}$$
$$+\left[-\sum_i m_i a_i (z_i^{(s)} - a_i \beta_i^{(s)}) + \sum_i I_\beta \beta_i^{(s)}\right]\ddot{\beta} = 0$$

Similarly, the left wing generalized loads are obtained and then, combined with the right wing to obtain the following expressions.

$$\begin{bmatrix} F_x \\ F_y \\ F_z \\ M_\alpha \\ M_\beta \\ M_\gamma \end{bmatrix} = \begin{bmatrix} M\omega^2 & & & & & \\ & M\omega^2 & & & & Ma\omega^2 \\ & & M\omega^2 + \sum_s \frac{2\sigma_{zs}^2\omega^2}{I_s\left(\frac{\omega_s^2}{\omega^2}-1\right)} & & -Ma\omega^2 + \sum_s \frac{2\sigma_{zs}\sigma_{\beta s}\omega^2}{I_s\left(\frac{\omega_s^2}{\omega^2}-1\right)} & \\ & & & I_\alpha\omega^2 + \sum_s \frac{2\sigma_{\alpha s}^2\omega^2}{I_s\left(\frac{\omega_s^2}{\omega^2}-1\right)} & & \\ & & -Ma\omega^2 + \sum_s \frac{2\sigma_z\sigma_\beta\omega^2}{I_s\left(\frac{\omega_s^2}{\omega^2}-1\right)} & & I_\beta\omega^2 + \sum_s \frac{2\sigma_\beta^2\omega^2}{I_s\left(\frac{\omega_s^2}{\omega^2}-1\right)} & \\ & Ma\omega^2 & & & & I_\gamma\omega^2 \end{bmatrix} \begin{bmatrix} x \\ y \\ z \\ \alpha \\ \beta \\ \gamma \end{bmatrix}$$

Combining the deflections with the above load expression, the effective wing matrix is,

EFFECTIVE WING MATRIX
(H-21 RANGE EXTENSION)

F_z		1				$-2Ma_{cg}\omega^2 + \sum_s \frac{2\sigma_{\beta s}\omega^2\sigma_z}{I_s\left(\frac{\omega_s^2}{\omega^2}-1\right)}$	$2M\omega^2 + \sum_s \frac{2\sigma_{zs}^2\omega^2}{I_s\left(\frac{\omega_s^2}{\omega^2}-1\right)}$								F_z
M_β			1			$2I_\beta\omega^2 + \sum_s \frac{2\sigma_{\beta s}^2\omega^2}{I_s\left(\frac{\omega_s^2}{\omega^2}-1\right)}$	$-2Ma_{cg}\omega^2 + \sum_s \frac{2\sigma_{zs}\sigma_{\beta s}\omega^2}{I_s\left(\frac{\omega_s^2}{\omega^2}-1\right)}$								M_β
F_x				1	$2M\omega^2$										F_x
x					1										x
β						1									β
z							1								z
F_y	=							1				$2Ma_{cg}\omega^2$	$2M\omega^2$		F_y
M_γ									1			$2I_\gamma\omega^2$	$2Ma_{cg}\omega^2$		M_γ
M_α										1	$2I_\alpha\omega^2 + \sum_s \frac{2\sigma_{\alpha s}^2\omega^2}{I_s\left(\frac{\omega_s^2}{\omega^2}-1\right)}$				M_α
α											1				α
γ												1			γ
$\tilde{\gamma}$													1		$\tilde{\gamma}$
Q														1	Q

$n+1$ $\qquad$ n

APPENDIX B

METHOD OF SOLUTION FOR COUPLED MATRIX PROGRAM

Method of Solution - Free Vibration

These matrices are now "building blocks" from which a dynamic representation of the helicopter fuselage may be constructed.

The boundary conditions for such a representative helicopter fuselage are that the loads F_x, F_y, F_z, M_α, M_b and M_γ just before the forward rotor mass and just after the aft rotor mass are zero, that is a "free-free" beam. Even ground springs do not affect the boundary conditions, because they are taken to act on the fuselage side before the boundaries are reached. Matrix multiplications from the forward to aft rotor are conducted repeatedly for trial frequencies, until the boundary conditions are met. Note that since the forward end boundary conditions, $F_x = F_y = F_z = M_\alpha = M_b = M_\gamma = 0$, appear in the single column end matrix, and since only these forces need be determined for comparison with the aft end boundary conditions, it is then necessary to use only the terms shown on the next page in the final collapsed matrix for the frequency calculation.

$$
\begin{bmatrix} F_z \\ M_\beta \\ F_\gamma \\ X \\ \beta \\ Z \\ F_\eta \\ M_\gamma \\ M_\alpha \\ \alpha \\ \gamma \\ \gamma \end{bmatrix}
=
\begin{bmatrix}
 & & & a_{14} & a_{15} & a_{16} & & & & a_{110} & a_{111} & a_{112} \\
 & & & a_{24} & a_{25} & a_{26} & & & & a_{210} & a_{211} & a_{212} \\
 & & & a_{34} & a_{35} & a_{36} & & & & a_{310} & a_{311} & a_{312} \\
 & & & & & & & & & & & \\
 & & & & & & & & & & & \\
 & & & & & & & & & & & \\
 & & & a_{74} & a_{75} & a_{76} & & & & a_{710} & a_{711} & a_{712} \\
 & & & a_{84} & a_{85} & a_{86} & & & & a_{810} & a_{811} & a_{812} \\
 & & & a_{94} & a_{95} & a_{96} & & & & a_{910} & a_{911} & a_{912} \\
 & & & & & & & & & & & \\
 & & & & & & & & & & & \\
 & & & & & & & & & & &
\end{bmatrix}
\cdot
\begin{bmatrix} \\ \\ \\ X \\ \beta \\ Z \\ \\ \\ \\ \alpha \\ \gamma \\ \gamma \end{bmatrix}
$$

Aft End **Fwd End**

Repeated trials of frequency, w, are made, and each one of the thirty-six terms shown above are obtained numerically. To meet the boundary requirement, the residual, Δ, of the matrix array must be zero.

$$
\Delta =
\begin{bmatrix}
a_{14} & a_{15} & a_{16} & a_{110} & a_{111} & a_{112} \\
a_{24} & a_{25} & a_{26} & a_{210} & a_{211} & a_{212} \\
a_{34} & a_{35} & a_{36} & a_{310} & a_{311} & a_{312} \\
a_{74} & a_{75} & a_{76} & a_{710} & a_{711} & a_{712} \\
a_{84} & a_{85} & a_{86} & a_{810} & a_{811} & a_{812} \\
a_{94} & a_{95} & a_{96} & a_{910} & a_{911} & a_{912}
\end{bmatrix}
= 0
$$

In practice, the residual may be plotted against the frequency trials, and when

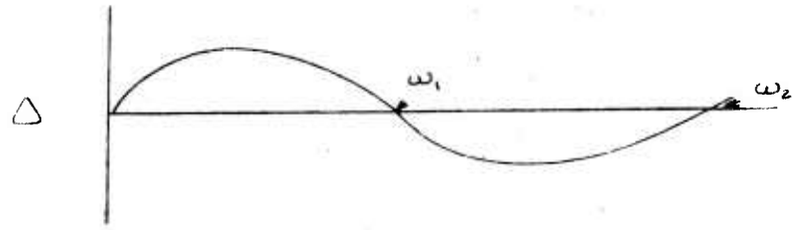

a zero intersection occurs, natural frequencies $\omega_1, \omega_2 \cdots\cdots \omega_n$ are determined.

For each natural mode, it is desirable to normalize in terms of the largest relative linear deflection value which exist at the ends of the beam. Now, calculating the relative linear deflections at both ends of the beam.

Rewriting the collapsed matrix with the zero columns removed,

$$
\begin{bmatrix} \\ \\ \\ X \\ \beta \\ Z \\ \\ \\ \\ \alpha \\ \gamma \\ \gamma \end{bmatrix}
\begin{bmatrix}
a_{14} & a_{15} & a_{16} & a_{1\bar{0}} & a_{1\bar{1}} & a_{1\bar{2}} \\
a_{24} & a_{25} & a_{26} & a_{2\bar{0}} & a_{2\bar{1}} & a_{2\bar{2}} \\
a_{34} & a_{35} & a_{36} & a_{3\bar{0}} & a_{3\bar{1}} & a_{3\bar{2}} \\
a_{44} & a_{45} & a_{46} & a_{4\bar{0}} & a_{4\bar{1}} & a_{4\bar{2}} \\
a_{64} & a_{55} & a_{56} & a_{5\bar{0}} & a_{5\bar{1}} & a_{5\bar{2}} \\
a_{64} & a_{65} & a_{66} & a_{6\bar{0}} & a_{6\bar{1}} & a_{6\bar{2}} \\
a_{74} & a_{75} & a_{76} & a_{7\bar{0}} & a_{7\bar{1}} & a_{7\bar{2}} \\
a_{84} & a_{85} & a_{86} & a_{8\bar{0}} & a_{8\bar{1}} & a_{8\bar{2}} \\
a_{94} & a_{95} & a_{96} & a_{9\bar{0}} & a_{9\bar{1}} & a_{9\bar{2}} \\
a_{\bar{0}4} & a_{\bar{0}5} & a_{\bar{0}6} & a_{\bar{0}\bar{0}} & a_{\bar{0}\bar{1}} & a_{\bar{0}\bar{2}} \\
a_{\bar{1}4} & a_{\bar{1}5} & a_{\bar{1}6} & a_{\bar{1}\bar{0}} & a_{\bar{1}\bar{1}} & a_{\bar{1}\bar{2}} \\
a_{\bar{2}4} & a_{\bar{2}5} & a_{\bar{2}6} & a_{\bar{2}\bar{0}} & a_{\bar{2}\bar{1}} & a_{\bar{2}\bar{2}}
\end{bmatrix}
\begin{bmatrix} X \\ \beta \\ Z \\ \alpha \\ \gamma \\ \gamma \end{bmatrix}
$$

Fwd Rotor

Aft Rotor

Using the aft rotor load equations,

$$
\begin{bmatrix} \\ \\ \\ \\ \\ \\ \end{bmatrix}
\begin{bmatrix}
a_{14} & a_{15} & a_{16} & a_{1\bar{0}} & a_{1\bar{1}} & a_{1\bar{2}} \\
a_{24} & a_{25} & a_{26} & a_{2\bar{0}} & a_{2\bar{1}} & a_{2\bar{2}} \\
a_{34} & a_{35} & a_{36} & a_{3\bar{0}} & a_{3\bar{1}} & a_{3\bar{2}} \\
a_{74} & a_{75} & a_{76} & a_{7\bar{0}} & a_{7\bar{1}} & a_{7\bar{2}} \\
a_{84} & a_{85} & a_{86} & a_{8\bar{0}} & a_{8\bar{1}} & a_{8\bar{2}} \\
a_{94} & a_{95} & a_{96} & a_{9\bar{0}} & a_{9\bar{1}} & a_{9\bar{2}}
\end{bmatrix}
\cdot
\begin{bmatrix} X \\ \beta \\ Z \\ \alpha \\ \gamma \\ \gamma \end{bmatrix}
$$

Fwd Rotor

Solving for the fwd rotor deflections in terms of

$$
\begin{bmatrix} X \\ B \\ Z \\ \alpha \\ \gamma \end{bmatrix}
= -\gamma
\begin{bmatrix}
a_{14} & a_{15} & a_{16} & a_{1\bar{0}} & a_{1\bar{1}} \\
a_{24} & a_{25} & a_{26} & a_{2\bar{0}} & a_{2\bar{1}} \\
a_{34} & a_{35} & a_{36} & a_{3\bar{0}} & a_{3\bar{1}} \\
a_{74} & a_{75} & a_{76} & a_{7\bar{0}} & a_{7\bar{1}} \\
a_{84} & a_{85} & a_{86} & a_{8\bar{0}} & a_{8\bar{1}}
\end{bmatrix}^{-1}
\cdot
\begin{bmatrix} a_{1\bar{2}} \\ a_{2\bar{2}} \\ a_{3\bar{2}} \\ a_{7\bar{2}} \\ a_{8\bar{2}} \end{bmatrix}
$$

Fwd Rotor

or letting $y = 1$, and then rewriting the equations

$$\begin{bmatrix} X \\ \beta \\ Z \\ \alpha \\ \gamma \\ y \end{bmatrix} = - \begin{bmatrix} a_{14} & a_{15} & a_{16} & a_{1\bar{0}} & a_{1\bar{1}} & \\ a_{24} & a_{25} & a_{26} & a_{2\bar{0}} & a_{2\bar{1}} & \\ a_{34} & a_{35} & a_{36} & a_{3\bar{0}} & a_{3\bar{1}} & \\ a_{74} & a_{75} & a_{76} & a_{7\bar{0}} & a_{7\bar{1}} & \\ a_{84} & a_{85} & a_{86} & a_{8\bar{0}} & a_{8\bar{1}} & \\ & & & & & -1 \end{bmatrix}^{-1} \begin{bmatrix} a_{1\bar{2}} \\ a_{2\bar{2}} \\ a_{3\bar{2}} \\ a_{7\bar{2}} \\ a_{8\bar{2}} \\ 1 \end{bmatrix}$$

Fwd Rotor

Solving for the aft rotor deflections,

$$\begin{bmatrix} X \\ \beta \\ Z \\ \alpha \\ \gamma \\ y \end{bmatrix} = - \begin{bmatrix} a_{44} & a_{45} & a_{46} & a_{4\bar{0}} & a_{4\bar{1}} & a_{4\bar{2}} \\ a_{54} & a_{55} & a_{56} & a_{5\bar{0}} & a_{5\bar{1}} & a_{5\bar{2}} \\ a_{64} & a_{65} & a_{66} & a_{6\bar{0}} & a_{6\bar{0}} & a_{6\bar{2}} \\ a_{\bar{0}4} & a_{\bar{0}5} & a_{\bar{0}6} & a_{\bar{0}\bar{0}} & a_{\bar{0}\bar{1}} & a_{\bar{0}\bar{2}} \\ a_{\bar{1}4} & a_{\bar{1}5} & a_{\bar{1}6} & a_{\bar{1}\bar{0}} & a_{\bar{1}\bar{1}} & a_{\bar{1}\bar{2}} \\ a_{\bar{2}4} & a_{\bar{2}5} & a_{\bar{2}6} & a_{\bar{2}\bar{0}} & a_{\bar{2}\bar{1}} & a_{\bar{2}\bar{2}} \end{bmatrix} \cdot \begin{bmatrix} a_{14} & a_{15} & a_{16} & a_{1\bar{0}} & a_{1\bar{1}} & \\ a_{24} & a_{25} & a_{26} & a_{2\bar{0}} & a_{2\bar{1}} & \\ a_{34} & a_{35} & a_{36} & a_{3\bar{0}} & a_{3\bar{1}} & \\ a_{74} & a_{75} & a_{76} & a_{7\bar{0}} & a_{7\bar{1}} & \\ a_{84} & a_{85} & a_{86} & a_{8\bar{0}} & a_{8\bar{1}} & \\ & & & & & -1 \end{bmatrix}^{-1} \begin{bmatrix} a_{1\bar{2}} \\ a_{2\bar{2}} \\ a_{3\bar{2}} \\ a_{7\bar{2}} \\ a_{8\bar{2}} \\ 1 \end{bmatrix}$$

Aft Rotor

The program inspects the linear deflections calculated as shown above and continues the normalizing procedure relative to the linear deflection with the largest magnitude. The normalization in terms of any linear deflection can be performed by adjusting the fwd rotor boundary conditions

$$\underline{x} \qquad \begin{bmatrix} X \\ \beta \\ Z \\ \alpha \\ \gamma \\ y \end{bmatrix} = \frac{1}{X} \begin{bmatrix} X \\ \beta \\ Z \\ \alpha \\ \gamma \\ y \end{bmatrix} \qquad \underline{y} \qquad \begin{bmatrix} X \\ \beta \\ Z \\ \alpha \\ \gamma \\ y \end{bmatrix} = 1 \begin{bmatrix} X \\ \beta \\ Z \\ \alpha \\ \gamma \\ y \end{bmatrix}$$

Fwd Rotor Column — **Fwd Rotor** — **Fwd Rotor Column** — **Fwd Rotor**

FWD ROTOR

$$Z \begin{bmatrix} X \\ \beta \\ Z \\ \alpha \\ \gamma \\ y \end{bmatrix} = \frac{1}{Z} \begin{bmatrix} X \\ \beta \\ Z \\ \alpha \\ \gamma \\ y \end{bmatrix}$$

Fwd Rotor Column — Fwd Rotor

AFT ROTOR

X

$$\begin{bmatrix} X \\ \beta \\ Z \\ \alpha \\ \gamma \\ y \end{bmatrix} = \frac{1}{X_{(Aft)}} \begin{bmatrix} a_{44} & a_{45} & a_{46} & a_{4\bar{0}} & a_{4\bar{1}} & a_{4\bar{2}} \\ a_{54} & a_{55} & a_{56} & a_{5\bar{0}} & a_{5\bar{1}} & a_{5\bar{2}} \\ a_{64} & a_{65} & a_{66} & a_{6\bar{0}} & a_{6\bar{1}} & a_{6\bar{2}} \\ a_{\bar{0}4} & a_{\bar{0}5} & a_{\bar{0}6} & a_{\bar{0}\bar{0}} & a_{\bar{0}\bar{1}} & a_{\bar{0}\bar{2}} \\ a_{\bar{1}4} & a_{\bar{1}5} & a_{\bar{1}6} & a_{\bar{1}\bar{0}} & a_{\bar{1}\bar{1}} & a_{\bar{1}\bar{2}} \\ a_{\bar{2}4} & a_{\bar{2}5} & a_{\bar{2}6} & a_{\bar{2}\bar{0}} & a_{\bar{2}\bar{1}} & a_{\bar{2}\bar{2}} \end{bmatrix}^{-1} \begin{bmatrix} X \\ \beta \\ Z \\ \alpha \\ \gamma \\ y \end{bmatrix}$$

Fwd Rotor Column — Rotor

y

$$\begin{bmatrix} X \\ \beta \\ Z \\ \alpha \\ \gamma \\ y \end{bmatrix} = \frac{1}{y_{(Aft)}} \begin{bmatrix} a_{44} & a_{45} & a_{46} & a_{4\bar{0}} & a_{4\bar{1}} & a_{4\bar{2}} \\ a_{54} & a_{55} & a_{56} & a_{5\bar{0}} & a_{5\bar{1}} & a_{5\bar{2}} \\ a_{64} & a_{65} & a_{66} & a_{6\bar{0}} & a_{6\bar{1}} & a_{6\bar{2}} \\ a_{\bar{0}4} & a_{\bar{0}5} & a_{\bar{0}6} & a_{\bar{0}\bar{0}} & a_{\bar{0}\bar{1}} & a_{\bar{0}\bar{2}} \\ a_{\bar{1}4} & a_{\bar{1}5} & a_{\bar{1}6} & a_{\bar{1}\bar{0}} & a_{\bar{1}\bar{1}} & a_{\bar{1}\bar{2}} \\ a_{\bar{2}4} & a_{\bar{2}5} & a_{\bar{2}6} & a_{\bar{2}\bar{0}} & a_{\bar{2}\bar{1}} & a_{\bar{2}\bar{2}} \end{bmatrix}^{-1} \begin{bmatrix} X \\ \beta \\ Z \\ \alpha \\ \gamma \\ y \end{bmatrix}$$

Fwd Rotor Column — Aft Rotor

Z

$$\begin{bmatrix} X \\ \beta \\ Z \\ \alpha \\ \gamma \\ y \end{bmatrix} = \frac{1}{Z_{(Aft)}} \begin{bmatrix} a_{44} & a_{45} & a_{46} & a_{4\bar{0}} & a_{4\bar{1}} & a_{4\bar{2}} \\ a_{54} & a_{55} & a_{56} & a_{5\bar{0}} & a_{5\bar{1}} & a_{5\bar{2}} \\ a_{64} & a_{65} & a_{66} & a_{6\bar{0}} & a_{6\bar{1}} & a_{6\bar{2}} \\ a_{\bar{0}4} & a_{\bar{0}5} & a_{\bar{0}6} & a_{\bar{0}\bar{0}} & a_{\bar{0}\bar{1}} & a_{\bar{0}\bar{2}} \\ a_{\bar{1}4} & a_{\bar{1}5} & a_{\bar{1}6} & a_{\bar{1}\bar{0}} & a_{\bar{1}\bar{1}} & a_{\bar{1}\bar{2}} \\ a_{\bar{2}4} & a_{\bar{2}5} & a_{\bar{2}6} & a_{\bar{2}\bar{0}} & a_{\bar{2}\bar{1}} & a_{\bar{2}\bar{2}} \end{bmatrix}^{-1} \begin{bmatrix} X \\ \beta \\ Z \\ \alpha \\ \gamma \\ y \end{bmatrix}$$

Fwd Rotor Column — Aft Rotor

Forced mode shapes can be obtained by collapsing the matrix array representing the fuselage into a single matrix considering the unknown frequency, ω as the frequency of forced excitation. Including the known magnitude of the shaking loads in the fuselage system the single matrix for the entire fuselage becomes,

$$
\begin{bmatrix} F_z \\ M_\beta \\ F_x \\ X \\ \beta \\ Z \\ F_y \\ M_\gamma \\ M_\alpha \\ \alpha \\ \gamma \\ y \\ Q \end{bmatrix}
=
\begin{bmatrix}
a_{11} & a_{12} & a_{13} & a_{14} & a_{15} & a_{16} & a_{17} & a_{18} & a_{19} & a_{1\bar{0}} & a_{1\bar{1}} & a_{1\bar{2}} & a_{1\bar{3}} \\
a_{21} & a_{22} & a_{23} & a_{24} & a_{25} & a_{26} & a_{27} & a_{28} & a_{29} & a_{2\bar{0}} & a_{2\bar{1}} & a_{2\bar{2}} & a_{2\bar{3}} \\
a_{31} & a_{32} & a_{33} & a_{34} & a_{35} & a_{36} & a_{37} & a_{38} & a_{39} & a_{3\bar{0}} & a_{3\bar{1}} & a_{3\bar{2}} & a_{3\bar{3}} \\
a_{41} & a_{42} & a_{43} & a_{44} & a_{45} & a_{46} & a_{47} & a_{48} & a_{49} & a_{4\bar{0}} & a_{4\bar{1}} & a_{4\bar{2}} & a_{4\bar{3}} \\
a_{51} & a_{52} & a_{53} & a_{54} & a_{55} & a_{56} & a_{57} & a_{58} & a_{59} & a_{5\bar{0}} & a_{5\bar{1}} & a_{5\bar{2}} & a_{5\bar{3}} \\
a_{61} & a_{62} & a_{63} & a_{64} & a_{65} & a_{66} & a_{67} & a_{68} & a_{69} & a_{6\bar{0}} & a_{6\bar{1}} & a_{6\bar{2}} & a_{6\bar{3}} \\
a_{71} & a_{72} & a_{73} & a_{74} & a_{75} & a_{76} & a_{77} & a_{78} & a_{79} & a_{7\bar{0}} & a_{7\bar{1}} & a_{7\bar{2}} & a_{7\bar{3}} \\
a_{81} & a_{82} & a_{83} & a_{84} & a_{85} & a_{86} & a_{87} & a_{88} & a_{89} & a_{8\bar{0}} & a_{8\bar{1}} & a_{8\bar{2}} & a_{8\bar{3}} \\
a_{91} & a_{92} & a_{93} & a_{94} & a_{95} & a_{96} & a_{97} & a_{98} & a_{99} & a_{9\bar{0}} & a_{9\bar{1}} & a_{9\bar{2}} & a_{9\bar{3}} \\
a_{\bar{0}1} & a_{\bar{0}2} & a_{\bar{0}3} & a_{\bar{0}4} & a_{\bar{0}5} & a_{\bar{0}6} & a_{\bar{0}7} & a_{\bar{0}8} & a_{\bar{0}9} & a_{\bar{0}\bar{0}} & a_{\bar{0}\bar{1}} & a_{\bar{0}\bar{2}} & a_{\bar{0}\bar{3}} \\
a_{\bar{1}1} & a_{\bar{1}2} & a_{\bar{1}3} & a_{\bar{1}4} & a_{\bar{1}5} & a_{\bar{1}6} & a_{\bar{1}7} & a_{\bar{1}8} & a_{\bar{1}9} & a_{\bar{1}\bar{0}} & a_{\bar{1}\bar{1}} & a_{\bar{1}\bar{2}} & a_{\bar{1}\bar{3}} \\
a_{\bar{2}1} & a_{\bar{2}2} & a_{\bar{2}3} & a_{\bar{2}4} & a_{\bar{2}5} & a_{\bar{2}6} & a_{\bar{2}7} & a_{\bar{2}8} & a_{\bar{2}9} & a_{\bar{2}\bar{0}} & a_{\bar{2}\bar{1}} & a_{\bar{2}\bar{2}} & a_{\bar{2}\bar{3}} \\
a_{\bar{3}1} & a_{\bar{3}2} & a_{\bar{3}3} & a_{\bar{3}4} & a_{\bar{3}5} & a_{\bar{3}6} & a_{\bar{3}7} & a_{\bar{3}8} & a_{\bar{3}9} & a_{\bar{3}\bar{0}} & a_{\bar{3}\bar{1}} & a_{\bar{3}\bar{2}} & a_{\bar{3}\bar{3}}
\end{bmatrix}
\cdot
\begin{bmatrix} F_z \\ M_\beta \\ F_x \\ X \\ \beta \\ Z \\ F_y \\ M_\gamma \\ M_\alpha \\ \alpha \\ \gamma \\ y \\ Q \end{bmatrix}
$$

Aft Rotor

Fwd Rotor

To solve for the unknown quantities at the forward rotor, consider the boundary conditions of the forward and aft rotor as part of its corresponding column matrix and then, simplify the solution. As an example, consider a free-free beam; the boundary conditions are defined by making all external loads equal to zero. Therefore, the matrix can be written as,

$$
\begin{bmatrix} \\ \\ \\ x \\ \beta \\ z \\ \\ \\ \\ \alpha \\ \gamma \\ y \\ Q \end{bmatrix}
=
\begin{bmatrix}
a_{14} & a_{15} & a_{16} & a_{1\bar{0}} & a_{1\bar{1}} & a_{1\bar{2}} & a_{1\bar{3}} \\
a_{24} & a_{25} & a_{26} & a_{2\bar{0}} & a_{2\bar{1}} & a_{2\bar{2}} & a_{2\bar{3}} \\
a_{34} & a_{35} & a_{36} & a_{3\bar{0}} & a_{3\bar{1}} & a_{3\bar{2}} & a_{3\bar{3}} \\
a_{44} & a_{45} & a_{46} & a_{4\bar{0}} & a_{4\bar{1}} & a_{4\bar{2}} & a_{4\bar{3}} \\
a_{54} & a_{55} & a_{56} & a_{5\bar{0}} & a_{5\bar{1}} & a_{5\bar{2}} & a_{5\bar{3}} \\
a_{64} & a_{65} & a_{66} & a_{6\bar{0}} & a_{6\bar{1}} & a_{6\bar{2}} & a_{6\bar{3}} \\
a_{74} & a_{75} & a_{76} & a_{7\bar{0}} & a_{7\bar{1}} & a_{7\bar{2}} & a_{7\bar{3}} \\
a_{84} & a_{85} & a_{86} & a_{8\bar{0}} & a_{8\bar{1}} & a_{8\bar{2}} & a_{8\bar{3}} \\
a_{94} & a_{95} & a_{96} & a_{9\bar{0}} & a_{9\bar{1}} & a_{9\bar{2}} & a_{9\bar{3}} \\
a_{\bar{0}4} & a_{\bar{0}5} & a_{\bar{0}6} & a_{\bar{0}\bar{0}} & a_{\bar{0}\bar{1}} & a_{\bar{0}\bar{2}} & a_{\bar{0}\bar{3}} \\
a_{\bar{1}4} & a_{\bar{1}5} & a_{\bar{1}6} & a_{\bar{1}\bar{0}} & a_{\bar{1}\bar{1}} & a_{\bar{1}\bar{2}} & a_{\bar{1}\bar{3}} \\
a_{\bar{2}4} & a_{\bar{2}5} & a_{\bar{2}6} & a_{\bar{2}\bar{0}} & a_{\bar{2}\bar{1}} & a_{\bar{2}\bar{2}} & a_{\bar{2}\bar{3}} \\
a_{\bar{3}4} & a_{\bar{3}5} & a_{\bar{3}6} & a_{\bar{3}\bar{0}} & a_{\bar{3}\bar{1}} & a_{\bar{3}\bar{2}} & a_{\bar{3}\bar{3}}
\end{bmatrix}
\cdot
\begin{bmatrix} x \\ \beta \\ z \\ \alpha \\ \gamma \\ y \\ Q \end{bmatrix}
$$

Now, the general solution considers only the equation which are equal to zero. Therefore the boundary conditions can be represented by six linear equations. The matrix for the free-free beam becomes,

$$
\begin{bmatrix} \\ \\ \\ \\ \\ \\ \end{bmatrix}
=
\begin{bmatrix}
a_{14} & a_{15} & a_{16} & a_{1\bar{0}} & a_{1\bar{1}} & a_{1\bar{2}} & a_{1\bar{3}} \\
a_{24} & a_{25} & a_{26} & a_{2\bar{0}} & a_{2\bar{1}} & a_{2\bar{2}} & a_{2\bar{3}} \\
a_{34} & a_{35} & a_{36} & a_{3\bar{0}} & a_{3\bar{1}} & a_{3\bar{2}} & a_{3\bar{3}} \\
a_{74} & a_{75} & a_{76} & a_{7\bar{0}} & a_{7\bar{1}} & a_{7\bar{2}} & a_{7\bar{3}} \\
a_{84} & a_{85} & a_{86} & a_{8\bar{0}} & a_{8\bar{1}} & a_{8\bar{2}} & a_{8\bar{3}} \\
a_{94} & a_{95} & a_{96} & a_{9\bar{0}} & a_{9\bar{1}} & a_{9\bar{2}} & a_{9\bar{3}}
\end{bmatrix}
\cdot
\begin{bmatrix} x \\ \beta \\ z \\ \alpha \\ \gamma \\ y \\ Q \end{bmatrix}
$$

The 6 x 6 boundary condition matrix may be obtained directly by considering only the elements common to rows of zero boundary at the aft rotor and to columns of non-zero boundary condition at fwd rotor. Considering the use of this procedure in the free-free beam case

$$
\begin{bmatrix} \\ \\ \\ X \\ \beta \\ Z \\ \\ \\ \\ \alpha \\ \gamma \\ y \\ Q \end{bmatrix}
=
\begin{bmatrix}
 & & & a_{14} & a_{15} & a_{16} & & & & a_{1\bar{0}} & a_{1\bar{1}} & a_{1\bar{2}} & a_{1\bar{3}} \\
 & & & a_{24} & a_{25} & a_{26} & & & & a_{2\bar{0}} & a_{2\bar{1}} & a_{2\bar{2}} & a_{2\bar{3}} \\
 & & & a_{34} & a_{35} & a_{36} & & & & a_{3\bar{0}} & a_{3\bar{1}} & a_{3\bar{2}} & a_{3\bar{3}} \\
 & & & & & & & & & & & & \\
 & & & & & & & & & & & & \\
 & & & & & & & & & & & & \\
 & & & a_{74} & a_{75} & a_{76} & & & & a_{7\bar{0}} & a_{7\bar{1}} & a_{7\bar{2}} & a_{7\bar{3}} \\
 & & & a_{84} & a_{85} & a_{86} & & & & a_{8\bar{0}} & a_{8\bar{1}} & a_{8\bar{2}} & a_{8\bar{3}} \\
 & & & a_{94} & a_{95} & a_{96} & & & & a_{9\bar{0}} & a_{9\bar{1}} & a_{9\bar{2}} & a_{9\bar{3}} \\
 & & & & & & & & & & & & \\
 & & & & & & & & & & & & \\
 & & & & & & & & & & & & \\
 & & & & & & & & & & & &
\end{bmatrix}
\cdot
\begin{bmatrix} \\ \\ \\ X \\ \beta \\ Z \\ \\ \\ \\ \alpha \\ \gamma \\ y \\ Q \end{bmatrix}
$$

Aft Rotor Fwd Rotor

Continuing, the matrix can be rewritten in terms of Q which is a known value for the free-free beam,

$$\begin{bmatrix} a_{14} & a_{15} & a_{16} & a_{1\bar{5}} & a_{1\bar{1}} & a_{1\bar{2}} \\ a_{24} & a_{25} & a_{26} & a_{2\bar{5}} & a_{2\bar{1}} & a_{2\bar{2}} \\ a_{34} & a_{35} & a_{36} & a_{3\bar{5}} & a_{3\bar{1}} & a_{3\bar{2}} \\ a_{74} & a_{75} & a_{76} & a_{7\bar{5}} & a_{7\bar{1}} & a_{7\bar{2}} \\ a_{84} & a_{85} & a_{86} & a_{8\bar{5}} & a_{8\bar{1}} & a_{8\bar{2}} \\ a_{94} & a_{95} & a_{96} & a_{9\bar{5}} & a_{9\bar{1}} & a_{9\bar{2}} \end{bmatrix} \cdot \begin{bmatrix} X \\ \beta \\ Z \\ \alpha \\ \gamma \\ \psi \end{bmatrix} = -Q \begin{bmatrix} a_{1\bar{3}} \\ a_{2\bar{3}} \\ a_{3\bar{3}} \\ a_{7\bar{3}} \\ a_{8\bar{3}} \\ a_{9\bar{3}} \end{bmatrix}$$

The equations can now be solved for the unknown values by inversion of the square matrix. The solution for the free-free beam can be written as,

$$\begin{bmatrix} X \\ \beta \\ Z \\ \alpha \\ \gamma \\ \psi \end{bmatrix} = -Q \begin{bmatrix} a_{14} & a_{15} & a_{16} & a_{1\bar{5}} & a_{1\bar{1}} & a_{1\bar{2}} \\ a_{24} & a_{25} & a_{26} & a_{2\bar{5}} & a_{2\bar{1}} & a_{2\bar{2}} \\ a_{34} & a_{35} & a_{36} & a_{3\bar{5}} & a_{3\bar{1}} & a_{3\bar{2}} \\ a_{74} & a_{75} & a_{76} & a_{7\bar{5}} & a_{7\bar{1}} & a_{7\bar{2}} \\ a_{84} & a_{85} & a_{86} & a_{8\bar{5}} & a_{8\bar{1}} & a_{8\bar{2}} \\ a_{94} & a_{95} & a_{96} & a_{9\bar{5}} & a_{9\bar{1}} & a_{9\bar{2}} \end{bmatrix}^{-1} \begin{bmatrix} a_{1\bar{3}} \\ a_{2\bar{3}} \\ a_{3\bar{3}} \\ a_{7\bar{3}} \\ a_{8\bar{3}} \\ a_{9\bar{3}} \end{bmatrix}$$

Following evaluation of the fwd rotor boundary conditions the forced mode shape at each station is obtained by progressive matrix multiplication and print-out starting with the known column elements.

DISTRIBUTION LIST
WIND TUNNEL TESTS AND FURTHER ANALYSIS OF THE
FLOATING WING FUEL TANKS FOR HELICOPTER RANGE EXTENSION

Chief U. S. Army R&D Liaison Group (9851 DU) ATTN: USATRECOM LO APO 757 New York, New York	(1)
President United States Army Aviation Board ATTN: ATBG-DB Fort Rucker, Alabama	(1)
Chief of Research and Development ATTN: Air Mobility Division Department of the Army Washington 25, D. C.	(1)
Chief of Transportation ATTN: TCDRD	(1)
ATTN: TCAFO-R	(1)
Department of the Army Washington 25, D. C.	
Commanding General U. S. Army Transportation Materiel Command ATTN: TCMAC-APU P. O. Box 209, Main Office St. Louis 66, Missouri	(1)
Commanding Officer U. S. Army Transportation Research Command ATTN: Executive for Programs	(1)
ATTN: Research Reference Center	(4)
ATTN: Aviation Directorate	(4)
ATTN: Military Liaison & Advisory Office	(4)
ATTN: Deputy Commander for Aviation	(1)
ATTN: Long Range Technical Forecast Office Fort Eustis, Virginia	(1)
Commanding Officer U. S. Army Transportation Research Command Liaison Office ATTN: MCLATS Wright-Patterson Air Force Base, Ohio	(1)

Chief, Bureau of Naval Weapons
Department of the Navy
ATTN: RAAE-34 (1)
Washington 25, D. C.

Headquarters
U. S. Army Aviation Test Office
ATTN: FTZAT (1)
Edwards Air Force Base, California

Commanding Officer and Director
David Taylor Model Basin
Aerodynamics Laboratory Library (1)
Washington 7, D. C.

National Aeronautics and Space Administration
ATTN: Mr. Bertram A. Mulcahy
Assistant Director for Technical Information (1)
1520 H. Street, N. W.
Washington 25, D. C.

National Aviation Facilities Experimental Center
ATTN: Library (1)
Atlantic City, New Jersey

Librarian
Langley Research Center
National Aeronautics & Space Administration (1)
Langley Field, Virginia

Ames Research Center
National Aeronautics and Space Agency
ATTN: Library
Moffett Field, California (1)

U. S. Army Standardization Group, U. K.
Box 65, U. S. Navy 100
FPO New York, New York (1)

Office of the Senior Standardization Representative
U. S. Army Standardization Group, Canada
c/o Director of Equipment Policy (1)
Canadian Army Headquarters
Ottawa, Canada

Canadian Army Liaison Officer
Liaison Group, Room 208
U. S. Army Transportation School
Fort Eustis, Virginia (3)

British Joint Services Mission (Army Staff)
ATTN: Lt. Col. R. J. Wade, RE (3)
DAQMG (Mov & Tn)
3100 Massachusetts Avenue, N. W.
Washington 8, D. C.

Commander
Armed Services Technical Information Agency
ATTN: TIPCR (10)
Arlington Hall Station
Arlington 12, Virginia

Cornell Aeronautical Laboratory, Inc.
ATTN: Mr. Richard White
4455 Genesee Street (1)
Buffalo 21, New York

Sikorsky Aircraft
Division of United Aircraft Corporation
ATTN: John Rabbott (1)
Stratford, Connecticut

Hiller Aircraft Corporation
ATTN: Library (1)
Palo Alto, California

Doman Helicopters, Incorporated
Danbury Municipal Airport
P. O. Box 603
Danbury, Connecticut (1)

Bell Helicopter Company
Division of Bell Aerospace Corporation
ATTN: Robert Lynn (1)
P. O. Box 482
Fort Worth 1, Texas

Hughes Tool Company
Aircraft Division
ATTN: Library
Culver City, California (1)

Kaman Aircraft Corporation
ATTN: Library
Bloomfield, Connecticut (1)

Kellett Aircraft Corporation
ATTN: Library
P. O. Box 35
Willow Grove, Pennsylvania (1)

McDonnell Aircraft Corporation
ATTN: Library
St. Louis, Missouri (1)

Georgia Institute of Technology
ATTN: Library
Atlanta, Georgia (1)

Massachusetts Institute of Technology
Department of Aeronautics and Astronautics
Cambridge, Massachusetts (1)

Mississippi State College
ATTN: Library
State College, Mississippi (1)

University of Wichita
ATTN: Library
Wichita 14, Kansas (1)

VERTOL DIVISION, THE BOEING COMPANY, Morton Pennsylvania

WIND TUNNEL TESTS AND FURTHER ANALYSIS OF THE FLOATING WING FUEL TANKS FOR HELICOPTER RANGE EXTENSION

Volume 4-Coupled Wing-Fuselage Forced Vibration Analysis, 45° Skewed Hinge, by R. Ricks, R. Gabel, May 1961, 104 p. incl. figs. and app. (TCREC 61-105 Proj. 9X38-09-006). (Contract DA 44-177-TC-550)

Unclassified Report

Forced response calculations are performed on the H-21 helicopter equipped with floating fuel wings for the 0% and 100% fuel configurations. Using third harmonic shaft loads measured on an H-21 helicopter, and a deflection test obtained analytical model of the H-21 fuselage, the Associated Matrix Method is employed to calculate the fuselage forced response. Results of the response calculations are presented as modal time histories of the fuselage for third harmonic azimuth positions of 0, 45, 90, and 135 degrees, (Over)

UNCLASSIFIED

1. Range Extension - Dynamics
2. Fuselage Forced Vibration

I. Ricks, R.
II. Gabel, R.

UNCLASSIFIED

and the resultant vertical and lateral responses at the cockpit floor during an rpm sweep.

Results of the analysis indicate that at the 0% fuel configuration, vertical response compares closely to that of the standard helicopter. Laterally, the response increases with rotor speed, having an acceptable level at the lower rotor speed range and somewhat higher amplitude at 268 rpm. For the 100% fuel configuration, the forced response calculations indicate the presence of a lateral natural frequency close to, but below the 3Ω excitation at 250 rpm. In both the lateral and vertical directions, the calculated undamped vibration levels are high at the lower rotor speeds, but appear satisfactory at 268 rpm. Past experience indicates that predicted vibration levels near resonance are reduced by damping. Nevertheless, as a result of the calculations, it is recommended that a simplified ground shake test be performed to substantiate the calculations and provide some reasonable prediction of the effect of damping.

UNCLASSIFIED

UNCLASSIFIED

VERTOL DIVISION, THE BOEING COMPANY, Morton Pennsylvania

WIND TUNNEL TESTS AND FURTHER ANALYSIS OF THE FLOATING WING FUEL TANKS FOR HELICOPTER RANGE EXTENSION

Volume 4-Coupled Wing-Fuselage Forced Vibration Analysis, 45° Skewed Hinge, by R. Ricks, R. Gabel, May 1961, 104 p. incl. figs. and app. (TCREC 61-105 Proj. 9X38-09-006). (Contract DA 44-177-TC-550)

Unclassified Report

Forced response calculations are performed on the H-21 helicopter equipped with floating fuel wings for the 0% and 100% fuel configurations. Using third harmonic shaft loads measured on an H-21 helicopter, and a deflection test obtained analytical model of the H-21 fuselage, the Associated Matrix Method is employed to calculate the fuselage forced response. Results of the response calculations are presented as modal time histories of the fuselage for third harmonic azimuth positions of 0, 45, 90, and 135 degrees, (Over)

UNCLASSIFIED

1. Range Extension - Dynamics
2. Fuselage Forced Vibration

I. Ricks, R.
II. Gabel, R.

UNCLASSIFIED

and the resultant vertical and lateral responses at the cockpit floor during an rpm sweep.

Results of the analysis indicate that at the 0% fuel configuration, vertical response compares closely to that of the standard helicopter. Laterally, the response increases with rotor speed, having an acceptable level at the lower rotor speed range and somewhat higher amplitude at 268 rpm. For the 100% fuel configuration, the forced response calculations indicate the presence of a lateral natural frequency close to, but below the 3Ω excitation at 250 rpm. In both the lateral and vertical directions, the calculated undamped vibration levels are high at the lower rotor speeds, but appear satisfactory at 268 rpm. Past experience indicates that predicted vibration levels near resonance are reduced by damping. Nevertheless, as a result of the calculations, it is recommended that a simplified ground shake test be performed to substantiate the calculations and provide some reasonable prediction of the effect of damping.

UNCLASSIFIED

UNCLASSIFIED

VERTOL DIVISION, THE BOEING COMPANY, Morton Pennsylvania

WIND TUNNEL TESTS AND FURTHER ANALYSIS OF THE FLOATING WING FUEL TANKS FOR HELICOPTER RANGE EXTENSION

Volume 4-Coupled Wing-Fuselage Forced Vibration Analysis, 45° Skewed Hinge, by R. Ricks, R. Gabel, May 1961, 104 p. incl. figs. and app. (TCREC 61-105 Proj. 9X38-09-006). (Contract DA 44-177-TC-550)

Unclassified Report

Forced response calculations are performed on the H-21 helicopter equipped with floating fuel wings for the 0% and 100% fuel configurations. Using third harmonic shaft loads measured on an H-21 helicopter, and a deflection test obtained analytical model of the H-21 fuselage, the Associated Matrix Method is employed to calculate the fuselage forced response. Results of the response calculations are presented as modal time histories of the fuselage for third harmonic azimuth positions of 0, 45, 90, and 135 degrees, (Over)

UNCLASSIFIED

1. Range Extension - Dynamics
2. Fuselage Forced Vibration

I. Ricks, R.
II. Gabel, R.

UNCLASSIFIED

and the resultant vertical and lateral responses at the cockpit floor during an rpm sweep.

Results of the analysis indicate that at the 0% fuel configuration, vertical response compares closely to that of the standard helicopter. Laterally, the response increases with rotor speed, having an acceptable level at the lower rotor speed range and somewhat higher amplitude at 268 rpm. For the 100% fuel configuration, the forced response calculations indicate the presence of a lateral natural frequency close to, but below the 3Ω excitation at 250 rpm. In both the lateral and vertical directions, the calculated undamped vibration levels are high at the lower rotor speeds, but appear satisfactory at 268 rpm. Past experience indicates that predicted vibration levels near resonance are reduced by damping. Nevertheless, as a result of the calculations, it is recommended that a simplified ground shake test be performed to substantiate the calculations and provide some reasonable prediction of the effect of damping.

UNCLASSIFIED

UNCLASSIFIED

VERTOL DIVISION, THE BOEING COMPANY, Morton Pennsylvania

WIND TUNNEL TESTS AND FURTHER ANALYSIS OF THE FLOATING WING FUEL TANKS FOR HELICOPTER RANGE EXTENSION

Volume 4-Coupled Wing-Fuselage Forced Vibration Analysis, 45° Skewed Hinge, by R. Ricks, R. Gabel, May 1961, 104 p. incl. figs. and app. (TCREC 61-105 Proj. 9X38-09-006). (Contract DA 44-177-TC-550)

Unclassified Report

Forced response calculations are performed on the H-21 helicopter equipped with floating fuel wings for the 0% and 100% fuel configurations. Using third harmonic shaft loads measured on an H-21 helicopter, and a deflection test obtained analytical model of the H-21 fuselage, the Associated Matrix Method is employed to calculate the fuselage forced response. Results of the response calculations are presented as modal time histories of the fuselage for third harmonic azimuth positions of 0, 45, 90, and 135 degrees, (Over.

UNCLASSIFIED

1. Range Extension - Dynamics
2. Fuselage Forced Vibration

I. Ricks, R.
II. Gabel, R.

UNCLASSIFIED

and the resultant vertical and lateral responses at the cockpit floor during an rpm sweep.

Results of the analysis indicate that at the 0% fuel configuration, vertical response compares closely to that of the standard helicopter. Laterally, the response increases with rotor speed, having an acceptable level at the lower rotor speed range and somewhat higher amplitude at 268 rpm. For the 100% fuel configuration, the forced response calculations indicate the presence of a lateral natural frequency close to, but below the 3Ω excitation at 250 rpm. In both the lateral and vertical directions, the calculated undamped vibration levels are high at the lower rotor speeds, but appear satisfactory at 268 rpm. Past experience indicates that predicted vibration levels near resonance are reduced by damping. Nevertheless, as a result of the calculations, it is recommended that a simplified ground shake test be performed to substantiate the calculations and provide some reasonable prediction of the effect of damping.

UNCLASSIFIED

UNCLASSIFIED

VERTOL DIVISION, THE BOEING COMPANY, Morton Pennsylvania

WIND TUNNEL TESTS AND FURTHER ANALYSIS OF THE FLOATING WING FUEL TANKS FOR HELICOPTER RANGE EXTENSION

Volume 4-Coupled Wing-Fuselage Forced Vibration Analysis, 45° Skewed Hinge, by R. Ricks, R. Gabel, May 1961, 104 p. incl. figs. and app. (TCREC 61-105 Proj. 9X38-09-006). (Contract DA 44-177-TC-550)

Unclassified Report

Forced response calculations are performed on the H-21 helicopter equipped with floating fuel wings for the 0% and 100% fuel configurations. Using third harmonic shaft loads measured on an H-21 helicopter, and a deflection test obtained analytical model of the H-21 fuselage, the Associated Matrix Method is employed to calculate the fuselage forced response. Results of the response calculations are presented as modal time histories of the fuselage for third harmonic azimuth positions of 0, 45, 90, and 135 degrees, (Over)

UNCLASSIFIED

1. Range Extension - Dynamics
2. Fuselage Forced Vibration

I. Ricks, R.
II. Gabel, R.

UNCLASSIFIED

and the resultant vertical and lateral responses at the cockpit floor during an rpm sweep.

Results of the analysis indicate that at the 0% fuel configuration, vertical response compares closely to that of the standard helicopter. Laterally, the response increases with rotor speed, having an acceptable level at the lower rotor speed range and somewhat higher amplitude at 268 rpm. For the 100% fuel configuration, the forced response calculations indicate the presence of a lateral natural frequency close to, but below the 3Ω excitation at 250 rpm. In both the lateral and vertical directions, the calculated undamped vibration levels are high at the lower rotor speeds, but appear satisfactory at 268 rpm. Past experience indicates that predicted vibration levels near resonance are reduced by damping. Nevertheless, as a result of the calculations, it is recommended that a simplified ground shake test be performed to substantiate the calculations and provide some reasonable prediction of the effect of damping.

UNCLASSIFIED

VERTOL DIVISION, THE BOEING COMPANY, Morton Pennsylvania

WIND TUNNEL TESTS AND FURTHER ANALYSIS OF THE FLOATING WING FUEL TANKS FOR HELICOPTER RANGE EXTENSION

Volume 4-Coupled Wing-Fuselage Forced Vibration Analysis, 45° Skewed Hinge, by R. Ricks, R. Gabel, May 1961, 104 p. incl. figs. and app. (TCREC 61-105 Proj. 9X38-09-006). (Contract DA 44-177-TC-550)

Unclassified Report

Forced response calculations are performed on the H-21 helicopter equipped with floating fuel wings for the 0% and 100% fuel configurations. Using third harmonic shaft loads measured on an H-21 helicopter, and a deflection test obtained analytical model of the H-21 fuselage, the Associated Matrix Method is employed to calculate the fuselage forced response. Results of the response calculations are presented as modal time histories of the fuselage for third harmonic azimuth positions of 0, 45, 90, and 135 degrees, (Over

UNCLASSIFIED

1. Range Extension - Dynamics
2. Fuselage Forced Vibration

I. Ricks, R.
II. Gabel, R.

UNCLASSIFIED

and the resultant vertical and lateral responses at the cockpit floor during an rpm sweep.

Results of the analysis indicate that at the 0% fuel configuration, vertical response compares closely to that of the standard helicopter. Laterally, the response increases with rotor speed, having an acceptable level at the lower rotor speed range and somewhat higher amplitude at 268 rpm. For the 100% fuel configuration, the forced response calculations indicate the presence of a lateral natural frequency close to, but below the 3Ω excitation at 250 rpm. In both the lateral and vertical directions, the calculated undamped vibration levels are high at the lower rotor speeds, but appear satisfactory at 268 rpm. Past experience indicates that predicted vibration levels near resonance are reduced by damping. Nevertheless, as a result of the calculations, it is recommended that a simplified ground shake test be performed to substantiate the calculations and provide some reasonable prediction of the effect of damping.

UNCLASSIFIED

VERTOL DIVISION, THE BOEING COMPANY, Morton Pennsylvania

WIND TUNNEL TESTS AND FURTHER ANALYSIS OF THE FLOATING WING FUEL TANKS FOR HELICOPTER RANGE EXTENSION

Volume 4-Coupled Wing-Fuselage Forced Vibration Analysis, 45° Skewed Hinge, by R. Ricks, R. Gabel, May 1961, 104 p. incl. figs. and app. (TCREC 61-105 Proj. 9X38-09-006). (Contract DA 44-177-TC-550)

Unclassified Report

Forced response calculations are performed on the H-21 helicopter equipped with floating fuel wings for the 0% and 100% fuel configurations. Using third harmonic shaft loads measured on an H-21 helicopter, and a deflection test obtained analytical model of the H-21 fuselage, the Associated Matrix Method is employed to calculate the fuselage forced response. Results of the response calculations are presented as modal time histories of the fuselage for third harmonic azimuth positions of 0, 45, 90, and 135 degrees, (Over)

UNCLASSIFIED

1. Range Extension - Dynamics
2. Fuselage Forced Vibration

I. Ricks, R.
II. Gabel, R.

UNCLASSIFIED

and the resultant vertical and lateral responses at the cockpit floor during an rpm sweep.

Results of the analysis indicate that at the 0% fuel configuration, vertical response compares closely to that of the standard helicopter. Laterally, the response increases with rotor speed, having an acceptable level at the lower rotor speed range and somewhat higher amplitude at 268 rpm. For the 100% fuel configuration, the forced response calculations indicate the presence of a lateral natural frequency close to, but below the 3Ω excitation at 250 rpm. In both the lateral and vertical directions, the calculated undamped vibration levels are high at the lower rotor speeds, but appear satisfactory at 268 rpm. Past experience indicates that predicted vibration levels near resonance are reduced by damping. Nevertheless, as a result of the calculations, it is recommended that a simplified ground shake test be performed to substantiate the calculations and provide some reasonable prediction of the effect of damping.

UNCLASSIFIED

VERTOL DIVISION, THE BOEING COMPANY, Morton Pennsylvania

WIND TUNNEL TESTS AND FURTHER ANALYSIS OF THE FLOATING WING FUEL TANKS FOR HELICOPTER RANGE EXTENSION

Volume 4-Coupled Wing-Fuselage Forced Vibration Analysis, 45° Skewed Hinge, by R. Ricks, R. Gabel, May 1961, 104 p. incl. figs. and app. (TCREC 61-105 Proj. 9X38-09-006). (Contract DA 44-177-TC-550)

Unclassified Report

Forced response calculations are performed on the H-21 helicopter equipped with floating fuel wings for the 0% and 100% fuel configurations. Using third harmonic shaft loads measured on an H-21 helicopter, and a deflection test obtained analytical model of the H-21 fuselage, the Associated Matrix Method is employed to calculate the fuselage forced response. Results of the response calculations are presented as modal time histories of the fuselage for third harmonic azimuth positions of 0, 45, 90, and 135 degrees, (Over

UNCLASSIFIED

1. Range Extension - Dynamics
2. Fuselage Forced Vibration

I. Ricks, R.
II. Gabel, R.

UNCLASSIFIED

and the resultant vertical and lateral responses at the cockpit floor during an rpm sweep.

Results of the analysis indicate that at the 0% fuel configuration, vertical response compares closely to that of the standard helicopter. Laterally, the response increases with rotor speed, having an acceptable level at the lower rotor speed range and somewhat higher amplitude at 268 rpm. For the 100% fuel configuration, the forced response calculations indicate the presence of a lateral natural frequency close to, but below the 3Ω excitation at 250 rpm. In both the lateral and vertical directions, the calculated undamped vibration levels are high at the lower rotor speeds, but appear satisfactory at 268 rpm. Past experience indicates that predicted vibration levels near resonance are reduced by damping. Nevertheless, as a result of the calculations, it is recommended that a simplified ground shake test be performed to substantiate the calculations and provide some reasonable prediction of the effect of damping.

UNCLASSIFIED

UNCLASSIFIED

UNCLASSIFIED